August 1991

EUROPEAN ORGANIZATION FOR EXPERIMENTAL PHOTOGRAMMETRIC RESEARCH

TEST OF TRIANGULATION OF SPOT DATA

Report edited by I. J. Dowman

Official Publication N° 26

Wir bitten, die vorgedruckte Empfangsbestätigung auf der unteren Hälfte dieses Blattes herauszutrennen, Ihre Adresse, bei Änderung auch die frühere, einzutragen und die Karte zurückzusenden. Bei mehreren Heften in einer Lieferung genügt es, nur eine Karte zurückzusenden, wenn die Nummern der anderen Hefte auf dieser notiert sind. *Sollten die Bestätigungskarten ausbleiben, müssen wir annehmen, daß Sie am Tauschverkehr mit uns nicht mehr interessiert sind, und weitere Lieferungen einstellen.*

Please detach the acknowledgement of receipt attached below, enter your address, in case of change enter your former address, too, and return the card.
If a shipment comprises several volumes, please return one card only listing all numbers. *If the receipt is not acknowledged we understand that you are no longer interested in our exchange of publications and that you wish to be cancelled from our mailing list.*

Ayez la bontē de dētacher l'accusē de rēception que vous trouvez sur la partie infērieure de cette page, d'y inscrire votre adresse et, le cas échéant, votre ancienne adresse et de retourner la carte.
Si la livraison se compose de plusieurs fascicules, il suffit de ne retourner qu'une seule carte portant également les numēros des autres fascicules. *Le fait d'avoir expēdiē un envois sans avoir reçu la carte de réception nous donnera raison à supposer que vous n'êtes plus intēressēs à continuer l'échange de publications et que vous approuverez l'arrêt de nos envois.*

Le rogamos sacar el acuse de recibo figurando en la parte inferior de esta pāgina, inscribir su direcciōn y si ha cambiado, inscribir la direcciōn anterior, y retornar esta tarjeta.
Si el envío se compone de varios fascículos es bastante retornarnos una sola tarjeta indicando también los nūmeros de los otros fascículos. *Si quedamos sin acuses de recibo tenemos que suponer que ya no tiene Vd interēs en nuestro cambio de publicaciones y que desea Vd suspender otros envíos.*

Absender:
Sender:
Expēditeur:
Expedidor:

Es sind hier eingegangen:
We received:
Nous avons reçu:
Han llegado en nuestras manos:

OEEPE
Publ. off. No. 26

Institut für Angewandte Geodäsie
Richard-Strauss-Allee 11
D-6000 Frankfurt am Main 70
Germany · Allemagne · Alemania

August 1991

EUROPEAN ORGANIZATION FOR EXPERIMENTAL PHOTOGRAMMETRIC RESEARCH

TEST OF TRIANGULATION OF SPOT DATA

Report edited by I.J. Dowman

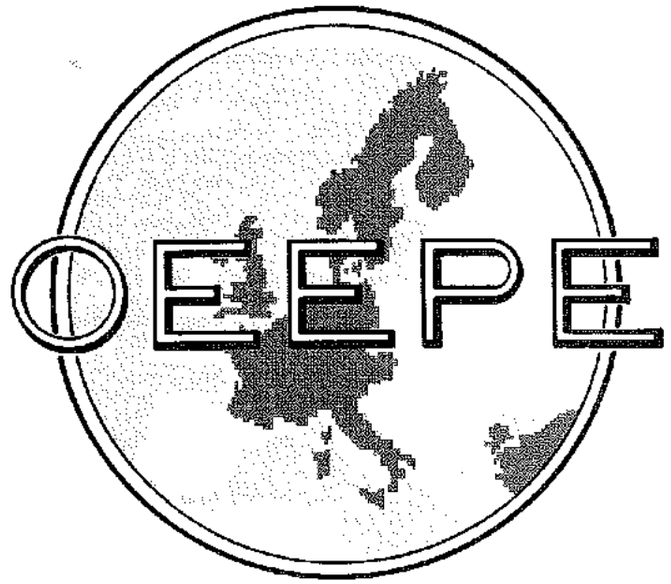

Official Publication N° 26

ISSN 0257-0505

EUROPEAN ORGANIZATION
for
EXPERIMENTAL PHOTOGRAMMETRIC RESEARCH

STEERING COMMITTEE

(composed of Representatives of the Governments of the Member Countries)

Prof. Dr. E. KILPELÄ — Finland
Institute of Photogrammetry Helsinki
University of Technology
SF-02150 Espoo 15

Mr. A. JAEGLE — France
Institut Géographique National
2, Avenue Pasteur
F-94160 Saint Mandé

Mr. G. BEGNI
Centre National
d'Etudes Spatiales
18, Avenue E. Belin
F-31055 Toulouse Cedex

Prof. R. GALETTO — Italy
Istituto di Topografia della
Facolta di Ingegneria della Universita
Via Strada Nuova
I-27100 Pavia

Dr. Eng. L. SURACE
Geographical Military Institute
Via Cesare Battista 8—10
I-50122 Firence

Prof. Dr. G. LIGTERINK — Netherlands
Technical University Delft
Thijsseweg 11
NL-2600 GA Delft

Ir. C. J. REMYNSE
Hoofddirecteur Hoofddirectie
v. h. Kadaster en de Openbare Registers
Waltersingel 1
NL-7300 GH Apeldoorn

Mr. Ø. BRANDSÆTER — Norway
Deputy Director
Mapping Division
Statens Kartverk
N-3500 Hønefoss

Mr. I. INDSET
Statens Kartverk
N-3500 Hønefoss

Prof. J. TALTS — Sweden
National Land Survey of Sweden
S-80112 Gävle

Prof. K. TORLEGÅRD
Royal Institute of Technology
Dept. of Photogrammetry
S-10044 Stockholm 70

Prof. Dr. O. KÖLBL — Switzerland
Institut de Photogrammétrie, EPFL
GR-Ecublens
CH-1015 Lausanne

Mr. R. KNÖPFLI
Vize-Direktor
Bundesamt für Landestopographie
Seftigenstrasse 264
CH-3084 Wabern

Col. A. EMIN YALIN — Turkey
Ministry of National Defence
General Command of Mapping
TR-06100 Ankara

Major M. ÖNDER
Ministry of National Defence
General Command of Mapping
TR-06100 Ankara

Director General P. Mc MASTER — United Kingdom
Ordnance Survey
Romsey Road
Maybush
Southampton S09 4DH

Dr. I. J. DOWMAN
Dept. of Photogrammetry and Surveying
University College London
Gower Street 6
London WC 1E BT

SCIENCE COMMITTEE

Dr. I. J. DOWMAN — United Kingdom
Dept. of Photogrammetry and Surveying
University College London
Gower Street 6
London WC 1E BT

EXECUTIVE BUREAU

Mr. J. KURE
Secretary General of the OEEPE
International Institute for Aerospace Survey
and Earth Sciences (ITC)
350 Boulevard 1945, P. O. Box 6
NL-7500 AA Enschede (Netherlands)

Prof. Dr. H. G. JERIE
International Institute for Aerospace Survey
and Earth Sciences (ITC)
350 Boulevard 1945, P. O. Box 6
NL-7500 AA Enschede (Netherlands)

Mr. G. DUCHER
Institut Géographique National
2, Avenue Pasteur
F-94160 Saint Mandé (France)

SCIENTIFIC COMMISSIONS

Commission A — **Aerotriangulation**

President: Mrs. P. NOUKKA
National Board of Survey
Box 84
SF-00521 Helsinki 52

Commission B — **Digital Elevation Models**

President: Dr. K. TEMPFLI
International Institute for Aerospace Survey
and Earth Sciences (ITC)
350 Boulevard 1945, P. O. Box 6
NL-7500 AA Enschede

Commission C — **Large Scale Restitution**

President: Prof. Dr. O. KÖLBL
Institut de Photogrammétrie, EPFL
GR-Ecublens
CH-1015 Lausanne

Commission D — **Photogrammetry and Cartography**

President: Major General C. THOMPSON
Burgh House
Burgh by Sands
Carlisle CA5 6AN
United Kingdom

Commission E — **Topographic Interpretation**

President: Dr. B.-S. SCHULZ
Institut für Angewandte Geodäsie
Richard-Strauss-Allee 11
D-6000 Frankfurt am Main 70

Commission F — **Fundamental Problems of Photogrammetry**

President: Prof. Dr. G. LIGTERINK
Technical University Delft
Thijsseweg 11
NL-2600 GA Delft

APPLICATION COMMISSIONS

Commission I — **Topographic Mapping**

President: Mr. M. J. D. BRAND
Director
Ordnance Survey of N. Ireland
Colby House, Stranmillis Court
Belfast BT 9 5BJ
United Kingdom

Commission II — **Cadastral Mapping**

President: Ir. L. A. KOEN
Hoofddirectie
v. h. Kadaster en de Openbare Registers
Waltersingel 1
NL-7300 GH Apeldoorn

Commission III — **Engineering Surveys**

President: Mr. A. FLOTRON
Gemeindemattenstrasse 4
CH-3860 Meiringen

Commission IV — **Environmental/Thematic Surveys**

Commission V — **Land Information Systems**

President: Prof. Dr. W. GÖPFERT
Technische Hochschule Darmstadt
Petersenstrasse 13
D-6100 Darmstadt

DK 528.88:528.067.4

Test of Triangulation of Spot Data

(with 67 Figures, 52 Tables and 3 Appendices)

Report edited by I.J. Dowman

Table of Contents

ABSTRACT:

This publication is a record of the OEEPE test of triangulation of SPOT data. The first part comprises a report of the objectives and requirements of the test and a summary of the results. The second part consists of the reports from all the participants on their method and results. The administrative details of the test and information from SPOT Image are included in the appendices.

Six centres participated fully in the test and two additional organisations also contributed. The data consisted of two strips of stereoscopic images, each of four models, thus forming a block of 8 models. 255 ground control points were provided by IGN which were used to control the strips and to check the accuracy of the triangulation. 10 control configurations were specified. Some centres carried out additional tests and these included investigations into the order of polynomials to be used for modelling attitude change, and the effect of using different types of ground control.

The results show that strips and blocks can be adjusted to give the same accuracy as single models when using the same number of control points. The results from all centres varied very little when control was reduced from 20 to 6 points and in some cases down to 4 points. However in general when four of less points were used the results deteriorated. Accuracy varied between 9.3 m and 20.9 m vector root mean square error when using 6 points in a strip and between 13.7 m and 21.3 m vector rmse when two points are used at either end of a strip. Blocks could be set up to similar accuracies with 4 to 6 control points. In all cases height was more accurate than plan.

The tests were repeated by four centres using data observed on digital images displayed in a screen and the results followed the same pattern but were more accurate. Thus the relative performance of the different methods could be assessed.

In summary the report shows that high accuracies can be obtained from strips and blocks of SPOT data with very little control. The potential of SPOT data for mapping large areas without the need for a large ground control campaign is thus demonstrated. The report also contains a comprehensive set of descriptions of geometric models used for SPOT data and an assessment of their performance.

RESUME:

Cette publication constitue le rapport final de l'essai qu'a conduit l'OEEPE sur une triangulation spatiale à partir de données du satellite SPOT. La première partie contient une description des objectifs de l'essai, ses caractéristiques et un résumé des résultats obtenus. La seconde partie regroupe les rapports de l'ensemble des participants, avec description des méthodes qu'ils ont utilisées et des résultats correspondants. On a placé en annexe les détails concernant le déroulement et la gestion de cet essai ainsi que des informations fournies par SPOT-Image.

Six centres ont participé à la totalité de l'essai et deux organismes supplémentaires y ont également contribué. Les données comprenaient deux bandes de quatre modèles stéréoscopiques chacune, formant ainsi un bloc de 8 modèles SPOT. Un canevas de 255 points de coordonnées connues a été fourni par l'IGN (F). Ces points ont servi soit de points d'appui aux bandes, soit de points de vérification, permettant ainsi de déterminer la précision de la spatio-triangulation. Il avait été préconisé de travailler sur 10 configurations différentes concernant les points d'appui à utiliser. Quelques centres ont effectué des essais supplémentaires, notamment sur le degré des polynomes à utiliser dans la modélisation des variations d'attitude et sur l'influence de la nature des points d'appui.

Les résultats montrent que l'on peut compenser des bandes et des blocs dans les mêmes conditions de précision résultante qu'avec des modèles séparés, tout en utilisant le même nombre de points d'appui. Tous les centres ont fourni des résultats qui varient très peu lorsque le nombre de points d'appui tombe de 20 à 6, voire dans certains cas à 4 points. En revanche les résultats se dégradent généralement dès que ce nombre devient inférieur ou égal à 4 points.

Lorsque l'on utilise 6 points d'appui par bande, l'exactitude des résultats peut se caractériser par une erreur moyenne quadratique (emq) dans l'espace comprise entre 9,3 m et 20,9 m (vecteur xyz) et si l'on ne garde que 2 points d'appui à chaque extrémité de la bande, l'emq se situe entre 13,7 m et 21,3 m. On obtient des précisions analogues pour les blocs en utilisant de 4 à 6 points d'appui. La précision altimétrique s'est révélée meilleure que la précision planimétrique dans tous les cas étudiés.

Quatre centres ont recommencé les essais en utilisant des données observées directement à partir d'images numériques affichées sur un écran et les résultats s'échelonnent de façon similaire, tout en étant plus précis. On a pu ainsi évaluer la qualité relative des différentes méthodes.

En conclusion, ce rapport démontre la possibilité d'accès à la haute précision avec une spatio-triangulation de bandes et de blocs SPOT, tout en ne s'appuyant que sur un très petit nombre de points connus. L'aptitude des données de SPOT à la cartographie de vastes zones, en évitant de recourir à de grandes campagnes d'établissement de canevas d'appui sur le terrain, est donc établie. Ce rapport contient également un jeu complet de descriptions des modèles géométriques utilisés pour des données SPOT et l'évaluation de leur performances.

ZUSAMMENFASSUNG:

In dieser Veröffentlichung wird über den OEEPE-Triangulationstest von SPOT-Daten berichtet. Im ersten Teil werden die Ziele und die Testanforderungen beschrieben und die Ergebnisse zusammengefaßt. Im zweiten Teil berichten alle Teilnehmer über ihre Methoden und Ergebnisse. Administrative Einzelheiten des Versuchs und Informationen von Spot Image sind in den Anlagen enthalten.

Sechs Auswertestellen waren an dem Versuch voll beteiligt und zwei weitere Organisationen lieferten Beiträge. Die Daten bestanden aus zwei Streifen stereoskopischer Bilder, jeder mit vier Modellen, die auf diese Weise einen Block von 8 Modellen bildeten. 255 Kontrollpunkte wurden vom IGN geliefert, die dazu verwendet wurden, die Streifen einzupassen und die Triangulationsgenauigkeit zu überprüfen. Es wurden 10 verschiedene Paßpunktanordnungen festgelegt. Einige Stellen führten zusätzliche Versuche durch, diese enthielten Untersuchungen zur Wahl des Grades von Polynome, wie sie zur Beschreibung von Lageänderungen (des Satelliten) gebraucht werden, und über die Auswirkung der Verwendung zweier unterschiedlicher Paßpunktarten.

Die Ergebnisse zeigten, daß Streifen und Blöcke mit der gleichen Genauigkeit ausgeglichen werden können wie Einzelmodelle, wenn die gleiche Anzahl von Paßpunkten verwendet wird. Die Ergebnisse aus allen Stellen unterschieden sich sehr wenig voneinander, wenn die Paßpunkte von 20 auf 6, in einigen Fällen sogar auf 4 verringert wurden. Die Ergebnisse wurden jedoch im allgemeinen schlechter, wenn 4 Punkte oder weniger verwendet wurden. Die Genauigkeit schwankte zwischen 9,3 m und 20, 9 m mittlerer quadratischer Vektorfehler bei Verwendung von 6 Punkten in einem Streifen und zwischen 13,7 m und 21,3 m mittlerer quadratischer Fehler, wenn zwei Punkte am jeweiligen Streifenende verwendet wurden. Blöcke konnten mit 4 bis 6 Paßpunkten auf ähnliche Genauigkeiten gebracht werden. In allen Fällen war die Höhe genauer als die Lage.

Die Tests wurden von vier Stellen wiederholt, wobei Daten verwendet wurden, die auf digitalen, am Bildschirm dargestellten Bildern beobachtet wurden, und die Ergebnisse zeigten das gleiche Erscheinungsbild, waren jedoch genauer. Auf diese Weise konnte die relative Leistung der verschiedenen Methoden beurteilt werden.

Zusammenfassend zeigt der Bericht, daß hohe Genauigkeiten von SPOT-Streifen und -Blöcken mit nur wenigen Paßpunkten erzielt werden können. Damit wird nachgewiesen, daß SPOT-Daten zur Kartierung großer Gebiete ohne große terrestrische Vermessungskampagnen geeignet sind. Der Bericht enthält außerdem umfangreiche Beschreibungen der für die SPOT-Daten verwendeten geometrischen Modelle und eine Beurteilung ihrer Leistungsfähigkeit.

Acknowledgements

This test has been possible only because of the generosity of SPOT Image in allowing the 16 SPOT scenes to be used for the work. The data had already been supplied to IGN who undertook to reproduce the tapes and images for distribution to the participants. OEEPE gratefully acknowledges the contribution of SPOT Image and also of IGN and UCL who have supported the project in the supply of ground co-ordinates, measurements and administrative effort.

The editor would also like to thank his colleagues and students at UCL, particularly Francelina Neto and Gordon Bentley, who have contributed to the organisation of the workshop and the preparation of the report.

PART 1

DESCRIPTION OF THE TEST AND SUMMARY OF RESULTS

By I.J.Dowman, F.Neto and I. Veillet.

1. Introduction

It has now been shown by many organisations that SPOT data can be used for topographical mapping. Methods have been developed and implemented at a number of centres and of the problems which have been identified, the use of ground control is a major one. Particularly in remote areas, those areas where SPOT data is most useful, ground control points are difficult to identify and very costly to co-ordinate. It has therefore become necessary to reduce control requirements to a minimum and, so, to develop methods of aerial triangulation and to develop the use of auxilliary data.

The OEEPE therefore set up a test with the following objectives:

> to determine the accuracy which can be obtained when determining control points from a strip covered by stereo SPOT data;
>
> to determine the number of control points which are necessary;
>
> to investigate the way in which information provided by tracking and on board measurement can be used in triangulation of SPOT data;
>
> to compare different methods which are available for triangulation of SPOT data.

It was hoped to include a large number of the centres which have used SPOT data for mapping and who have a capability to triangulate SPOT data. This aim was successful and this report is a comprehensive survey of methods for triangulating SPOT data and of accuracies attainable.

The report describes the data which was provided and the results obtained. A description of each method, prepared by the participants, is included, together with comments on their results.

2. Organisation of the test

The test was carried out in two phases. In the first phase the participants were provided with SPOT data and ground control information and asked carry out a triangulation and determine the co-ordinates of check points. This phase was concluded with a workshop which was held on 27th and 28th September 1989 at UCL and
at which all centres presented their results and details of their method.

In the second phase participants were provided with a set of image co-ordinates observed at the Institut Géographique National, France (IGN) and asked to carry out the same computation.

University College London (UCL) acted as pilot centre, responsible for distributiung the data, collating results and preparation of the report. UCL also organised the workshop a the end of phase 1.

The Institut Geographique Nationale (IGN) provided the SPOT data and the ground control information. SPOT Image generously agreed that the SPOT data already purchased by IGN should be made available to the participants without additional charge. IGN also observed the image data used in phase 2 of the test.

Because of the limited number of centres in Europe capable of handling SPOT data, organisations outside of Europe were invited to participate. Two such centres, The Canadian Centre for Mapping and the Department of Geographic Information in Queensland participated as full partners, The Triffid Corporation of the USA also carried out some of the tests and attended the workshop. The full list of participants is shown in Table 1.

CENTRE	ABBREVIATION
Canadian Centre for Mapping, Ottawa.	CCM
Institute for Photogrammetry and Engineering Surveys, University of Hannover.	HAN
Institut Géographique National, France.	IGN
Istituto di Topografia, Fotogrammetria e Geofisica, Politecnico di Milano.	MIL
Department of Geographic Information, Queensland, Australia	QLD
Department of Photogrammetry and Surveying, University College London in collaboration with Laser-scan Laboratories.	UCL
Trifid Corporation, St Louis, USA.	TRI

Table 1. Participants in the OEEPE test of triangulation of SPOT data

3. Preparation of the test data

3.1 Introduction

Within its Action for Development, Evaluation and Training in spatial photogrammetry with SPOT data, IGN acquired SPOT images and prepared the ground control data. Experiments were then conducted on the data for the OEEPE test on triangulation using SPOT data. IGN supplied the pilot centre with all the test data, SPOT images and ground control points.

3.2 Location of the test site

The French test site for the evaluation of spatial triangulation of SPOT images is located in the South East of France, between the Rhone valley and the Alps. This area covers approximately 200 kms from North to South and 110 kms from East to West, or from Grenoble to Aix en Provence, and from Gap to Valence. This site was chosen because there were already some check data prepared for the in-flight evaluation and because it is the driest French region, which could make SPOT image acquisition easier.

3.3 SPOT data

The test area is divided into two zones (A and B). Each zone covers two overlapping strips of SPOT images. Figure 1 shows the location of all the sixteen SPOT images. The common part of A and B strips is quite narrow. A SPOT strip is a series of images taken succesively by the same instrument, the same day, along the same track of the satellite. Each strip is four SPOT images long. The acquisition was ordered this way so as to have as few models as possible, since modelisation of a stereopair of strips is nearly the same as modelisation of a stereopair of images.

The zone A acquisition took place in summer 1986, and the zone B in spring 1987. The images were required to be taken so that the two images of a stereopair would be as close in time as possible, in order to have the best pointing accuracy. The details are given in Table 2.

The SPOT images were supplied to the pilot centre as level 1A CCT, or as IGN level 1A film diapositives of second generation. Original positives were made on the IGN Vizircolor system. The images have been processed and locally enhanced. The panchromatic pixel size is 25 micrometers. The images have been linearly extended along each line (across the track), in order to have the

same scale across the track as along track.

K - J	Day and of view	Angle	Image centre in ° ' "		Cloud cover
A. stereoscopic pair 50 : 50E and 50W					
050-259	of 28.07.86	20.5°E	N0450713	E0055700	0000
050-260	of 28.07.86	20.5°E	N0443820	E0054348	0000
050-261	of 28.07.86	20.5°E	N0440924	E0053047	0000
050-262	of 28.07.86	20.5°E	N0434026	E0051757	0000
050-259	of 30.08.86	22.3°W	N0450713	E0060222	2110
050-260	of 30.08.86	22.3°W	N0443820	E0055345	0000
050-261	of 30.08.86	22.3°W	N0440924	E0054514	0201
051-262	of 30.08.86	22.3°W	N0434026	E0053647	0000
B. stereoscopic pair 49 : 49E and 49W					
049-259	of 19.04.87	22.6°E	N0450713	E0052905	1202
049-260	of 19.04.87	22.6°E	N0443820	E0051536	1202
049-261	of 19.04.87	22.6°E	N0440944	E0050218	0100
049-262	of 19.04.87	22.6°E	N0434026	E0044912	0000
049-259	of 26.04.87	21.7°W	N0450713	E0051353	0202
049-260	of 26.04.87	21.7°W	N0443820	E0050511	0200
049-261	of 26.04.87	21.7°W	N0440944	E0045635	0000
049-262	of 26.04.87	21.7°W	N0434026	E0044803	0000

Table 2. Description of the SPOT images used.

3.3 SPOT Data quality

As shown by the cloud cover figures, some of the images are quite cloudy. The main inconvenience lies in the difficulty of finding ground controls on the east part of stereopair 049-259. The images could be suitable for geometric evaluation but are not convenient for stereoplotting the whole area. The snowy parts were not a great problem, because only the highest summits were masked. Clouds and snow partly explain the irregular density of points.

3.4 Ground control

The points of this test set, which can be used as well as control points or check points, were gathered from various origins. All of them were sketched manually from the actual SPOT images, and then located on a SPOT small scale paper print. Points were observed stereoscopically, they were not chosen to be observed on single images.

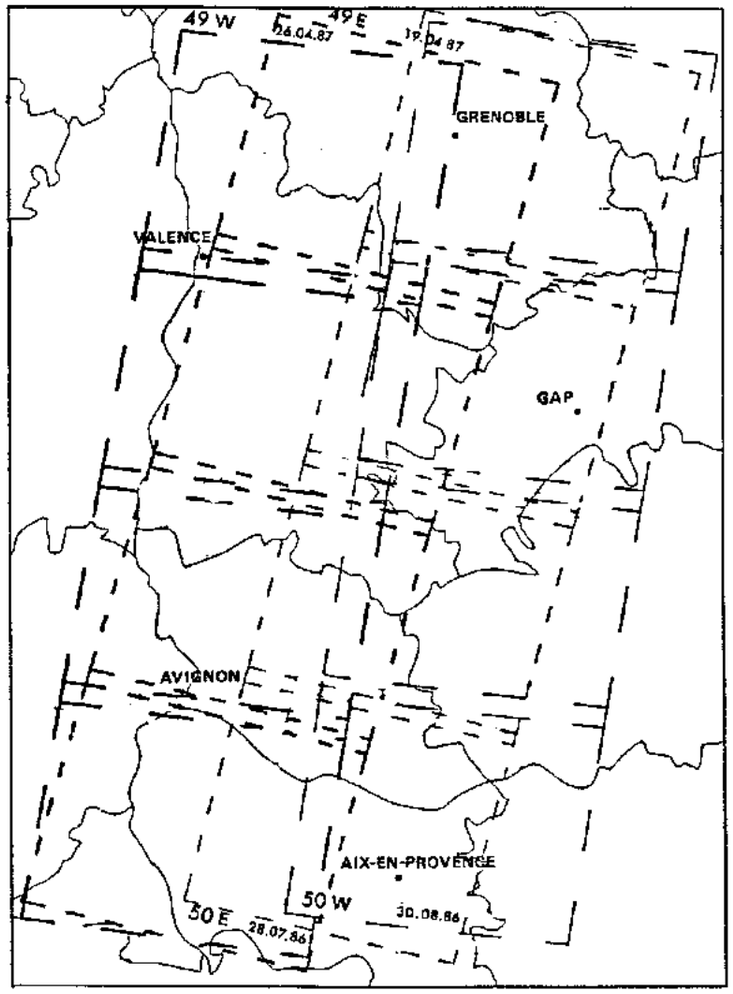

Figure 1. Spot images location

129 points were provided in area A and 132 in area B. Six points of area A can also be observed on area B. Figure 2 shows the location of points.

Inventories giving all the elements about the ground control points were supplied to participants. Their contents are as follows:

- general information
- list of points coordinates
- sketch and definition for all points
- print of each SPOT scene with the location of the points
- a geoid map over the area.

3.5 Quality of ground control points.

Points were chosen in four different ways:

Field stereopreparation, they are numbered 0-- and 109 (class 1).
From 1:30000 aerial stereopairs, they are numbered 20-- (class 2).
From 1:60000 aerial stereopairs, but chosen without refering to SPOT images, they are numbered 1 --- and 3--- (class 3).
From 1:25000 IGN topographic maps, they are numbered --, 1-- and 9--- (class 4).

The accuracy of computation of the points varies from 2 to 10 metres for the coordinates computation. There is also an identification error which can reach 10 metres. It is really hard to give precise figures about accuracies because those points were prepared by different methods from different source materials. For the computation accuracy of the co-ordinates figures can be given only as indicative values, to check relative results between the four groups of points.

Class	1	2	3	4
Planimetric accuracy (m)	3	2	4	5
Altimetric accuracy (m)	2	2	2	2

Table 3. Indicative accuracy of control points.

3.6 Conclusion

A considerable amount of time was taken to collect this set of data, and it may not be fully consistent and may not be ideal. However, it was available at the time OEEPE planned to organize tests on triangulation of SPOT images and is a convenient data set to test triangulation processing over a large area.

4. Test requirements

Participants were sent the data on computer compatible tape or diapositive as required, together with photographic prints and descriptions of all control points. 10 control point configurations were specified using 20 control points. The configurations are shown in figure 3.

Control in strip A was designed to provide even distribution except for case (f) which uses only two points at each end of the strip. In strip B control is used only down one side of the strip, the asumption being that a block adjustment with strip A will give full control; there are common control points in the overlap area.

The full test instructions are given in Appendix I.

After the centres had carried out their adjustments using the control provided, the full set of control points was provided by the pilot centre.

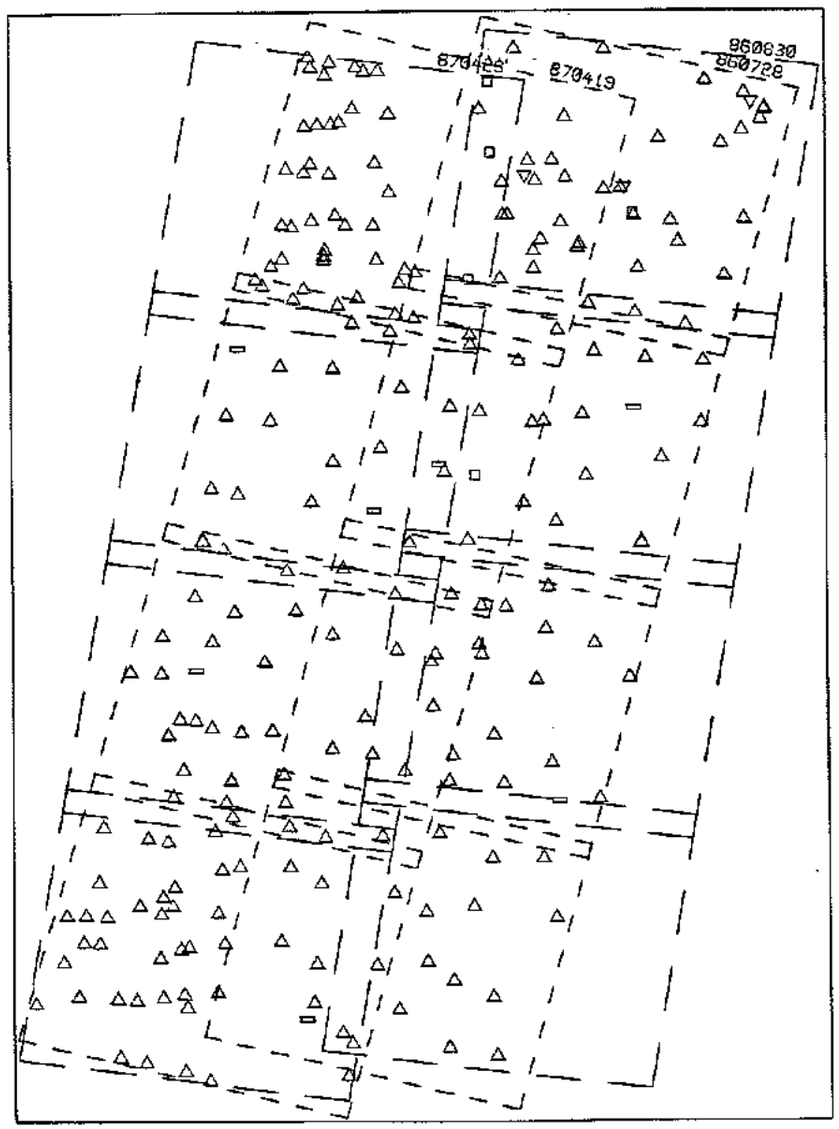

Figure 2. Ground control points distribution

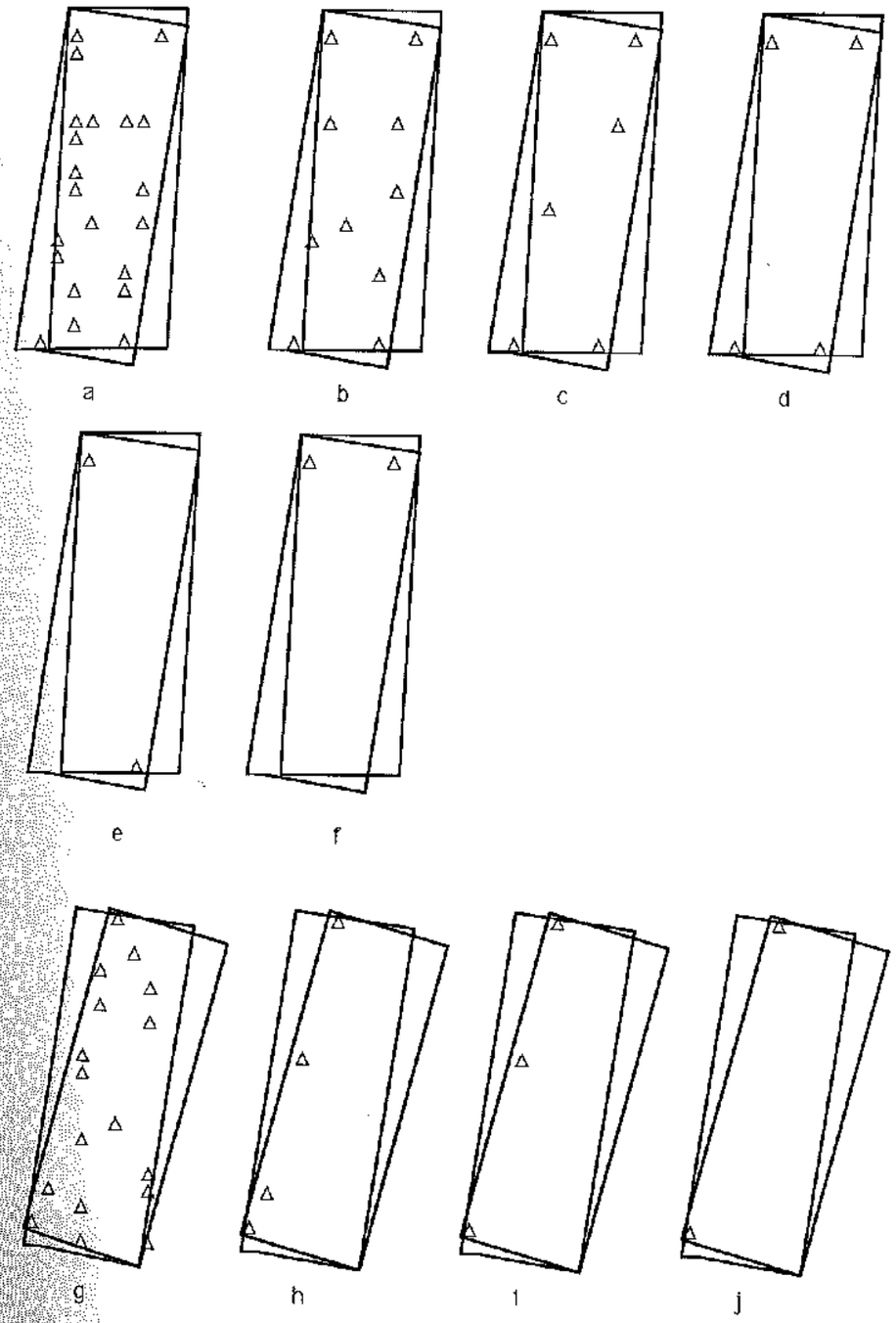

Figure 3. The control configurations for the test.

CENTRE	DESCRIPTION OF MODEL	UNKNOWNS	HEADER DATA	CONSTRAINTS
CCM	Bundle adustment with orbit constraints	12 elements ext. orient'n	No	Orbit constraints
	Does not use header data	12 rates of change		
		df1,df2, q1,q2		
HAN	Modified BINGO bundle adjustment		Yes	
	Does not use w or ø			
IGN	Bundle adjustment with orbital contraints	4 - 7 parameters	Yes	
		Position and attitude		
MIL	Bundle adustment with orbit constraints	Sat. state vectors	Posn and attitude	Pseudo w,ø
		attitude functions	data. Inst. settings	range
		instrument settings		
QLD	Geometric model with conjugate points	r,i,Ω,w,e	c,to,	Orbit and
	x = k,t	wo,w1.., ø0,ø1.., ko,k1..	initial attitude	attitude
			Position and att.	
UCL (Gugan)	Single model space resection	r,i,Ω,w,e	No	None
		wo,w1.., ø0,ø1.., ko,k1..		
UCL (O'Neill)	Orbital model with relaxation using	Sensor attitude and pos'n	Yes	Orbit
	conjgate points			
Trifid	Bundle adjustement	Pos'n and att.	Pos'n and att. for	No
			initial values	

Table 4. Sensor models used by participants

5. Methods used

The methods used by the participants are described in part 2 of this report. Their features are described in Table 4.

The basis of all the models except UCL (O'Neill) and Hannover are similar. All use a model which describes the orbit in terms of orbital parameters or co-ordinates with constraints, and attitude in terms of a polynomial, and relate object space to image space with collinearity equations. This can be described as a bundle adjustment. All except UCL (Gugan), which only uses single images or strips, use conjugate points in the solution but the methods differ in the use of constraints and method of determining initial values of the unknowns. Hannover also uses a bundle adjustment but one which is based on the Bingo block adjustment for aerial photographs, and additional parameters are used to allow for the different geometry of SPOT. UCL (O'Neill) uses the SPOT header data and conjugate points only to carry out a relative orientation by minimising the ray skewness by relaxation. A further relaxation is applied when control points are introduced to give the absolute orientation.

6. Results of phase 1

6.1 Observations

Various methods were used to observe the image co-ordinates of the control points, these are summarised in Table 5

CENTRE	METHOD OF OBSERVATION	NO. OF POINTS OBSERVED CONTROL A (21)*	B(14)	CHECK PTS A(129)	B(132)
CCM	Stereo observation on NRC Anaplot I	19		63	
HAN	Stereo observation on Planicomp C100	20	10	101	124
IGN	Stereo observation on Matra Traster	21	14	101	144
MIL	Mono observation on ZeissPK-1	21	14	86	103
QLD	Stereo observation on Planicomp C100	21	14	108	123
UCL	Stereo observation on Kern DSR1	18	14	106	135

Table 5 Method of observation and number of points observed.

* numbers in brackets indicate the number of points available.

Every point was not observed for a number of reasons. In most cases points could not be identified or were not available on both images. Participants commented on the ease of using the control points and that very few points had been rejected as being difficult to identify and observe.

6.2 Results from determination of check point co-ordinates

The co-ordinates of the check points provided by the main participants were compared with the ground co-ordinates determined by IGN. In all cases a root mean square error was computed and

these results are shown in tables 6 - 11 and summarised graphically in figure 4 and 5. UCL (O'Neill) and Trifid carried out their own evaluation and did not use the specified control configurations and their results are treated separately. Some participants also carried out additional tests which are also treated separately.

The first point to note is that CCM and UCL (Gugan) did not produce results for all control configurations; this is because the model could not obtain a solution without a minimum number of control points. In the case of UCL this is because single image space resection was used with no support from conjugate points. In the case of CCM the solutions failed due to ill conditioning and singularity of the solution.

The results from strip A for 20, 10 and 6 GCPs are very similar except in the case of CCM where the 10 point solution is worse than the 6. The same applies to strip B, where the distribution is less regular.
The range of results is quite large and this is particularly noticable in the cases of more control points being used where there is a two times differential between IGN and UCL (Gugan) although the norm is closer to 1.5. When less control is available and less well distributed the fluctuation in results is much greater.

control	rms height	rms plan	rms 3D
A	5.5	12.1	13.3
B	6.4	13.5	14.9
C	7.5	13.6	15.5
D	10.4	14.0	17.4
E	8.9	14.5	17.0
F	19.2	20.0	27.7
G	4.5	13.5	14.3
H	5.4	15.3	16.2
I	5.7	17.6	18.5
J	5.9	17.1	18.1

Table 6 rms (m) of the results obtained by Hannover

control	rms height	rms plan	rms 3D
A	3.6	6.6	7.5
B	4.9	7.6	9.0
C	4.7	8.0	9.3
D	5.3	7.9	9.5
E	4.1	13.1	13.7
F	5.2	12.9	14.0
G	4.0	7.4	9.4
H	6.6	20.1	21.2
I	5.7	20.1	20.9
J	8.9	25.8	27.3

Table 7 rms (m) of the results obtained by IGN

control	rms height	rms plan	rms 3D
A	13.1	15.8	20.5
B	11.5	16.5	20.7
C	12.9	16.4	20.9
D	12.7	16.3	20.6
E	13.3	16.7	21.3
F	11.2	22.1	24.4
G	11.4	13.7	17.8
H	12.0	16.3	20.3
I	12.0	14.5	18.9
J	12.3	16.4	20.5

Table 8 rms (m) of the results obtained by Milan

control	rms height	rms plan	rms 3D
A	5.1	12.6	13.6
B	6.8	13.3	14.9
C	5.8	13.8	15.0
D	6.0	14.2	15.4
E	6.0	13.2	14.5
F	5.9	21.0	21.8
G	4.0	12.9	13.6
H	4.1	17.0	17.5
I	3.8	16.4	16.8
J	5.2	15.2	16.1

Table 9 rms (m) of the results obtained by Queensland

control	rms height	rms plan	rms 3D
A	5.3	12.8	13.8
B	6.7	21.1	22.2
C	13.2	15.0	20.0
D	21.5	17.2	27.5

Table 10 rms (m) of the results obtained by CCM

control	rms height	rms plan	rms 3D
A	7.3	15.6	17.2
B	7.3	16.1	17.7
G	8.4	12.6	15.2
H	8.9	14.1	16.6

Table 11 rms (m) of the results obtained by UCL (resection)

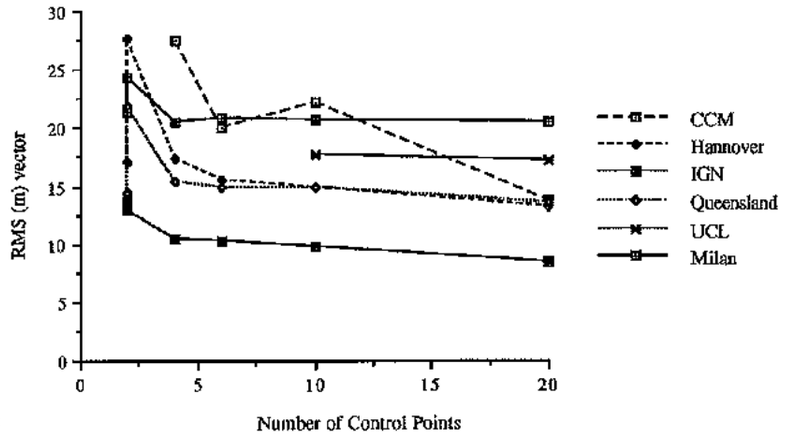

Figure 4 Vector errors of the measurements in strip A, obtained by the different centres

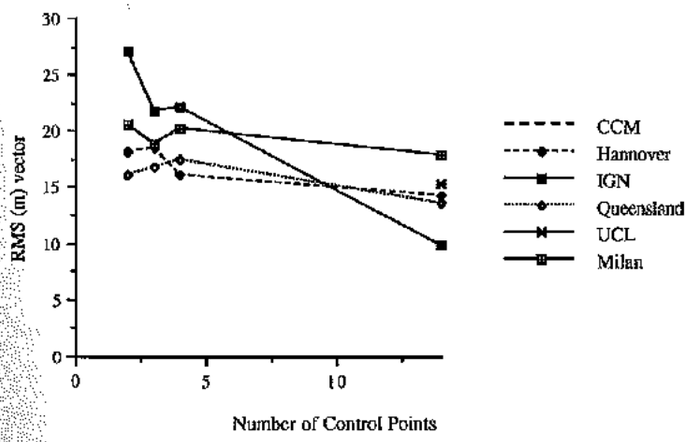

Figure 5 Vector errors of the measurements in strip B, obtained by the different centres

From these results the following conclusions can be drawn:

A similar accuracy can be obtained when triangulating strips of SPOT data as when setting up single models using the same number of control points.

Some of the methods are sensitive to the number and distribution of ground control points used. With these methods it was either impossible to set up models with less than 6 control points or else the accuracy deteriorated.

Height accuracy is better than plan, and height is less sensitive to control point number and distribution than plan.

6.3 Additional results

Some of the participants carried out additional tests to those specified by OEEPE.

6.3.1 Block adjustment

Four centres, Hannover, IGN, Queensland and UCL carried out a block adjustments on the two strips together. The results indicate that a similar result can be obtained with two strips as with one for a similar number of control points although the minimum number of control points which should be used is four. With four points there is no chance of detecting errors in the ground control points and so the use of more points is desirable.

CENTRE	No GCPs	No Chk Pts	X m	Y m	Z m
HANNOVER	6	194	11.2	10.0	6.5
IGN	4	232	8.4	5.8	4.9
			7.0	5.8	4.6
			11.5	5.5	5.4
QUEENSLAND	6	229	10.1	8.6	5.1
	35	229	9.3	7.8	5.1
UCL	4		12.2		7.3
	5		11.3		6.4
	8		11.6		5.7

Table 12. Results of adjustment of two strips together.

6.3.2 The order of polynomials

Queensland investigated the optimum order of polynomial to use for modelling the attitude changes and concluded that first order polynomials should be used for omega, phi and kappa, except where

control distribution is insufficient to produce meaningful values for these parameters.

6.3.3 Distribution and accuracy of control

A number of centres employed data snooping techniques to identify and allow removal of erroneous control points. It is well known that when minimum amounts of control are used in block adjustment that the result is sensitive to errors in control but this can be a greater problem with SPOT than with larger scale imagery because of the greater problems in identifying control points. This feature was apparent in the results from CCM which used similar control distibutions to those specified but with alternative points in the same location. IGN also carried out tests with additional control distributions.

Trifid carried out adjustments with 16, 12, 6 and 4 control points and concluded that six points are sufficient whereas systematic errors occur with four points.

UCL carried out tests on strips A and B using the O'Neill-Dowman relaxation model. The control configuration used were not the same as those specified by OEEPE. These and other non-standard results are shown in Table 13.

CENTRE	No GCPs	No Chk Pts	Plan m	Z m	Vector m	Comment
CCM	10	61	10.8	4.9	11.9	
	6	61	13.9	5.6	15.0	
Trifid	16	41	8.7	6.9	11.1	
	12	41	9.1	6.7	11.4	
	6	41	10.4	7.0	12.5	
	4	41	11.8	9.1	14.9	
UCL (O'Neill)	2	93	21.6	11.4	24.5	Strip A GCPs in across track direction.
	3	98	12.1	6.5	14.1	Strip A GCPs in Δ pattern
	3	130	15.3	8.6	17.6	Strip B GCPs in Δ pattern

Table 13. Results of adjustment of non standard control configurations.

6.3.4 Type of ground control point

UCL investigated the effect of using control points derived from different sources. It was not possible to come to any clear conclusion because there was correlation between control type and relief. However it is clear that control derived from maps is worse than than derived from aerial photographs or from ground survey. The overall result showed that the control derived from aerial photographs gives the best result.

Trifid also studied the accuracy using different groups of ground control points and concluded that the points derived from 1:25 000 scale maps were less reliable than those from ground control of stereo photographs.

6.4 Discussion of phase 1 results

At the workshop a number of points which arose from the results were discussed and the conclusions are reported.

6.4.1 Precision of the image co-ordinates

Participants indicated that image co-ordinates had been observed with precision varying from 5 -10μm. This corresponds to 2-4m on the ground, about 0.25 pixels. Weights used in the adjustments are given below. Milan also used weights for focal length (0.1mm), Psi X (0.018^0), Psi Y(0.008^0), satellite veolocities (0.05 m s^{-1}) and pitch yaw and roll velocities (0.1^0 s^{-1}).

CENTRE	IMAGE	ORBIT					CONTROL		
		X	Y	Z	Ω	K	X	Y	Z
IGN	12μm		300m			400mrads	6m	6m	6m
QLD	10	85	170	85		0.02^o		infinity	
HAN	10	400	400	400		1mgon	7.5	7.5	5
TRIFFID	7	1000	1000	1000		3arcmin	11	11	7
CCN	2000	200	500						
MIL	6	150	150	150			6	6	6

Table 14. Weights used by participants.

6.4.2 Image quality

There was noticable variation in the quailty of the images and although this cannot be quantified it is likely that the better results of strip B may be attributable to this cause. All participants noted the importance of good preprocessing of the hardcopy data and also of the desirability of SPOT Image providing additional information to control film stability such as additional fiducial marks of appropriate size. SPOT Image now produce a level 1AP product which solves many of these problems.

6.4.3 Quality of height measurement

The question was raised as to why the height accuracy is better than plan and why the height accuracy is less dependent on number of control points than plan? There was considerable discussion on this point and it was concluded that such a reseult could be justified theoretically on the gropunds that accuracy would be greater in the cross track direction, this is the direction of parallax measurement and on the grounds that an error in plan over a 10m pixel would give a larger result in the final fit than would an error in height.

7. Phase 2

7.1 Background

There was general agreement at the workshop that the test should continue with the following objectives:

To compare the methods used with a single set of data;

To repeat the test with digital data.

It was decided to combine these two objectives into a single test using digital data observed by IGN. IGN prepared the data for distribution by the Pilot Centre. Instructions for phase 2 are given in appendix I.

7.2 Results

Four centres carried out the test with digital data observed at IGN. A summary of the results are given in tables 15-16 and figures 6-10, full results are presented in part 2.

Centre	using IGN digital data			using own data		
	rms(m)			rms(m)		
	height	plan	3D	height	plan	3D
UCL	11.4	15.6	19.3	7.3	15.6	17.2
Milan	14.8	14.6	20.8	13.1	15.8	20.5
Queensland	10.7	13.4	17.2	7.7	12.0	14.3
Hannover	10.4	15.1	18.4	5.5	12.1	13.3
IGN	5.2	9.0	10.4	3.6	6.6	7.5

Table 15 rms (m) obtained by different centres using IGN data for configuration A

Centre	using IGN digital data			using own data		
	rms(m)			rms(m)		
	height	plan	3D	height	plan	3D
UCL	11.0	16.1	19.5	7.3	16.1	17.7
Milan	13.6	16.1	21.1	11.5	16.5	20.7
Queensland	10.1	14.4	17.6	9.4	12.3	15.5
Hannover	10.2	16.4	19.3	6.4	13.5	14.9
IGN	6.3	10.0	11.8	4.0	7.4	9.4

Table 16 rms (m) obtained by different centres using IGN data for configuration B

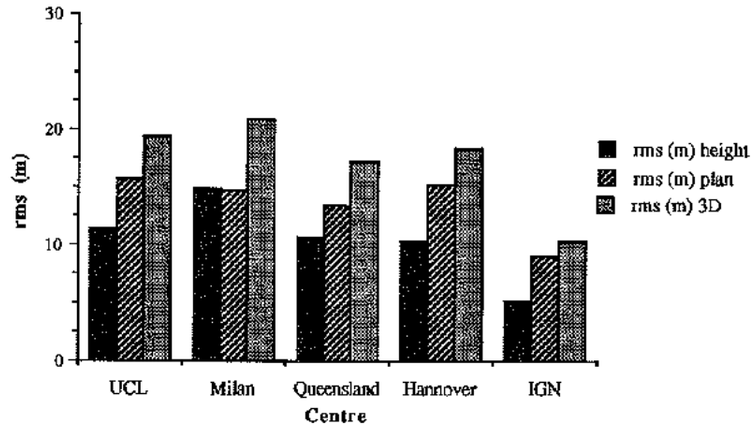

Figure 6. Rms (m) obtained by different centres using IGN data for control configuration A

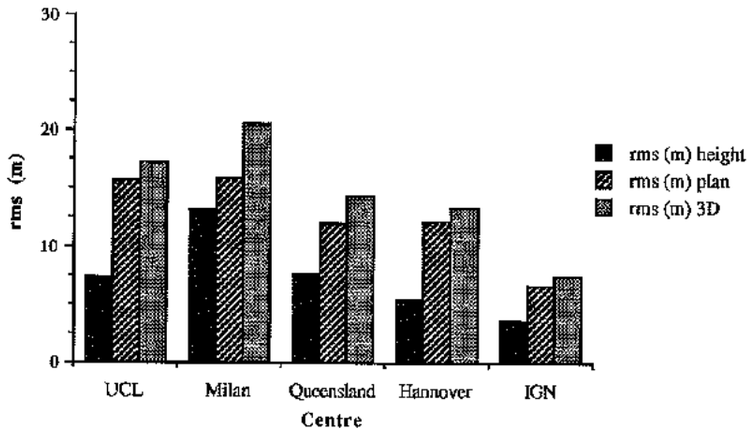

Figure 7. Rms (m) obtained by different centres using their own data for control configuration A

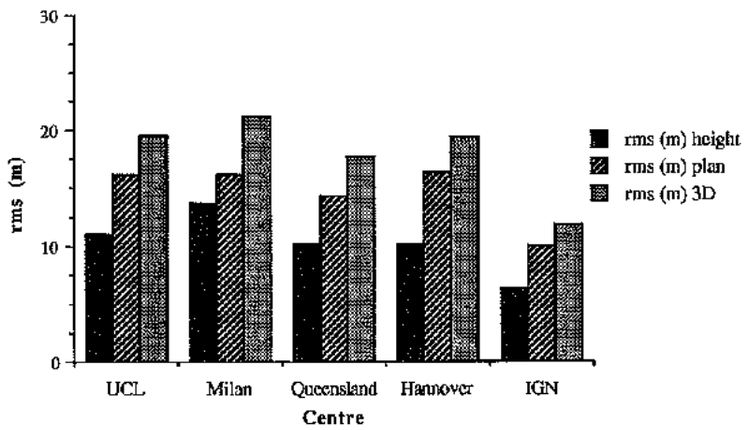

Figure 8. Rms (m) obtained by different centres using IGN data for control configuration B

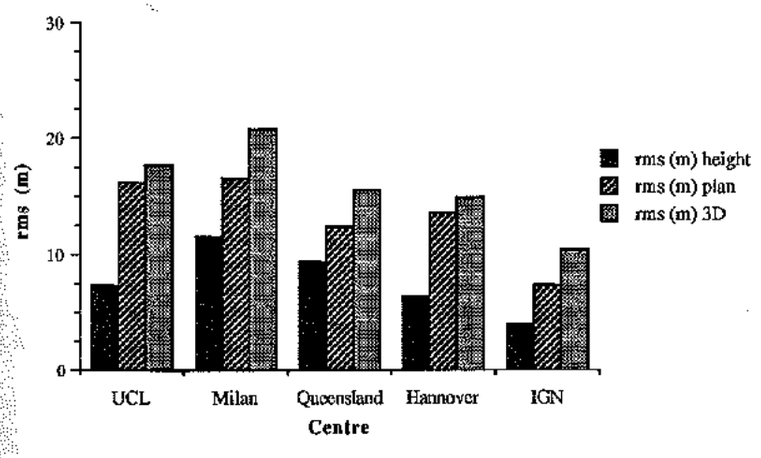

Figure 9. Rms (m) obtained by different centres using their own data for control configuration B

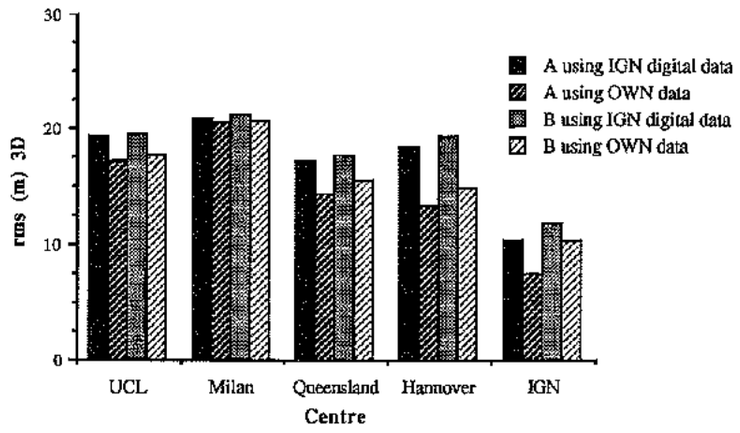

Figure 10. Rms (m) in 3D obtained by different centres using either IGN or OWN data, and configurations A and B

In all cases the centres achieved worse results with the digital data than with hardcopy data observed by themselves. This may be due to the fact that the digital data was observed monoscopically, without the benefit of stereo observation for identification of points. There is also a clear order in the accuracy of the results showing in both sets. This indicates that the accuracy of the digital data is better and that the results are independent of the instrument used for observation as the same differentials apply in both sets of data. In other words there is confirmation that the results reflect the fidelity of the geometric models used.

8. Future work

The test has given useful insight into the orientation of SPOT data and the methods used to determine ground co-ordinates. It has shown that high accuracy, similar to that from single models, can be obtained with strips and blocks of SPOT data. It has further shown that the results are sensitive to distribution and type of ground control and that the use of ephemeris and attitude data can reduce the amount of control and improve the results.

It appears that data observed directly from a digital display, monoscopically, gives less accurate results than that observed from hardcopy on an analytical plotter.

Other work which could be useful would be a more rigorous analysis of the effect of different types of ground control points and in the longer term a test to investigate extension of control laterally to areas remote from those where control existed.

PART 2

PAPERS BY PARTICIPANTS IN THE TEST DESCRIBING THEIR METHODS AND RESULTS.

SUMMARY OF GRENOBLE TRIANGULATION TEST RESULTS

V. Kratky
Canada Centre for Mapping
Ottawa, CANADA

The method used is described in the following paper. We have chosen to process only the data from strip A and tested all features listed in requirements 1 to 4 as formulated in the Test Instructions of March 1989.

We have compiled with the suggested control distributions in variants a) to f), however, we had to substitute for two control points, Nr. 26 and 3036, which are not available in some of the images. The revised distributions are shown in figures 1 and 2. The following notes characterize our efforts:

Variant a)

Sigma 0	10.1 µm				
RMS discrepancies in 19 GCP	6.2	6.0	4.9	6.3 m	(in X, Y, Z, py)
RMS errors in 63 CHK (check p.)	6.6	8.3	4.5	11.9 m	

Variant b)

Sigma 0	8.0 µm			
RMS discrepancies in 10 GCP	3.9	2.7	3.8	5.0 m
RMS errors in 9 INTersections	9.6	25.5	9.4	8.0 m
RMS errors in 63 CHK	7.4	18.1	5.7	12.2 m

Unfortunately, the given control configuration does not support well the ties of all individual image segments and this fact resulted in excessive Y-errors. A modified configuration in variant b1) improved the results drastically.

Variant b1)

Sigma 0	10.2 µm			
RMS discrepancies in 10 GCP	3.5	6.9	4.8	4.1 m
RMS errors in 10 INT	9.1	5.1	4.6	8.9 m
RMS errors in 61 CHK	6.7	8.5	4.9	11.8 m

Variant c)

Sigma 0	5.0 µm			
RMS discrepancies in 6 GCT	0.5	0.1	0.1	7.9 m
RMS errors in 15 INT	8.4	10.4	11.6	7.2 m
RMS errors in 61 CHK	7.3	12.2	13.2	11.6 m

Again, the control configuration was not optimal. Two control points in the middle of the strip are not supporting the tie of two segments. A modified configuration in variant c1) was adopted.

Variant c1)

Sigma 0	7.2 µm			
RMS discrepancies in 6 GCP	2.3	1.4	4.4	1.8 m
RMS errors in 14 INT	7.9	11.5	6.1	9.0 m
RMS errors in 61 CHK	6.5	12.3	5.6	11.6 m

Compared with c) elevations are improved drastically.

Variant d)

Sigma 0	7.5 µm			
RMS discrepancies in 4 GCP	0.0	0.6	0.4	6.1 m
RMS errors in 17 INT	13.5	9.5	19.2	8.5 m
RMS errors in 61 CHK	11.3	11.7	21.7	11.1 m

The control configuration of this variant is not sufficient to support the solution. The errors are systematic. More control points are definitely needed.

Variants e) and f) were not expected to support a numerical solution or yield any reasonable results. When tried, the solutions failed, indicating ill-conditioning and singularity of the solution.

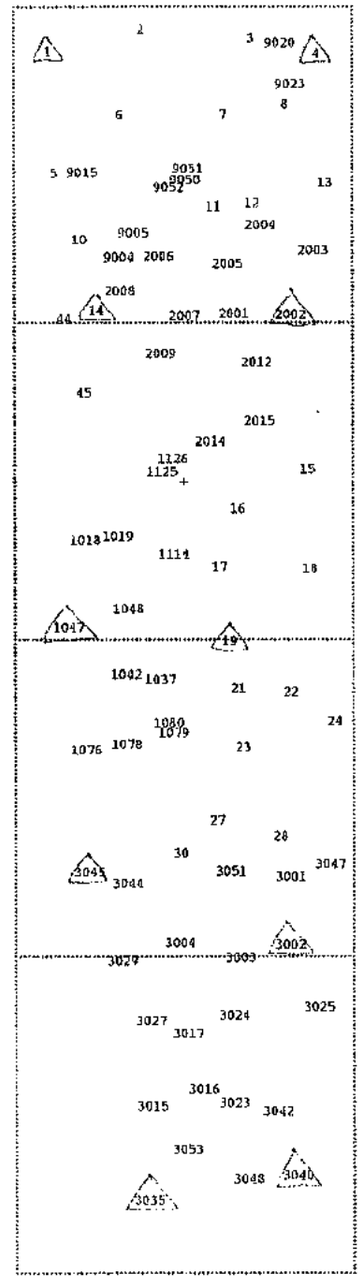

Figure 1. Configuration of GC points variant b1

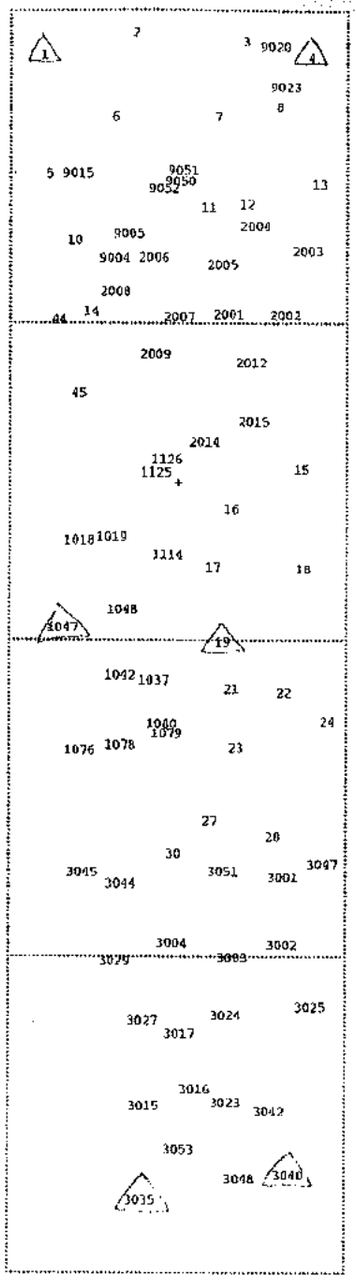

Figure 2. Configuration of GC points variant c1

RIGOROUS PHOTOGRAMMETRIC PROCESSING OF SPOT IMAGES AT CCM CANADA

Dr. V. Kratky
Canada Centre for Mapping (CCM)
615 Booth Street, Ottawa, Ontario
CANADA K1A 0E9

ABSTRACT

A method for rigorous photogrammetric reconstruction of three-dimensional stereomodels from SPOT images has been developed. The solution is universal as far as applications are concerned and can be implemented both in digital processing systems and in analytical photogrammetric instruments. The images are analyzed in their original raw form (SPOT IMAGE level 1a) corrected in radiometry, but containing no geometric corrections typical of the higher levels of image products. The geometric solution combines the principle of photogrammetric bundle formulation, modified in a time-dependent mode, with additional constraints derived from known orbital relations. The inherent accuracy of the geometric reconstruction in a rectangular coordinate system is supported and maintained by a series of rigorous auxiliary transformations between other orbital and cartographic systems involved in the process. The solution concept was successfuly expanded to process longer strips of stereoimagery in a photogrammetric triangulation mode and can be used for an efficient ground control extension. Extensive experiments have demonstrated the viability of the approach and very good accuracy of the solutions.

Invited Paper to the
International Symposium on Topographic Applications
of SPOT Data
Sherbrooke, October 13-14 1988

INTRODUCTION

Basic information on the SPOT satellite mission, its goals and technical parameters is available in numerous publications; here we refer to Chevrel, Weill (1981). To utilize the SPOT potential in the context of cartography and photogrammetry, that is with special emphasis on geometry, considerable research has been carried out especially in France, but also in other countries, as demonstrated, e.g., by Guichard (1983), Toutin (1985), Denis (1987), Salgé et al. (1987), Jaloux (1987), Dowman et al. (1987), Simard (1987), Cooper et al. (1987) and Priebbenow, Clerici (1987). Parallel efforts have also been directed at adaptation of existing on-line analytical photogrammetric instruments and their software to an accurate geometric evaluation of SPOT imagery, as reported by de Masson d'Autume (1980), Egels (1983), Dowman, Gugan (1985) and Koneeny et al. (1987). This paper represents a rigorous approach capable of supporting a universal application even in a fully digital environment. It is an extension of the author's earlier reports (Kratky, 1987, 1988b).

ORBITAL GEOMETRY

SPOT 1 satellite is placed on a close-to-circular elliptical orbit defined by Keplerian motion, with the centre of earth mass in one its foci. Even though the numeric eccentricity of the orbit is very low (E=0.00103919), the corresponding linear eccentricity is appreciable, displacing the focus of the ellipse from its centre by about 7.5 km. Fig. 1 illustrates the relationship between the orbital ellipse and the earth represented by the international reference ellipsoid GRS 80 (Vanicek, Krakiwsky, 1986). The inclination of the orbital plane from the equator i = 98.77° determines the geographic top T of the orbital track on the earth ellipsoid. The nominal orbit is supposed to have its perigee here. Geocentric distance c at this point is a function of ellipsoid semiminor axis b, its numeric eccentricity e and of the angle ε = i - 90° according to

$$c^2 = b^2/(1-e^2\sin^2\varepsilon) \quad . \tag{1}$$

The ground ellipse intersected by the orbital plane has dimensions a and c, where a is the length of semimajor ellipsoid axis. The nominal orbital ellipse has corresponding dimensions A, B and eccentricity E.

Fig. 1b shows the orbital ellipse with its perigee P at the top of the orbit where, after the initial orbit stabilization in 1986, the flying altitude was h_P = 818.269 km, while the altitude for the apogee is h_A = 833.198 km (SPOT Newsletter, 1986). Parameters of the nominal orbital ellipse can then be derived from these values as follows

$$A = c+(h_A+h_P)/2 \quad , \quad E = 0.5(h_A-h_P)/A \quad , \quad B^2 = A^2(1-E^2) \quad . \tag{2}$$

When SPOT traveled angle τ is measured from the top of the orbit, the geocentric radii r and R of the ground and orbital SPOT positions, respectively, are determined from

$$r^2 = c^2/(1 - e^2\sin^2\tau) \quad , \quad R = A(1 - E^2)/(1 + E\cos\tau) \tag{3}$$

and variable flying altitude h = R-r is also a function of angle τ. If the perigee does not coincide with the top of the orbit, a constant angular offset for τ must be considered.

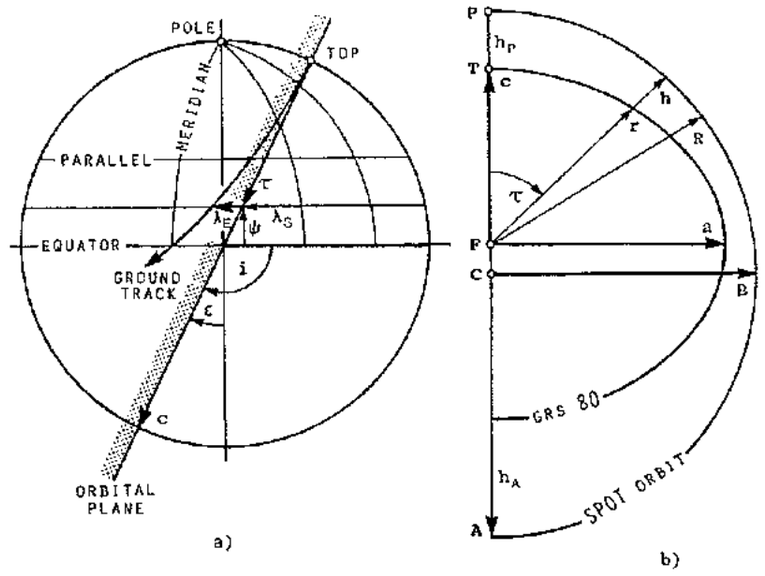

Fig. 1 a,b SPOT Orbital Relations

Time Dependence

Time t is the only independent variable in our orbital relations and one must be able to readily convert τ into t and vice versa. Because of the Keplerian character of the orbit the angular velocity ω_s of the satellite is variable, being highest at the perigee and lowest at the apogee. The radius vector R describes a constant area k in unit time, i.e. the instantaneous value of ω_s is indirectly proportional to R^2 : $\omega_s = d\tau/dt = 2k/R^2$. Consequently, traveled angle τ is not directly proportional to the elapsed time t. With reference to Vanicek (1986), angle τ represents true anomaly in Kepler's terms and can be converted, in succession, into eccentric anomaly N, mean anomaly M and eventualy into time t measured from the perigee by equations

$$\cos N = (E+\cos\tau)/(1+E\cos\tau) \quad , \tag{4}$$

$$M = N - E\sin N \quad , \tag{5}$$

$$t = M/\omega_m \quad , \tag{6}$$

where $\omega_m = dM/dt$ is the mean angular velocity derived from 369 SPOT orbits performed in 26 days. For the opposite task the sequence of the steps is reversed to calculate mean anomaly M from given time t first, $M = \omega_m t$, then computing N from Eq. (5) by iteration and eventually deriving traveled angle τ as

$$\cos\tau = (\cos N-E)/(1-E\cos N) \quad . \tag{7}$$

Area constant k can obviously be expressed from the total orbital area and time of a single orbit as $k = \pi AB/\Delta t_o$. This relation, together with the use of $\omega_m = 2\pi/\Delta t_o$, leads to the expression for instantaneous angular velocity

$$\omega_s = \frac{2k}{R^2} = \frac{AB}{R^2}\omega_m = \frac{B}{A}\frac{(1+E\cos\tau)^2}{(1-E^2)^2}\omega_m \quad . \tag{8}$$

Earth Rotation Effect

While the SPOT satellite travels, the earth revolves and both these angular changes combine in a composite motion which causes the satellite ground track to deviate from the nominal plane of orbit as shown in Fig. 1a. Corresponding geographic longitude increase λ_E changes linearly with time

$$\lambda_E = \omega_E t \quad , \tag{9}$$

where $\omega_E = 2\pi/24/60/60 = 0.072722$ mrad/s is the constant angular velocity of earth rotation. In the context of our analysis the composite motion $\tau(t)$ and $\lambda_E(t)$ can both be assigned to the satellite as if it orbited around a stationary earth. With reference to Fig. 1a and to derivations by Kratky (1973) the effect of traveled angle τ can be expressed by changes of geocentric latitude ψ and geographic longitude λ_S

$$\sin\psi = \cos\varepsilon\cos\tau \quad , \quad \tan\lambda_S = \tan\tau/\sin\varepsilon \quad , \quad \lambda = \lambda_S + \lambda_E \quad . \tag{10}$$

Geographic latitude ϕ is derived from ψ by

$$\tan\phi = a^2\tan\psi/b^2 \quad . \tag{11}$$

The satellite position is defined in terms of polar coordinates for any given time t from Eqs. (6), (5), (7), (10) and (3). Polar coordinates can then be converted into rectangular geocentric coordinates as needed.

COORDINATE SYSTEMS

Several coordinate systems are needed to apply photogrammetric formulations in the context of orbital and geodetic conditions. They are used to provide a rigorous link between the photogrammetric model, orbit and the reference ellipsoid as needed in the implementation of the solution. Transformation algorithms and computer subroutines were developed to perform all needed two-way conversions among the systems.

Photogrammetric Coordinates

IMG (x',y') - Image Coordinates. Input image coordinates are represented either by the pixel/scanline positions in the digital image record or by corresponding positions measured in transparencies reproduced as a raw image with no geometric corrections involved in the process. In either case the position of an image detail is converted into ideal image coordinates (x',y') with their origin set to the centre pixel of the centre scanline, i.e. to the centre of the corresponding transparency. This is done in the process of inner orientation.

PHG (U,V,W) - Photogrammetric Coordinates. All photogrammetric relations are expressed in a geocentric rectangular system of coordinates defined with

respect to the nominal plane of the left orbit as determined by its expected equator crossing, e.g., $\lambda = 93.174°$ for track 305. The U-axis is normal to the orbital plane while W-axis deviates from the top of orbit by angle τ, computed for the centre of the corresponding ground scene, in dependence on the side view angle of the sensor and on the ground elevation.

MDL (X,Y,Z) - Model Coordinates. In order to achieve a good numerical stability of photogrammetric computations, model X,Y,Z coordinates are obtained from PHG coordinates by their scaling to the size of image coordinates, i.e. by equating the flying height with the focal length of the HRV imaging sensor, and by setting their origin close to one of the projection centres. Hence, the IMG and MDL coordinate ranges closely correspond to each other.

Object Coordinates

UTM (E,N,h) - Universal Transverse Mercator Coordinates. Ground control points for topographical mapping in Canada are available in standard UTM coordinates of easting E and northing N in a system of 6° wide zones related to the regional reference ellipsoid (Clarke 1866) which represents the current North American Datum NAD 27. Heights h are related to the local geoid.

GEO (Φ,Λ,H) - Geographic Coordinates. They are represented by geographic latitude Φ and longitude Λ, supplemented by ellipsoidal height H measured in the normal to the local surface. In conversions to rectangular coordinates geocentric latitude ψ is used as an alternative to geographic latitude Φ. Geographic coordinates are related to a chosen reference ellipsoid, which can be defined regionally (NAD 27) or internationally (GRS 80). The relative orientation and offset of both ellipsoids must be known and considered in coordinate conversions.

GCP - Geocentric Coordinates in Polar Orientation. This coordinate system is geocentric with vertical axis going through the pole and another axis defined by the reference longitude of the related geographic system GEO.

Orbital Coordinates

ORB (ρ,δ,r) - Basic Orbital Coordinates. This is a polar coordinate system used mainly for ground points and expressing a geocentric position vector by length r and two orbital angles ρ, δ defined as consecutive rotations along and across the orbital plane, respectively.

CMP (τ,λ_E,R) - Composite Orbital Coordinates. This polar coordinate system is used to describe the composite SPOT position vector by geocentric distance R, SPOT traveled angle τ and longitudinal drift λ_E due to the effect of the earth revolution. These angles are obviously functions of time and represent rotations about axes which are not perpendicular to each other. The latter angle may also include an additional longitudinal displacement of the orbit with respect to its nominal position.

PHOTOGRAMMETRIC SOLUTION OF A SINGLE STEREOMODEL

In a rigorous system of geometric processing SPOT image information should be analyzed in its original geometric form which is not affected and biased by any spatial changes caused by resampling, modified display or photo-reproduction of images. The imagery on input should be represented by raw

image data containing no corrections except for those improving their radiometric rendition (SPOT IMAGE level 1a). This condition applies to both major classes of procedures operating either directly on digital images, or on their photoreproduced transparencies in on-line photogrammetric systems. The analytical reconstruction of geometric relations should always be carried out in three-dimensional Cartesian space with all related tasks of individual image rectification or resampling left to follow in subsequent operations. Only then can they be properly controlled by the previously established rigorous mathematical model of geometric relations.

The three-dimensional character of the photogrammetric formulation allows to consider, in a rigorous way, all physical aspects of satellite orbiting and of the earth imaging, together with geometric conditions of the time-dependent intersection of corresponding imaging rays in the model space. The orbital parameters, either predicted or extracted from SPOT ephemeris data, are not applied in an absolute way. Potential orbital perturbations due to the earth's gravitational field and accumulated irregularities in the control of the orbit are taken into account by allowing the SPOT orbital segment, corresponding to the viewed ground scene, to be additionally shifted with respect to its expected nominal position, in order to find the best fit of the image projecting rays with given ground control points and to preserve a good intersection of all additional corresponding projecting rays. Thus, the resulting reference SPOT position τ_o for the ground scene centre can move along the orbit and the orbit can also be offset sideways in geographic longitude λ. Simultaneously, a proper mathematical model for the imaging sensor's attitude variations is defined or modified in the process. It is worth mentioning that in this solution concept, there is no absolute need for using any additional information, such as from SPOT IMAGE supplemental data files. If available, however, the information can be used either directly to approximate or preset some of the solution unknowns, or indirectly for an assessment of the need for a more refined attitude model.

The annotation of raw images provides geographic coordinates of the ground scene centre, the orbit number and the view angle of the HRV sensor. All these values may not be fully consistent since the given view angle does not reflect the local attitude of the sensor. Consequently, only the remaining above values are used to derive reference angle τ_o, that is the orbital position from which the scene centre is seen from the given track, as shown by Kratky (1988b).

Inner Orientation

In the proces of inner orientation coordinates x' are adjusted to the physical length of the sensor's linear CCD array (6000 x 13 μm = 78 mm). Coordinates y' are assuming the same scale, however, during photogrammetric computations they are merely used as a measure of time which is the primary independent parameter in our solution. Their conversion into time t is possible by comparing the image y'-range with the time interval needed to make the 6000 consecutive scans in the scene (6000 x 1.504 ms = 9.024 s). The scale of the transparency is not important. Inner orientation will fit the measured corners of the raw image with an ideal square pattern of fictitious fiducial marks, with coordinate origin in their centre and a separation of 78 mm in both directions. Affine or bilinear transformation converts measurements into ideal IMG coordinates (x',y'). In digital systems, pixel and line numbers are converted into IMG coordinates directly, without any transformation.

Time Conversions

The conversion of y' into a time interval Δt is implemented with the use of a known constant rate $c_t = dt/dy' = 9.024/78 = 0.11569$ s/mm which yields

$$\Delta t(y') = - c_t y' \quad . \tag{12}$$

Traveled angle τ can be derived directly from y' with $\tau = \tau_o - c_\tau y'$ where

$$c_\tau = d\tau/dy' = (d\tau/dt)(dt/dy') = \omega_s c_t \quad , \tag{13}$$

or rigorously, if above formulated conversions $\tau_t = F_\tau(t)$ and $t_\tau = F_t(\tau)$ in Eqs. (4) to (7) are applied, by

$$\tau = F_\tau(F_t(\tau_o)+\Delta t(y')) \quad . \tag{14}$$

Analytical Considerations

The principle of an extended bundle formulation is applied to available ground control points and additional intersection points. The fact that the bundles of reconstructed image rays are restricted to a plane, and the field of sensor's view is very narrow, results in a high correlation between projection centre displacements and sensor's tilts defined in the same direction. These pairs of unknowns cannot be separated in a standard bundle solution and the inherent singularity of the solution must be compensated by inclusion of additional constraints derived from known orbital relations. The constraining values can be either estimated from expected nominal orbits or obtained from supplemental data file available in digital image tapes. There are numerous possibilities of including this type of information into a constrained photogrammetric solution and several variants were tested before the present approach was adopted.

The total number of unknown parameters of the solution is 28 and they are defined in the following way. 12 standard orientation elements are represented by the reference positions $(X,Y,Z)_o$ of SPOT projection centres and by the reference attitude elements $(\varkappa,\phi,\omega)_o$ of sensors, all corresponding to the centre of images (x'=y'=0). Additional 12 unknowns are linear and quadratic rates of change for attitude elements as modeled by polynomials dependent on y', that is on time. To compensate for the lack of information on the photogrammetric calibration of HRV sensors, four additional parameters are considered. Firstly, an auxiliary change of image scale in the direction of scanlines is allowed by defining corrections df to the nominal focal length f of both individual sensors, and finally, coefficients q of a quadratic distortion in x'-direction due to the residual misalignment of HRV sensors are introduced in two correction terms. The attitude model can be simplified by disregarding the quadratic terms, when judged appropriate. In this instance, the number of unknowns is reduced by six, down to the total of 22.

Weighted constraints are formulated in the CMP coordinate system to keep orbital position λ, τ of the left sensor, relative position $\Delta\lambda, \Delta\tau$ of the stereo related right sensor and their geocentric distances R - all for the image centres - within statistical limits specified at the outset of the solution. This adds six constraining conditions to the solution.

Twelve absolute constraints are enforced in order to keep projection centres moving strictly along appropriate elliptical orbital segments . The segments

must rigorously correspond to the reference position $(X,Y,Z)_o$, which is gradually refined in the iterative process of the solution. Currently known coordinates of the projection centre are used to define a coinciding auxiliary orbit and SPOT orbital position, both displaced by $d\lambda$ and $d\tau$ with respect to the initial reference values λ_o, τ_o in the nominal orbit. Then, we calculate the needed linear and quadratic rates of change in X,Y,Z which are eventually used as given, absolutely accurate values.

Every ground control point supported by all three coordinates contributes to the solution by four collinearity equations, while a planimetric, elevation or intersection point gives rise to three, two or a single equation, respectively. As we also have six additional constraining conditions, five full control points and two intersection points represent the minimum support needed to perform computations with no redundancy in input data. When linear model for HRV attitude changes is adopted, four ground control points would suffice. However, the lowest practical number of control points used should be between five and nine.

Analytical Formulation

The formulation of a standard bundle solution must be expanded by the effect of the time-dependent parameters. Resulting modifications of a standard approach are briefly reviewed here. In collinearity equations

$$F_x \equiv \Delta Xz - \Delta Zx = 0 \quad , \quad F_y \equiv \Delta Yz - \Delta Zy = 0 \tag{15}$$

the vector $(\Delta X\ \Delta Y\ \Delta Z)^T = (X-X_c\ \ Y-Y_c\ \ Z-Z_c)^T$ represents model coordinates reduced with respect to the projection centre, which is expressed in terms of quadratic polynomials

$$X_c = X_o+y'\dot{X}+y'^2\ddot{X} \quad , \quad Y_c = Y_o+y'\dot{Y}+y'^2\ddot{Y} \quad , \quad Z_c = Z_o+y'\dot{Z}+y'^2\ddot{Z} \tag{16}$$

with rates $\dot{X}$, $\ddot{X}$, $\dot{Y}$, $\ddot{Y}$, $\dot{Z}$, $\ddot{Z}$ computed for the currently known SPOT position from rigorous orbital equations. The transformed image coordinates are

$$(x\ y\ z)^T = T_t T_v\ (x'\ 0\ -f)^T \quad , \tag{17}$$

where T_v is a matrix corresponding to the side view angle of the sensor, while the time-dependent rotation matrix is defined as $T_t = F(\varkappa,\phi,\omega) = F_t(y')$ by relations

$$\varkappa = \varkappa_o+y'\dot{\varkappa}+y'^2\ddot{\varkappa} \quad , \quad \phi = \phi_o+y'\dot{\phi}+y'^2\ddot{\phi} \quad , \quad \omega = \omega_o+y'\dot{\omega}+y'^2\ddot{\omega} \quad . \tag{18}$$

In linearized standard condition equations $Av + Bg + u = 0$, with design matrices A, B and misclosure vector u, term Bg is expanded as

$$Bg = [B_c\ \ B_a\ \ y'B_a\ \ y'^2B_a\ \ B_s\ \ B_x](g_c\ \ g_a\ \ \dot{g}_a\ \ \ddot{g}_a\ \ g_s\ \ g_x)^T \quad , \tag{19}$$

which shows that the same design submatrix B_a, corresponding to attitude elements g_a is applied also in the terms for their linear and quadratic rates when premultiplied by y' and y'^2, respectively. Submatrices B_c, B_s and B_x correspond to projection centre coordinates g_c, sensor calibration parameters g_s and model coordinates g_x, respectively. As in conventional bundle solutions, vector g_x is eliminated from the equations by analytical means for each pair of intersecting rays with no control support, so leaving the number of unknowns in the solution invariable.

Submatrices corresponding to a single imaging ray have the following form

$$A = \begin{bmatrix} -\Delta Z & 0 \\ 0 & -\dot{Y}z \end{bmatrix} \quad , \quad B_t = \begin{bmatrix} -z & 0 & x \\ 0 & -z & y \end{bmatrix} = -B_x \quad ,$$

$$v = (\ v_x,\ v_y,\ )^T \quad , \quad g_c = (\ X_c\ \ Y_c\ \ Z_c\ )^T \quad , \quad g_x = (\ X\ Y\ Z\ )^T \tag{20}$$

$$B_a = \begin{bmatrix} -\Delta Zy & -(\Delta Xx+\Delta Zz) & -\Delta Xy \\ \Delta Zx & -\Delta Yx & -(\Delta Yy+\Delta Zz) \end{bmatrix} \quad , \quad B_s = \begin{bmatrix} \Delta Zt_{13}-\Delta Xt_{33} & x'^2(\Delta Xt_{31}-\Delta Zt_{11}) \\ \Delta Zt_{23}-\Delta Yt_{33} & x'^2(\Delta Yt_{31}-\Delta Zt_{21}) \end{bmatrix}$$

$$g_a = (\ \varkappa \qquad \phi \qquad \omega\ )^T \ , \ g_s = (\ df \qquad q\ )^T$$

where t_{ij} are elements of matrix product $T = T_t T_v$ defining the instantaneous orientation of the imaging sensor for current point position in y'.

CARTOGRAPHIC ASPECTS

The strength of a stereophotogrammetric approach in geometric satellite image processing results from the fact that spatial relations are formed and solved in a three-dimensional rectangular system, so avoiding or circumventing some of the complexities of curvilinear reference systems. However, ground control information has to be supplied from an external cartographic system and, vice versa, the reconstructed photogrammetric model has to be interpreted in terms of this external system.

A rigorous process of mutual cartographic-photogrammetric transformations was developed to suit the geodetic conditions in Canada represented by the North American Datum NAD 27. For scenes located elsewhere equivalent local conditions should apply. The following transformations are needed:

h - H : conversion of geoidal heights h to NAD 27 ellipsoidal heights H;
UTM - GEO: conversion of UTM coordinates to geographic coordinates φ, Λ in NAD 27;
GEO - GCP: conversion of geographic to geocentric coordinates in NAD 27;
GCP - GCP: offset of geocentric NAD 27 coordinates to international system GRS 80;
GCP - GEO: conversion of geocentric to geographic coordinates in GRS 80;
GEO - ORB: conversion to polar orbital coordinates ρ,σ,r in the chosen nominal orbital plane;
ORB - PHG: conversion to geocentric coordinates U,V,W oriented with respect to expected SPOT position τ_o;
PHG - MDL: translation and scaling into photogrammetric model coordinates X,Y,Z.

A reversed sequence of the above steps will transform photogrammetric MDL coordinates back to UTM system and to geoidal heights h in the NAD 27 system.

ON-LINE IMPLEMENTATION

Two major aspects must be considered when applying the SPOT solution in an on-line photogrammetric environment: 1. the control of image positioning must cope with dynamic changes in the position and attitude of the sensor and still retain its needed real-time performance; 2. in the continuous compilation mode, the elevations entered on input must be defined with respect to the curved ellipsoidal or geoidal surface. Similar considerations are also important for the digital environment of image analysis systems where the

real-time constraints of image matching, resampling and transformations are even more critical.

A detailed analysis of these and other on-line aspects of processing SPOT images and a description of the way in which the problems are resolved in our solution, is presented in Kratky (1988a). Here, only the main conclusions are briefly mentioned. The positioning control is feasible and efficient even with straight forward IMG-MDL and MDL-IMG transformations of coordinates when the algorithms are streamlined to shorten the iteration cycle inherent in the latter conversion and modified to speed up construction of orthogonal matrices. With the use of single precision arithmetics the duration of the positioning real-time cycle is 2 to 3 ms with the support of DEC VAX 750 computer. A significant improvement is achieved through modeling the effect of a sequence of rigorous transformations by a one-step, direct polynomial mapping of input-to-output values. A concept of a generalized parametric control of real-time operations for analytical instruments was developed and tested. With its use the real-time positioning cycle can be implemented with 24 multiplications only, as compared with about 124 needed in the above transformations, and the performance of an analytical plotter is boosted accordingly. In this arrangement, the NRC Anaplot I supported by DEC PDP 11/45 minicomputer achieves a frequency of 100 to 130 Hz. The approach is extended to control photogrammetric on-line operations with respect to curved geodetic surfaces, as needed for measurements of ellipsoidal or geoidal heights. For example, the control of elevations in the plotter input is handled through a 10-term polynomial function of 3rd degree which relates geoidal heights h with model heights Z in dependence on the current point position x',y' in the left image

$$Z = F_Z(x',y',h) = (1\ h\ x'\ y'\ hx'\ x'y'\ x'^2\ y'^2\ hx'^2\ x'^3)p_{10} \qquad (21)$$

so providing a fast and accurate transformation with maximum errors dZ well below 1 m for any possible range of elevations.

STRIP TRIANGULATION

SPOT imagery is acquired in a continuous strip mode and any scene segment represents an artificial window which is extracted from a digital image of an essentially indefinite length and defined in a uniform coordinate system. The simplest type of photogrammetric strip triangulation is a stereomodel extension over several standard scenes. Obviously, the orbits should be chosen to achieve the best base-to-height ratio (b/h) by using oblique images with extreme view angles in order to obtain a 100% image overlap. Because of the convergence of orbits, the overlap and the effective ground coverage is gradually changing; consequently, there are practical limits to the length of the strip. Finally, the geometric definition of the derived model can be further strengthened by adding a third vertical image in order to secure a triple intersection of imaging rays.

A block extension of individual strip formations is practical only if the imaging is arranged in a twin mode of both HRV sensors operating simultaneously. The ground coverage is then almost doubled, but strips will overlap only by 50 to 60%. Individual strips can be assembled in blocks in a cross-track bridging mode using the triple overlaps between strips.

The approach developed at CCM consists of expanding the above described stereomodel solution over several scene segments. This can be done directly,

as long as the digital image data is given in a fully continuous stream of scanlines in a uniform time frame. The only limiting problem here is to ensure that the analytical model of HRV attitude changes is general enough to represent the real variations during the flight. It can easily be established or checked from supplemental data file over what distance the strip can be geometrically controlled using existing quadratic formulation, or when a more general, cubic form is needed. The relation between time and y', as defined by Eq. (12), is valid for any length of the strip. In a digital environment, the application of our rigorous stereophotogrammetric algorithm is straight forward. However, in the analytical stereoplotter environment one deals with individual photo transparencies which are generated with a slight overlap. Their mutual relationship then has to be established by performing their inner orientations in a uniform system of corner pixel coordinates reflecting accurately their time acquisition. In general, the supplemental data file should identify the times of recording for the centre scanlines in each segment and the differences could determine the needed offsets in coordinates y' between individual transparencies.

However, this information may not always be available, or the times given may not be accurate. Practical experience with supplemental data shows that these times are truncated or rounded off to full seconds. In order to handle these cases our photogrammetric solution is extended to consider the y'-offsets as additional unknown parameters so expanding Eq. (19) by the effect of submatrix

$$B_{y'} = \begin{bmatrix} -\dot{X}z + \dot{Z}x \\ -\dot{Y}z + \dot{Z}y \end{bmatrix} \approx \begin{bmatrix} 0 \\ -\dot{Y}z \end{bmatrix} \quad , \quad \text{because } \dot{Y} >> \dot{X} >> \dot{Z} \quad , \qquad (22)$$

with corresponding vector $g_{y'} = dy'$ defined for 2(n-1) image segments, where n is the number of scenes in the strip. The solution then becomes fully independent of auxiliary information in supplemental data files.

PRACTICAL EVALUATION

Single Stereomodel

The solution for stereoimages usually requires 3 to 6 iterations and yields all parameters needed for any further geometric control and processing, as well as their stochastic evaluation. A practical solution is obtained with a minimum of 5 to 9 ground control points, depending on the degree of the polynomial SPOT attitude model. The inner accuracy of the algorithm as tested by fictitious data ensures a submicrometre least squares fit of image data, and RMS ground errors are within the range of 0.2 to 0.3 m for both planimetry and heights, when base-to-height ratio is around 1 .

The results reported here are from three different test areas: Ottawa, Sherbrooke (Canada) and Grenoble (France). The Ottawa test is based on two images taken four orbits apart (tracks 305 and 309) in August 1987, with view angles +27.89° and +7.31° and with a very poor base-to-height ratio of 0.4 . The results which are summarized in Table 1, are useful to demonstrate the practical effect of using certain unknown parameters in the solution. The first two tests, computed without using calibration correction q, demonstrate that there is no practical need for choosing quadratic form for the attitude model. When linear model of attitude variations was applied, the performance of the quadratic formulation was preserved. The same conclusion was confirmed from processing stereomodels in other test areas; within the 60 km image segment the non-linear attitude variations are usually negligible and the need

for a quadratic attitude model does not seem to be warranted. The computation of the third example included correction term with q (for sensor misalignment) and demonstrates a drastic improvement in elevations, even though the number of control points is reduced. The solution with 22 parameters appears to be optimal and is highly recommended as a standard approach.

Table 1

Test Ottawa: Aug. 87, view angles: +27.9°, +7.3°, b/h = 0.4

Attitude model	Number of UP	GCP	CHP	σ_o (μm)	RMS Errors in CHP E	N	h (m)
Q	26	6	65	12.0	4.8	6.0	12.9
L	20	6	65	9.0	4.9	6.3	12.2
L	22	5	62	9.7	4.6	5.3	8.4

Legend: σ_o - standard unit error; Q - quadratic; L - linear; UP - unknown parameters; GCP - ground control point; CHP - check point; E - UTM Easting; N - UTM Northing; h - height

Sherbrooke test results are comparable in planimetric accuracy to those from the Ottawa tests and, because of a better b/h ratio, they are improved in elevations. Considering the high number of available check points the statistical value of the evaluation is excellent. In view of this quality, the data were used to experiment with the number of control points needed to achieve a reliable solution and to establish how the selection and number of control points further affects the accuracy of the reconstructed geometric model. From the data listed in Table 2, it appears that a good solution can be expected even with five control points and that the results do not really show a noticeable improvement with additional points included. Using more than nine control points does not seem to be economically justified.

Table 2

Test Sherbrooke
Nov. 86 - Apr. 87, view angles: +27.0°, -3.0°, b/h = 0.61

Attitude model	Number of UP	GCP	CHP	σ_o (μm)	RMS Errors in CHP E	N	h (m)
L	22	16	237	6.8	4.9	5.1	7.3
L	22	9	244	6.1	5.2	5.8	7.9
L	22	7	246	6.8	5.3	6.1	7.9
L	22	5	248	8.8	5.6	5.3	7.5

Figures 2 and 3 show the values and distribution of height errors (in m) and planimetric error vectors, respectively, for 73 points selected from the last example of Table 2. The density of check points is too high to include all of them in the plot. Control points are marked by triangles and the point positions are plotted as they appear in the left SPOT image.

In the Grenoble test, three individual scenes available for a triangulation experiment were processed independently in order to check the quality of identification for ground control points, whose definition in images was in many cases very poor and whose description by hand-drawn sketches not always adequate. Single models were formed from extreme view angles yielding double convergent configuration with an excellent b/h ratio of 0.94, using all points considered to be reliable in definition. The RMS errors listed in Table 3

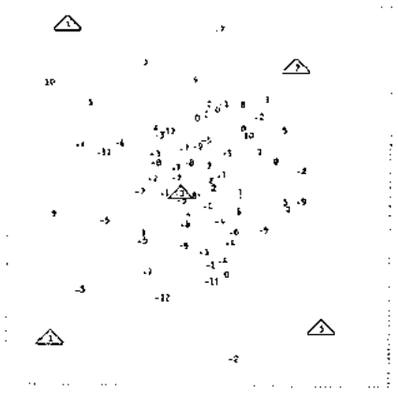

Fig. 2 Height Residuals

Fig. 3 Planimetric Residuals

correspond to discrepancies in control points after adjustment, except for the first scene, which was also restored with five control points only; the RMS values then also reflect the fit in check points as in the preceding tables. Coordinates X,Y are defined in Lambert III projection.

Grenoble models
July - Aug. 86, view angles: +23.4°, -25.5°, b/h = 0.94

Table 3

Scene	Att. model	Number of UP	GCP	CHP	σ_o (μm)	RMS Errors (m) in X	Y	h
260	L	22	17	0	7.6	5.5	4.4	2.3 GCP
260	L	22	5	12	3.7	8.1	5.8	3.3 CHK
261	L	22	12	0	8.6	5.8	5.1	3.5 GCP
262	L	22	10	0	7.1	2.0	5.7	3.5 GCP

Strip Triangulation

The only available material to test strip triangulation was from the Grenoble area. Four consecutive images from three orbits were taken in 1986 in order to conduct a series of international triangulation experiments. Transparencies were generated at level 1a and supplied, together with ground control data, by the Institute Geographique National in Paris. However, the first images in each orbit were not available at the time of our testing. The tests were conducted with three images in each of the two extreme orbits, using the above described formulation with unknown relative image offsets. The results of the triangulation are listed in Table 4. The first line shows the ground control point fit when all identifiable points were included in the solution, while the rest of the table represents a triangulation performed with 11 control points and yielding comparison in 28 independent check points. In this instance, RMS discrepancies for both groups are listed. Figures 4 and 5 illustrate the distribution of height errors and planimetric error vectors for check points, while the positions of control points are marked by triangles.

Grenoble strip (50/260-261-262) Table 4
July - Aug. 86, view angles: +23.4°, -25.5°, b/h = 0.94

Attitude model	Number of UP	GCP	CHP	σ_o (µm)	RMS Errors (m) in X	Y	h	
Q	32	39	0	7.9	4.9	6.1	4.1	GCP
Q	32	11	28	10.9	4.3	6.5	4.1	GCP
					5.9	6.5	5.1	CHK

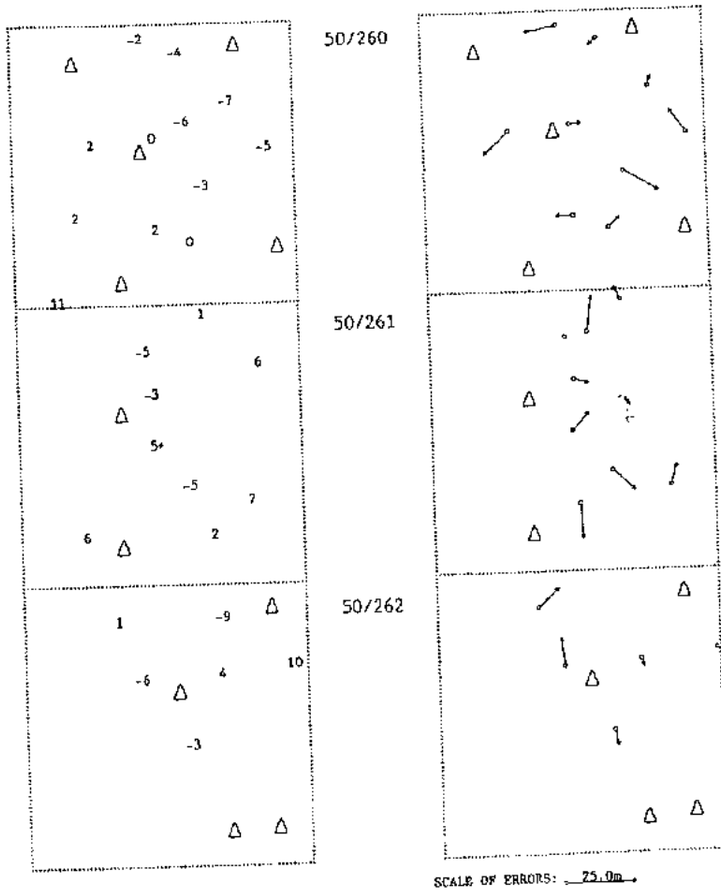

Fig. 4 Height Residuals

Fig. 5 Planimetric Residuals

CONCLUSIONS

The method described represents a rigorous photogrammetric reconstruction of a ground scene from SPOT stereoimages. The geometric model fully respects the physical reality of imaging, satellite orbiting and of the earth shape, instead of indirectly modeling their combined effect by empirical image fitting and warping, as frequently adopted in non-photogrammetric approaches. The solution is universal and can be implemented in digital processing systems, as well as in analytical photogrammetric instruments. No auxiliary information from ephemeris and telemetry sources is needed, but may be utilized when available. The formulations can accommodate single stereoscenes, as well as their extension in a triangulation mode. Resulting geometric parameters can be used to define simple polynomial mapping functions for accurate control of auxiliary, on-line or real-time functions, such as rigorous positioning, display, resampling and matching of images. The accuracy achieved is judged to be sufficient to support topographical mapping at 1 : 50,000 and smaller scales. For discrete points, it seems to be justified to expect RMS errors of 5 to 6 m in planimetry and, depending on the base-to-height ratio, RMS errors of 4 to 8 m in elevations.

REFERENCES

Chevrel, M. and G. Weill, 1981. The SPOT Satellite Remote Sensing Mission. Photogrammetric Engineering and Remote Sensing, 47(8): 1163-1171.

Cooper, P.R., D.E. Friedmann and S.A. Wood, 1987. The Automatic Generation of Digital Terrain Models from Satellite Images by Stereo. Acta Astronautica 15(3):171-180.

Denis, P., 1987. Applications métriques de la stéréoscopie latérale de SPOT. SPOT 1 - Utilisation des images, bilan, résultats, CNES, Paris, pp. 1267-1272.

Dowman, I.J. and D.J. Gugan, 1985. Application Potential of SPOT Imagery for Topographical Mapping. Advanced Space Research, 5(5):73-79.

Dowman, I.J., D.J. Gugan, J-P. Muller and G. Peacegood, 1987. The Use of SPOT Data for Mapping and DEM Production. SPOT 1 - Utilisation des images, bilan, résultats, CNES, Paris, pp. 1213-1220.

Egels, Y., 1983. Amelioration des logiciels TRASTER: restitution d'images a géométrie non conique. Bull. Inf. IGN, 1983(2):19-22.

Guichard, H., 1983. Étude théorique de la précision dans l'exploitation cartographique d'un satellite a défilement. Application a SPOT. Bull. SFPT, No. 90:15-26.

Jaloux, A., 1987. Contribution des images SPOT à la cartographie topographique. SPOT 1 - Utilisation des images, bilan, résultats, CNES, Paris, pp. 1195-1204.

Konecny, G., P. Lohmann, H. Engel and E. Kruck, 1987. Evaluation of SPOT Imagery on Analytical Photogrammetric Instruments. Photogrammetric Engineering and Remote Sensing, 53(9):1223-1230.

Kratky, V., 1973. Cartographic Accuracy of ERTS. Photogrammetric Engineering, 40(2):203-212.

Kratky, V., 1987. Rigorous Stereophotogrammetric Treatment of SPOT Images. SPOT 1 - Utilisation des images, bilan, résultats, CNES, Paris, pp.1281-1288.

Kratky, V., 1988a. On-Line Aspects of Stereophotogrammetric Processing of SPOT Images. International Archives of Photogrammetry and Remote Sensing, 27(B2):238-247, ISPRS, Kyoto.

Kratky, V., 1988b. Universal Photogrammetric Approach to Geometric Processing of SPOT Images. International Archives of Photogrammetry and Remote Sensing. 27(B4):180-189, ISPRS, Kyoto.
de Masson d'Autume, M.G., 1980. Le traitement géométrique des images de télédétection. Annales des Mines, 1980(2):53-62.
Priebbenow, R. and E. Clerici, 1987. Cartographic Applications of SPOT Imagery. SPOT 1 - Utilisation des images, bilan, résultats, CNES, Paris. pp. 1189-1194.
Salgé, F., M.-J. Roos-Josserand and P. Campagne, 1987. SPOT, un outil de saisie et de mise à jour pour la Base de données Cartographiques de l'IGN. SPOT 1 - Utilisation des images, bilan, résultats, CNES, Paris, pp. 1421-1428.
Simard, R. et al., 1987. Digital Terrain Modelling with SPOT Data and Geological Applications. SPOT 1 - Utilisation des images, bilan, résultats, CNES, Paris, pp. 1205-1210.
SPOT Newsletter, 1986(8), CNES.
Toutin, T., 1985. Analyse mathématique des possibilités cartographiques du système SPOT. Thèse du doctorat, Ecole Nationale des Sciences Géographique. Paris.
Vanicek, P. and E.J. Krakiwsky, 1986. Geodesy, The Concepts. North-Holland, Amsterdam, p. 697.

PROCESSING OF SPOT IMAGE BLOCKS WITH PROGRAM BINGO OEEPE TEST 1989

G. Picht, E. Kruck *), M. Guretzki
Institute for Photogrammetry and Engineering Surveys
University of Hannover
D-3000 Hannover 1, FRG
*) Carl Zeiss, D-7082 Oberkochen

0. Summary

A block of 16 SPOT scenes is processed with the BINGO program system. For different given control point distributions the orientation of the scenes and point coordinates are computed. The results are controlled by using independent check points.

1. Testdata

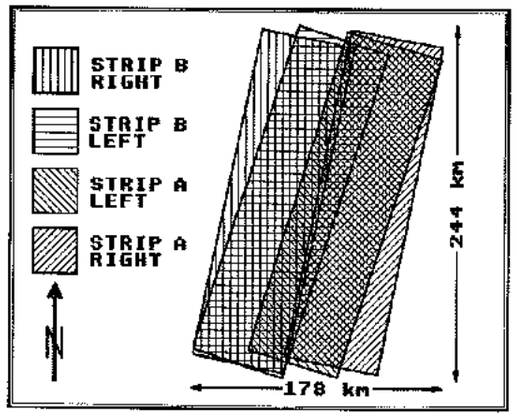

The testarea is covered by SPOT scenes of 4 satellite passes. For each pass the image data are diveded into 4 scenes. According to the OEEPE test rules this 16 images are forming 2 strips of 4 models each, fig. 1. The header data for the scenes are given. Control- and checkpoints are marked in paperprints and the test participants are also supplied with scetches of the point location. Because of the rough topography in the testarea a geoidmap is necessary part of the test.

Fig. 1: Testarea

The points have a very different nature, a part of them is very well defined, others are quite poor or invisible in some images. The coordinates of the control points are derived from several sources, so they do not have a homogeneous quality.

1.1 Preprocessing of control points

The control points are given in Lambert projection on the base of the Clark 1880 ellipsoid (french NTF system). Using the geoid map, the heights are corrected to heights above the ellipsoid. Then all coordinates are transformed in a local cartesian coordinate system, which has its origin close to the center of the testarea.

1.2 Measurement of image coordinates

The measurement of the image coordinates was done at a Planicomp C100 using the program system B159 /Jacobsen 1987/. After digitizing the points in the paperprints

a computer supported stereoscopically measurement was done at an analytical plotter. A precorrection of systematic errors caused by the film writer and the processing, which can exceed one pixel /Jacobsen, Picht 1988/, could not be done, because there was no overlay of digital introduced reseau marks in the images.

The two model strips of this test are overlapping, therefore also points of the neighbouring strip are measured in the overlapping area.

2 Bundle block adjustment with BINGO-SPOT

2.1 Program system

BINGO is an operational program system for bundle block adjustment of terrestrial and aerial images including geodetical observations, e.g. distances. Features like simultaneous camera calibration and data snooping are included /Kruck 1987, Krauss 1988/. The programs are implemented on several types of computers, e.g. VAX, PC and HP-1000. Optional the capability of processing of SPOT images is available. For the ZEISS Planicomp/Orthocomp families a full interface is existing to set up SPOT models for the measurement of e.g. DEM´s and generating orthophotos /Picht 1987, Engel 1987/. The images can be either standard scenes of Level 1a, 1p, 1ap or parts of them.

2.2 Mathematical model of BINGO-SPOT

2.2.1 Coordinate systems

The ground coordinate system for the bundle block adjustment is a local cartesian coordinate system. Transformations from/to the reference coordinate system of the user are done precisly by the pre- and postprocessing programs. Geoid undulations can be used for corrections, if they are available.

2.2.2 Sensor orientation

From the header data the 8-9 trace points are used to calculate polynoms of the sensor movement in the local coordinate system. These polynoms are a function of time. From the PSIX and PSIY angles of the sensors attitude also polynoms for the orientation angles are computed. These header data are given in the WGS-80 system, which is in general different to the geodetic reference system of ground coordinates.

2.2.3 Formulation of unknowns

The orientation of the scene center line is treated as unknown, i.e. the 6 coefficients of 0^{th} degree of the polynoms. The polynom coefficients of higher degree are introduced as known values. This strategy allows to fit the translations, which are necessary for the change of the ellipsiod and for absolute displacements in the trace points, and make use of the higher relative accuracy of the trace information. This formulation of unknowns is an update of the BINGO-SPOT software, presented the first time with this paper.

Smaller effects, like differential rotations between the ellipsoids or high frequent changes of the sensors attitude data may be compensated by the use of additional parameters. The results presented in 3.3 are obtained without additional parameters.

The sensor has a small angular field of view. For this reason the orientation angles φ and ω are introduced into the adjustment with a high weight, because they are strongly correlated with X_0 and Y_0. The values for the 6 orientation parameters are used as ´observed unknowns´.

2.2.4 Ground control

Control points are used to fix the datum parameters and to stabilize the orientation of images in the adjustment procedure. In BINGO they are supplied with standard deviations, so different qualities of control points can be regarded. Control points are used even if they are located only in one image. Errors in control point coordinates can be detected.

The BINGO-SPOT solution may be used with only few or without control points. The datum parameters are then fixed by the trace information. As mentioned above, the results are in the case of no ground control strongly influenced by the incertainty of the tracepoints and the neglected change of ellipsoids. For this reason it is recommended to use at least 4-6 control points of good quality.

2.2.5 Strip connections

If more then one scene of a satellite pass is available, there are several possibilities to use the information, that these scenes are from the same pass. In BINGO-SPOT observation equations are formulated, which connect the unknown orientation parameters of scenes to the pass, using the orientation polynoms. Following this way, it is possible to compute additional parameters separatly for each scene. The compensation of relative high frequent image distortions, caused e.g. by the changing of sensors attitude data, would be more complicate, if all single scenes are combined to a new long one.

3 Results of OEEPE test

In the first phase of the test all calculations are done with image coordinates measured seperatly by each participant (3.1 - 3.3). In a second phase the calculations for strip A are repeated with the same image coordinates for all participants (3.4).

3.1 Objectives of test

The main factors, that are influencing the computations and results are:

a) systematic distortions of the films,
b) accuracy of control points,
c) quality of points,
d) identification and interpretation errors of the operator,
e) mathematical model of used software.

The factor a) is unknown in this test. For factor b) and c) it is known, that the control point coordinates are derived using different methods resulting in different standard deviations, but it is stated, that all may include errors up to 10 m. The quality of the points is the biggest problem. From their nature wood corners and non rectangular street crossings are not very ideal targets. This leads to identification and interpretation errors of the operator. For this reason the standard deviation of control points was set to an unique level, independent from their origin.

3.2 Detection of errors in image coordinates

Identification and interpretation errors are the biggest problem of this dataset. For this reason the test pilot center supplied the test participants with the ground coordinates of all points. So the identification and interpretation errors could be detected in a preadjustment.

For the results presented in this paper the rejection of points was done using the data snooping, which is a standard feature of BINGO. All points were introduced as 'control' points, and those measurements were treated as faulty, where the data snooping indicated errors. Often the test detected errors in the coordinates of the 'control' points, a clear indicator for an identification error. Following the objective rules for data snooping, only those errors could be removed, which were significant.

Interpretation errors below the significance level still influence the results. This is obvious looking at table 1, which shows the relative low accuracy of the plane coordinates compared to the height. This relationship is not in accordance with the base/height ratio, so it has to be explained as problems to define the point location in the xy-plane.

Points, which are covered by clouds, and those, who are not identificable, are cancelled.

3.3 Computations of strip A and B

The computation of strip A was done with 101 points. For strip B 124 points could be used. The number of cancelled points are 18 and 16. The different control point configurations are shown in fig. 2 and 3.

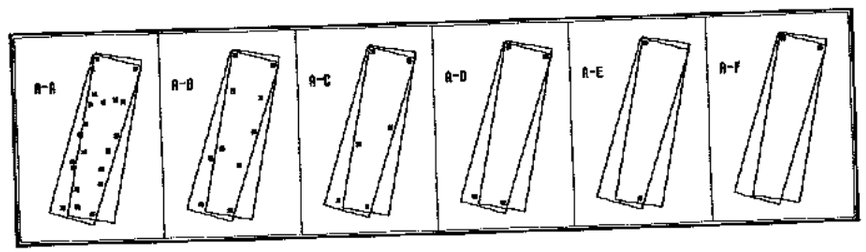

Fig. 2: Control point configurations of strip A

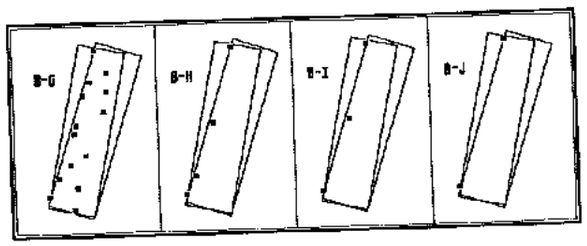

Fig. 3: Control point configurations of strip B

The results are tested by using independent check points. For each configuration and coordinate axes the following three values are computed:

- root mean square difference $\left(\frac{\sum d_i^2}{n}\right)^{0.5}$,
  d_i = difference for point i , i = 1, n
- linear mean difference $\frac{\sum d_i}{n} = lm$
- standard deviation $\left(\frac{\sum (d_i - lm)}{n}\right)^{0.5}$.

The results are shown in table 1, table 2 and fig. 4. They are computed in the local cartesian coordinate system.

It is obvious, that systematic errors increase by reducing the number of control points. Using only two or three of them, a significant shift of the coordinates appear. The redundancy becomes very low in the control points, so that identification problems influence the result. In case of configuration A-F the base of two control points is very short. The extrapolation of the orientation along the strip causes additionally systematic errors.

3.4 Digitally measured image coordinates

As stated in 3.2 the individual derived datasets are influenced by some errors. In order to get more comparable results, all test participants got the same dataset of strip A. This data were measured digitally by IGN. The method of measurement was declared as 'simultaneous monoscopically'.

With this dataset a preadjustment was carried out again to eliminate gross identification errors. Eight points had to be deleted, because their residuals were > 3.5 σ. The other points are used for the calculations. Table 4, 5 and fig. 1 show, that the results of this digitally derived dataset are not better than those of the analytical plotter. In plane there are the same problems of identification, and in height there is a significant loss of accuracy because of the monoscopic viewing. The disadvantage of monoscopic viewing is not compensated by the possibility of image enhancement in a digital system. Only digital stereo workstations may bring better results.

strip/ configur. | control points | independ. checkpoints

A	101	–
7.2	6.7	1.9
0.0	0.0	0.0
7.2	6.7	1.9
X	Y	Z

B	124	–	
7.0	7.6	1.8	← square mean
0.0	0.0	0.0	← linear mean
7.0	7.6	1.8	← standard dev.

Table 1: Differences of the preadjustment result

A-A	21	69
9.1	8.8	6.2
-0.3	0.5	-0.9
9.1	8.8	6.2

A-B	10	80
9.2	10.3	6.8
-2.5	0.8	-0.9
8.8	10.3	6.7

A-C	6	83
8.8	10.5	7.7
-1.4	1.5	-4.5
8.7	10.4	6.3

A-D	4	85
8.7	10.9	10.5
-1.5	1.2	-8.2
8.6	10.8	6.5

A-E	2	86
8.8	11.5	8.9
2.6	-2.1	-5.6
8.4	11.3	6.9

A-F	2	86
13.0	15.3	19.4
9.9	-8.2	-16.4
8.4	12.8	10.4

Table 2: differences at independent checkpoints strip A

B-G	14	110
8.8	11.5	4.8
-1.2	-5.0	1.5
8.7	10.3	4.6

B-H	4	120
8.7	12.7	5.6
2.0	-6.3	1.4
8.4	11.1	5.4

B-I	3	121
8.7	15.4	5.9
-1.2	-10.3	-0.1
8.6	11.5	5.9

B-J	2	122
8.9	14.7	6.0
-1.9	-9.3	1.2
8.6	11.5	5.9

Table 3: differences at independent check points strip B

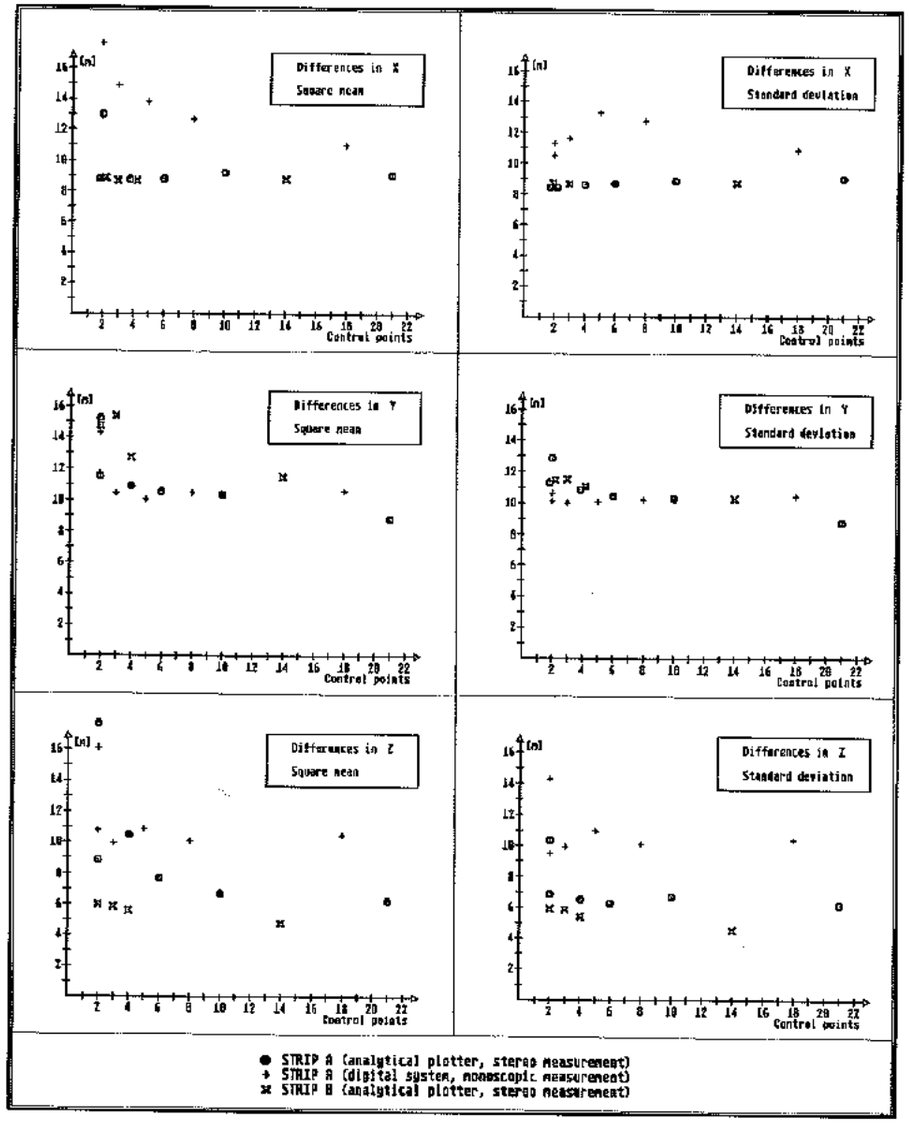

Fig. 4: Graphic representation of results strip A and B

A	92	-
9.0	7.4	2.5
0.0	0.1	0.0
9.0	7.4	2.5

Table 4: Differences of preadjustment result, digital data

A-A	18	74
11.0	10.6	10.7
1.5	2.4	-2.8
11.0	10.4	10.4

A-B	8	84
12.8	10.5	10.1
1.4	2.9	0.3
12.8	10.2	10.2

A-C	5	87
13.8	10.1	10.9
3.8	0.6	0.3
13.3	10.1	10.9

A-D	3	89
14.8	10.5	9.9
9.3	-3.2	-1.1
11.1	10.0	9.9

A-E	2	90
12.9	14.4	16.1
6.3	-9.7	-7.7
11.3	10.6	14.3

A-F	2	90
18.1	11.4	10.8
14.7	-5.2	-5.0
10.5	10.2	9.6

Table 5: differences at independent checkpoints strip A, digital data

3.5 Computation of the whole block

As an extension to the test an adjustment was carried out using all 16 scenes simultaneously. In this configuration, called AB-K, 6 control points were used. Four of them were placed into the overlapping area of the strips, fig. 5. Two control points were located at the border of the block in order to stabilize the sensor orientation in height.

The results, table 6, are in agreement with the other computations, there is no need for more ground control, although the number of scenes was doubled.

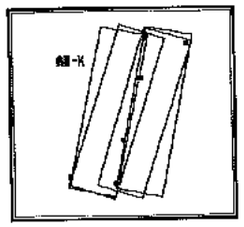

Fig. 5: Configuration AB-K

AB-K	6	194
11.2	10.0	6.5
6.8	-2.8	1.0
8.9	9.6	6.5

Table 6: results of configuration AB-K

4 Conclusions

This OEEPE test shows, that it is possible to reach absolute accuracies of about 5-6 m with the presented BINGO-SPOT solution by use of 4-6 control points. The necessary number of control points seems not to be dependent on the number of scenes in the block.

Limiting factor for practical applications is not the mathematical model but the problems in identifiing points, which may cause undetectable errors of several meters. Stereoscopically measurement is absolutely necessary.

5 References

/Jacobsen 1987/ Computer supported data acquisition for block adjustment, SSH

/Jacobsen, Picht 1988/ Aerial triangulation of SPOT and aerial photography, Int. Arch. of Phot. and R.S. Vol 27 III, p 436

/Engel 1987/ Orthocomp operation of SPOT imagery, SSH

/Krauss 1988/ Aktuelle Anwendungen der Nahbereichsphotogrammetrie bei Rheinbraun, BUL 56/1988, p 24

/Kruck 1987/ BINGO Bundle block adjustment program for SPOT data, SSH

/Picht 1987/ Planicomp operation of SPOT imagary, SSH

BUL = BUL Zeitschrift für Photogrammetrie und Fernerkundung
SSH = Seminar on Photogrammetric mapping from SPOT imagery, Hannover, Sep. 1987

TRIANGULATION of SPOT DATA at IGN for the OEEPE TEST

Isabelle Veillet
Ingénieur Geographe
Institut Géographique National. France
2 av Pasteur, 94160 ST MANDE

1. IGN and Spot triangulation

Photogrammetric investigations towards Spot system abilities for cartographic products were made even before launching.
IGN has facilities for Spot stereoplotting. Various experiments were conducted to evaluate Spot accuracies and the ability to handle together more than two Spot strips seemed to be useful. IGN gathered a set of data in the South of France and geometric results were tested.

The data supplied for the OEEPE test had already been processed in IGN on the Spot triangulation software written to supply Spot stereoplotting with points as is done in the aerotriangulation processing.

2. Method

Principle

The method used is based on a physical modelisation of Spot system geometry.
The collinearity equations are written in a system linked to the instrument platform and HRV.

The unknowns are ground coordinates for all the points measured, and orbit corrections (position and attitude) for the different tracks, i.e. one per strip. The attitude correction is supposed to be constant. The position correction is supposed to be linear (or constant) in time.

The equations come from collinearity equations for all the measures, from ground coordinates of controls and from assuming orbit corrections stay within CNES specifications.

Adjustment computation
The software is running on a Vax 730 computer, and is able to deal with Spot image blocks. It is possible to handle strips with or without ground controls, with any kind of distribution. Nearly as many strips as given can be joined together. The software has provision for disactivating or reactivating points as required. The different kinds of equations can be weighted as requested.

Measurements
The points were measured with the Matra Traster analytical stereoplotter. This equipment, used for Spot stereoplotting, can handle strips with controls distributed over them.
The points were extracted from the IGN generated level 1A films supplied for the test.
Other software is available to point simultaneously on two digital images, with the additional help of correlation around the point.

Output
The results of a block adjustment are statistics to check the computation and then elements for further stereoplotting.

3. Tests conducted

The same set of measures had been used for all the different distrubutions.

Reference computation
An adjustment was computed using all the points as controls to check their own quality with a low ground weight. After eliminating the points with residuals which were too large, the good points were selected to calculate the root mean square errors.

Ground residuals
The figures to check ground fitting are:

for control points	Residuals Mean Square
for check points	residuals Mean mean square of difference from residual to residuals mean (E) Residuals Mean Square

The RMS on check points is the figure used to classify the computation. A three class classification could be proposed, depending on planimetric and altimetric accuracies (RMS).

class	planimetric accuracy	altimetric accuracy
I	less than 10 m	around 6 m
II	around 15 m	more than 8 m
III	more than 20 m	

A class I computation is required for 1:50 000 topographic mapping.

Measurement residual
The Root Mean Square for measurement residuals is computed,

too. Actually this does not change a lot between the different distribution computations. It stays around the third of a pixel.

4. Independent stereostrips Tests results

4.1 OEEPE tests

Nota Bene
The scheduled distributions were slightly modified because two points could not be measured on the test stereopairs in the A strip. The closest measurable points were taken. Point 3045 was taken instead of 026, and 3035 instead of 3036.

Tested distributions

Strip 'A'

A :	all points provided									
B :	points 001,	004,	014,	2002,	1078,	018,	3045,	028,	3035,	3040
C :	points 001,	004			1078,	018,			3035,	3040
D :	points 001,	004							3035,	3040
E :	points 001,									3040
F :	points 001,	004								

The sketches are the following ones :

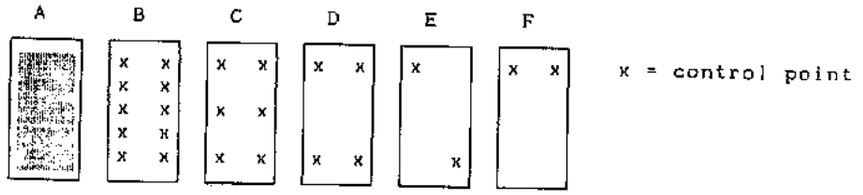

Strip 'B'

G :	all points provided			
H :	6,	1036,	78,	73
I :	6,	1036,		73
J :	6,			73

The sketches are the following ones :

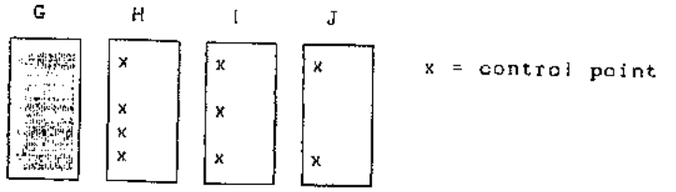

Results

Both 'all control' distributions (A and G) gave 5 m in X and Y, and 4 m in Z as RMS.

For the other distributions, the detailed figures are given below in Annex. Their classifications are:

Test number	B	C	D	E	F	H	I	J
Class	I	I	I	II	II	III	III	III

The first conclusion is that a two point distribution (E and F), even on both edges of the strip, is quite short to get valuable results. This kind of distribution belongs to class I.

A four corner distribution (D) is suitable for a 6 meter accuracy on each coordinate, X, Y and Z; it is classified II.

A one-edge distribution does not fit and is to be avoided. Both H, I and J are only in class III.

4.2 Additional tests

Between E or F destributions and D distribution, there may exist a mid-distribution, a three point one which is still a class I one. Three point distributions will be tested to see what can bring a third point to the result.

Before concluding, additional tests to have similar configurations on the second strip as the ones chosen on the first one could be really useful. At least, it gives another set of measurements, but also, it could show the influence of a bad measurement of a control point on the global result.

Tested distributions

Strip 'A'

Three point distributions to evaluate the third point advantage

N : points 001, 004, 3040
O : points 001, 004, 028
P : points 001, 004, 018
Q : points 001, 004 2002

Four point distributions to evaluate influence of Y distance between controls

R : points 001, 004, 014, 2002
S : points 001, 004 1078 018

The sketches are the following ones :

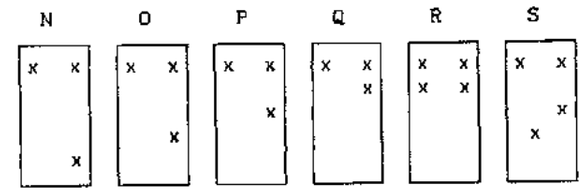

Results

Test number	N	O	P	Q	R	S
Class	I	I	II	II	I/II	I

Strip 'B'

Distributions to check the strip 'A' results

K : 6, 101
L : 72, 101
M : 6, 72, 101
U : 1025, 72, 101
V : 1036, 72, 101
W : 78, 72, 101
X : 1036, 72, 101, 1041

The sketches are the following ones :

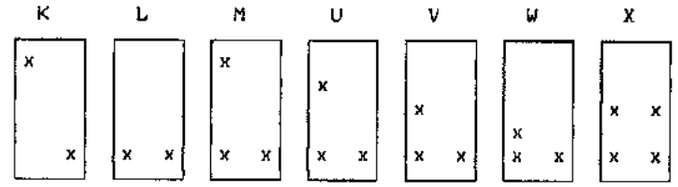

Tho distributions are to be compared respectively to :

E F N O P Q S

Results

Test number	K	L	M	U	V	W	X
Class	II	I	I	I	I	II	I

K and L confirm E and F results. R, S, and X show that a 'square' distribution should be as extended along the track as possible, at least one image long.

4.3 Conclusion

At least two points are necessary, one on the West edge and the other on the East one. This gives an accuracy of 15 m in planimetry and 10 m in altimetry.

With three points, one on each edge, and one North / one South distant from more than one image, the accuracy is around 12 m in planimetry and 6 m in altimetry.

The fourth point gives a planimetric accuracy lower than 10 m. It allows to lower a bad measurement influence on one of the points.

Then 6 to 8 points enable to control and eliminate gross errors.

5. Block adjustment

Block adjustments were computed. Pass points were created to join strips together.

The two sets of tests were made on slightly different data sets. In both cases a computation was made using all ground points as controls: it was called the reference computation.

5.1 Various four points or more distributions

In the examples b, c and d, to avoid bias, instead of using one point where a control was required, three points were used, those three points being as close as possible.

Distribution sketches

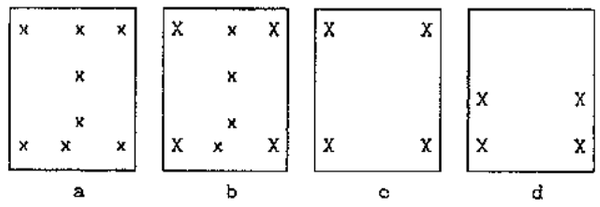

Results

This set of tests shows that a four corner distribution is quite suitable, and that a 'square' distribution must be spread along the track if possible. The general conclusions remain the same as they were for a one-strip block.

All these distributions give 8 to 10 meters in planimetry and around 5 meters in altimetry, as the root mean square of ground residuals on check points. There are all part of class I.

5.2 'Three point' distributions

In order to confirm the results obtained using three point distribution on one strip, tests were conducted on the two stereo strips block.

For the tests 'e', 'f' and 'g', 2 points were taken instead of one to link the two strips, because no point was well measured on the two strips in the North area.

Tested distributions

0 : all points provided
e : 73, 3040, 47, 006
f : 1072, 024, 47, 006
g : 1036, 018, 47, 006

Distribution sketches

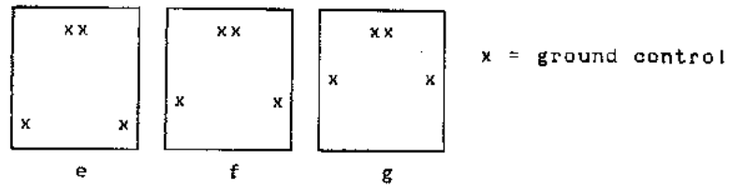

Results

Test number	e	f	g
Class	I/II	I	II

The 6 m mean residual in X for 'g' test, leads to assume that one of the ground controls was not good. The classification in class I of 'f' distribution enables to conclude that three good quality controls could be enough.

6. Conclusion

These tests were part of larger experimentation on a 32 images adjustment. The general results are mainly similar to these two stereo strip block adjustments.

The next step is to evaluate the extrapolation capacities of Spot system. The gross error detection and elimination is also to be studied.

This kind of tests leads IGN to use block triangulation of Spot images for cartographic production. A 32 images block was acquired and triangulated to extrapolate and is actually stereoplotted for making line maps over Djibouti country.

Annex I: Detailed results for the different tested distributions

All the figures are given in meters. in X, Y and Z cartographic coordinates.
M = residuals mean
E = mean square of difference from residual to M
RMS residual mean square

The classification of each distribution is given. The RMS on check points is the figure used to classify the computation. A three class classification could be proposed, depending on planimetric and altimetric accuracies (RMS).

class	planimetric accuracy	altimetric accuracy
I	less than 10 m	around 6 m
II	around 15 m	more than 8 m
III	more than 20 m	

Two stereo strip block

	Test number	residuals X	Y	Z	class
RMS	ø	5.1	5.2	4.2	
M	e	1.2	1.ø	-1.4	
E		8.2	5.7	4.7	
RMS		8.4	5.8	4.9	I/II
M	f	.ø	-1.8	.ø	
E		7.ø	5.8	4.6	
RMS		7.ø	5.8	4.6	I
M	g	6.ø	.4	.4	
E		9.8	5.5	5.4	
RMS		11.5	5.5	5.4	II

Annex I

One stereo strip adjustement

	Test number	residuals X	Y	Z	class	Test number	residuals X	Y	Z	class
RMS	A	4.2	5.1	3.6		G	5.2	5.2	4.ø	
M	B	.ø	1.9	-3.1		H	-11.4	11.4	2.8	
E		4.5	5.8	3.8			1ø.7	7.ø	6.ø	
RMS		4.5	6.1	4.9	I		15.3	13.1	6.6	III
M	C	2.2	1.1	-2.9		I	-11.ø	11.1	2.7	
E		5.ø	5.7	3.7			1ø.7	7.ø	6.ø	
RMS		5.5	5.8	4.7	I		15.3	13.1	6.6	III
M	D	1.8	.4	-3.8		J	-16.7	14.3	1.4	
E		5.1	5.8	3.7			11.6	7.3	5.5	
RMS		5.4	5.8	5.3	I		2ø.2	16.1	5.7	III
M	E	-2.3	.4	-1.ø		K	-.6	5.7	-5.7	
E		1ø.2	8.3	4.ø			7.ø	5.4	6.9	
RMS		1ø.4	8.ø	4.1	II		7.ø	7.8	8.9	II
M	F	8.3	1.ø	ø.6		L	-3.2	2.5	3.2	
E		5.8	8.1	5.2			6.9	6.ø	5.5	
RMS		1ø.1	8.1	5.2	II		7.6	6.5	6.3	I
M	N	2.3	2.3	-2.3		M	-2.5	6.ø	-2.7	
E		4.3	5.5	4.1			6.2	5.1	4.2	
RMS		4.9	5.9	4.7	I		8.7	7.9	5.ø	I
M	O	1.3	.2	-3.6		U	-.3	2.8	-2.7	
E		5.6	6.4	3.8			6.1	5.5	4.2	
RMS		5.8	6.4	5.3	I		8.1	6.1	5.ø	I
M	P	8.1	1.9	1.ø		V	2.7	2.ø	.5	
E		7.5	6.ø	5.3			5.9	5.6	4.7	
RMS		11.ø	6.3	5.4	II		6.5	5.9	4.7	I
M	Q	14.9	1.8	-4.3		W	-1.4	4.2	14.ø	
E		1ø.7	6.ø	3.6			6.2	5.4	13.1	
RMS		18.3	6.2	5.6	II		6.3	6.8	19.1	II
M	R	5.5	2.5	-4.3		X	2.ø	1.ø	-1.7	
E		6.2	5.9	3.6			6.1	5.4	4.ø	
RMS		8.3	6.4	5.6	I/II		6.4	5.5	4.4	I
M	S	.ø	.2	-1.3						
E		4.6	5.7	4.2						
RMS		4.6	5.7	4.4	I					

strip A

strip B

Annex 2

Residuals of some of the tested diastributions

A, F, N for strip 'A'

G, L, M for strip 'B'

Ø, e, f, g for the two strips block

The scale and symbols are the same for all of those graphics.
They are given below :

Points

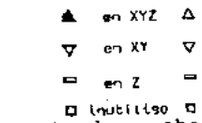

control check

Ground residuals

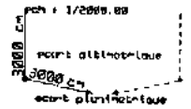

active inactive

OEEPE Test A

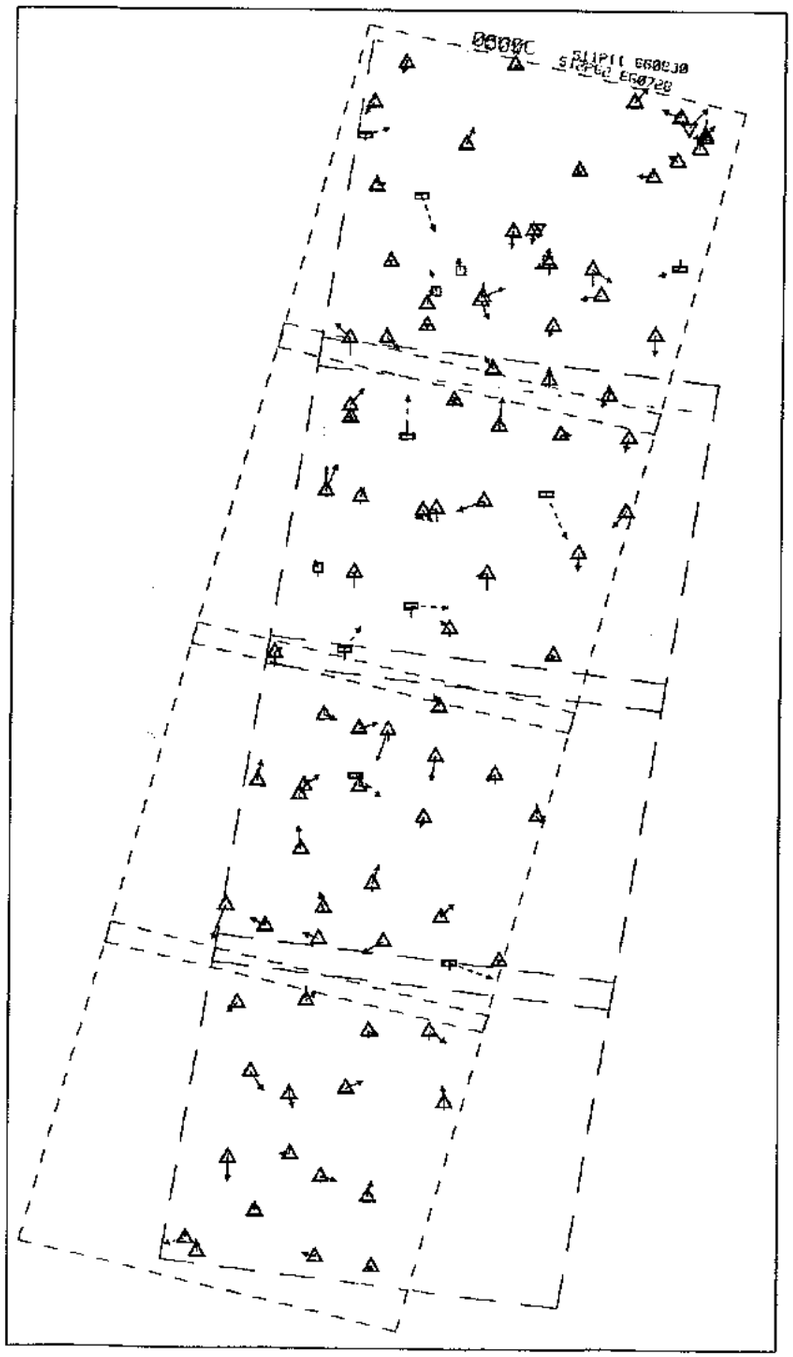

OEEPE Test F

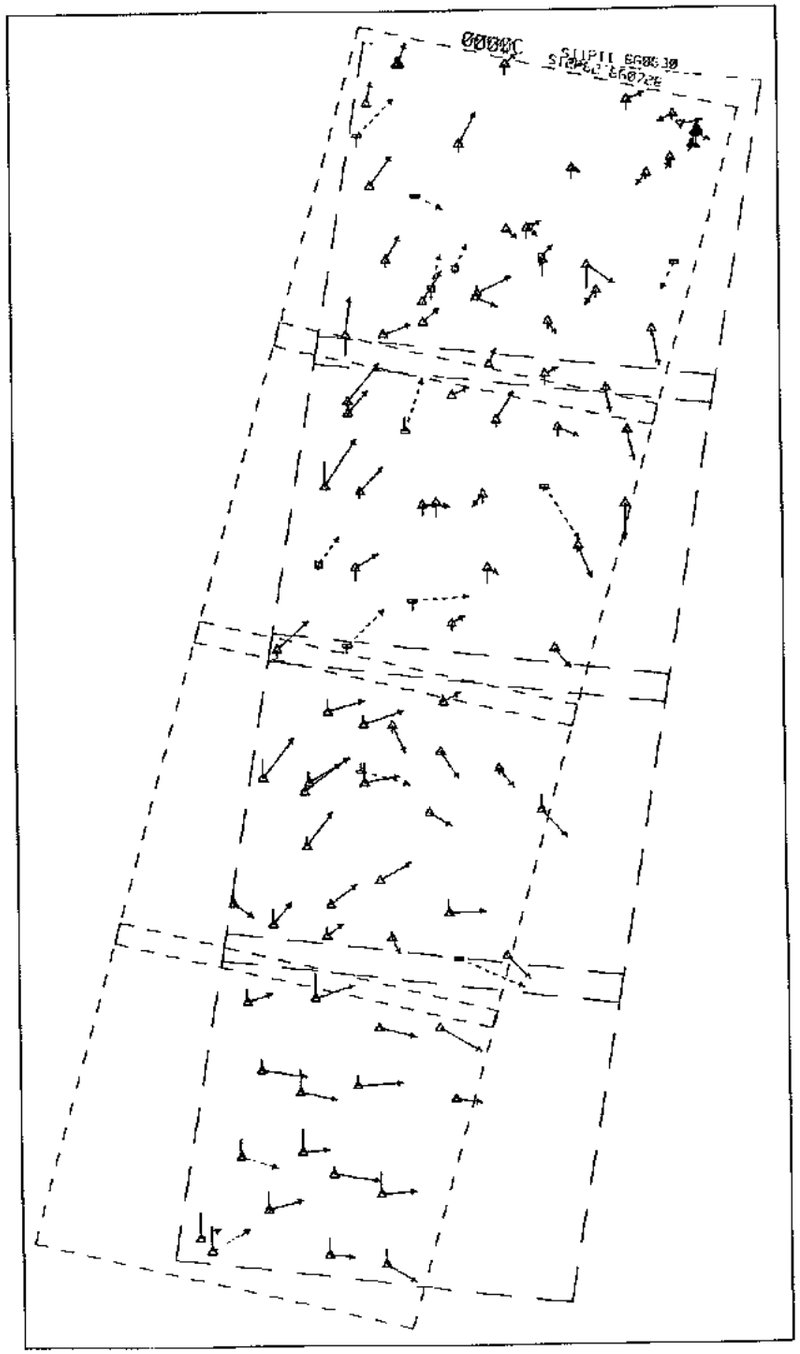

OEEPE Test N

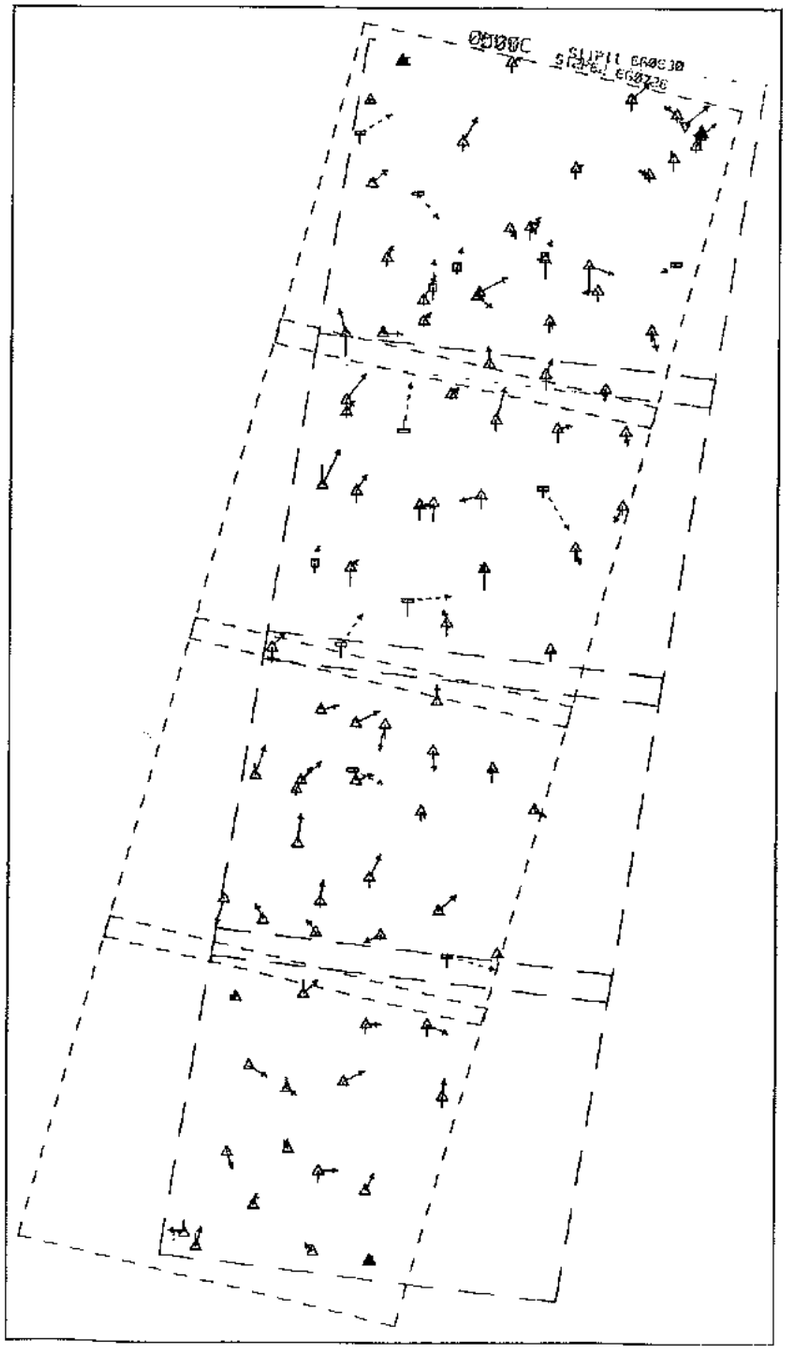

OEEPE Test G

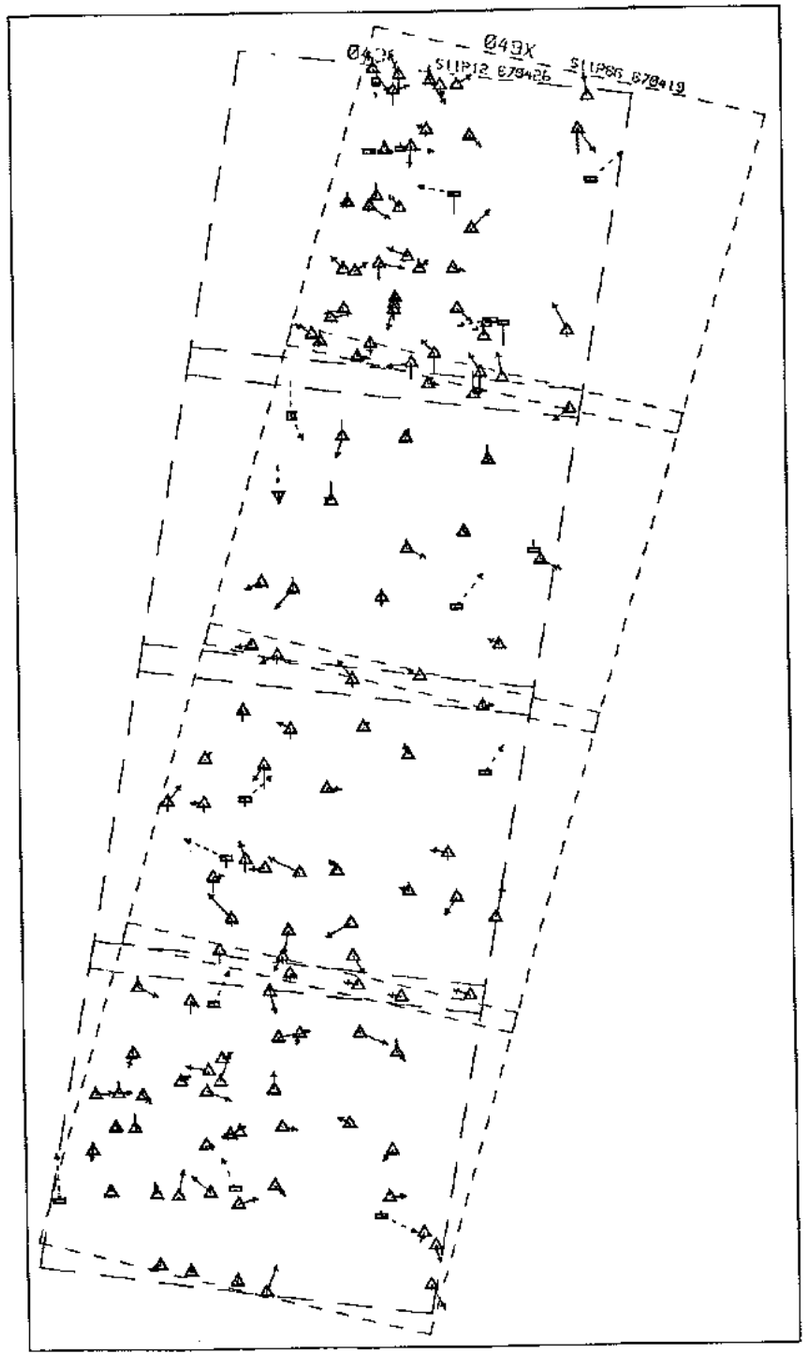

OEEPE Test L

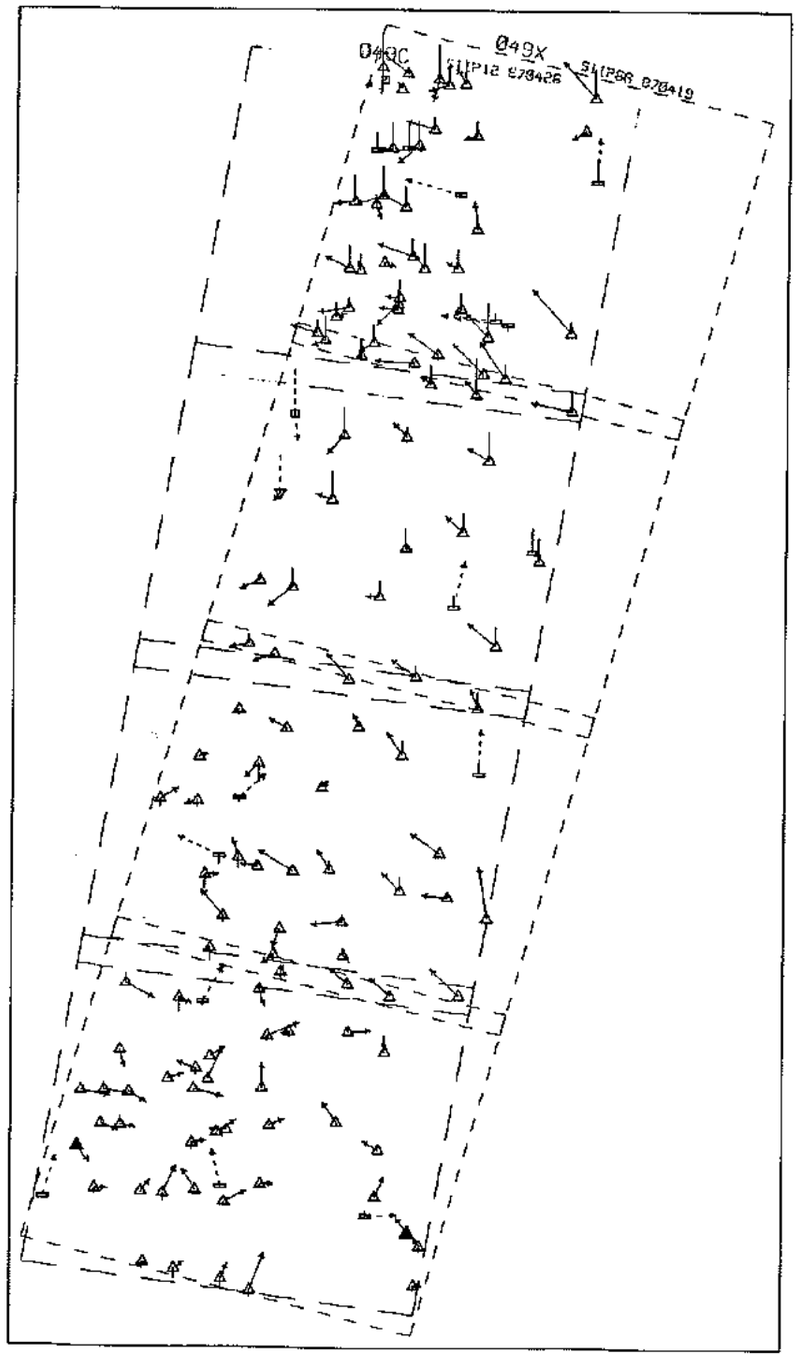

OEEPE Test M

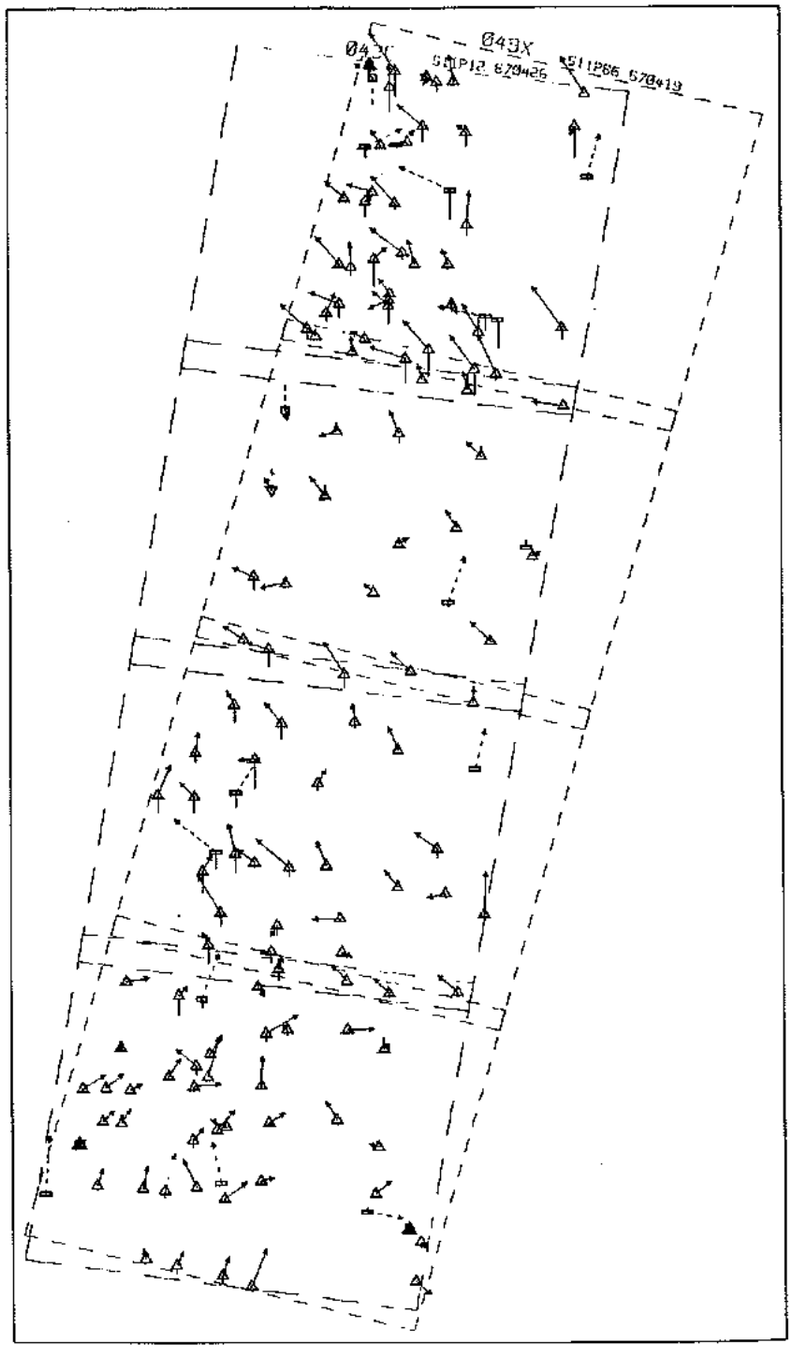

OEEPE Test Ø

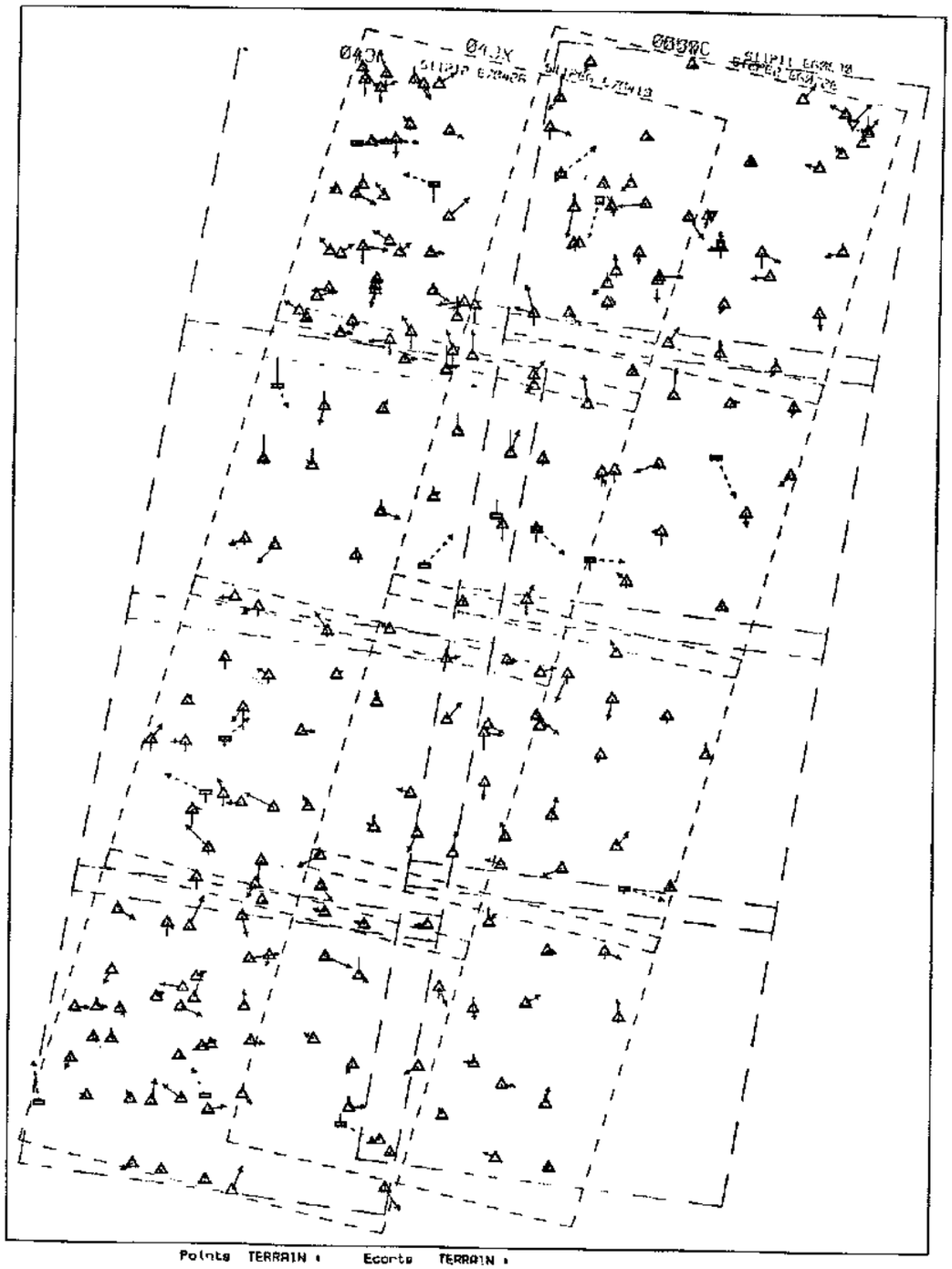

OEEPE Test e

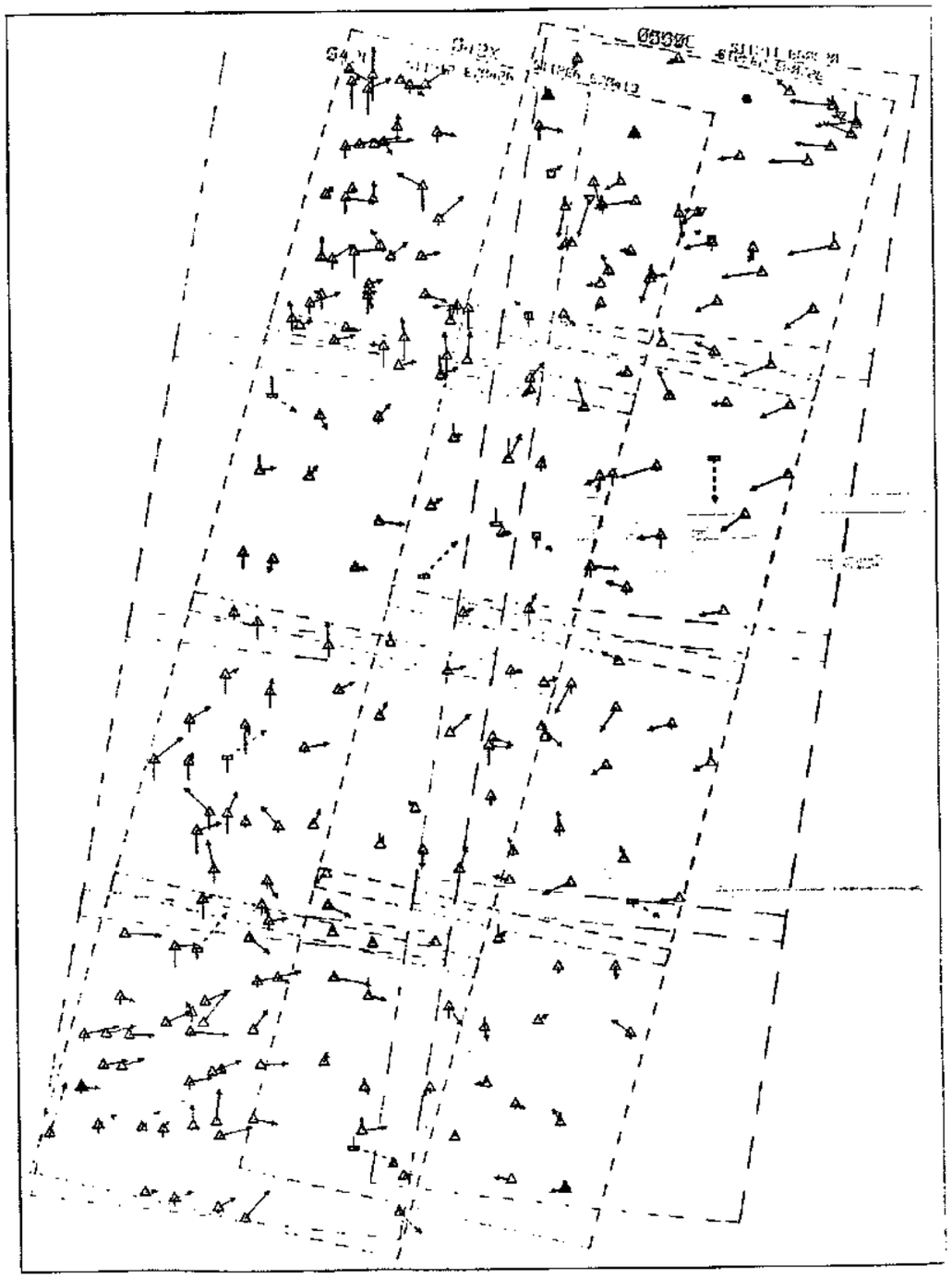

OEEPE Test f

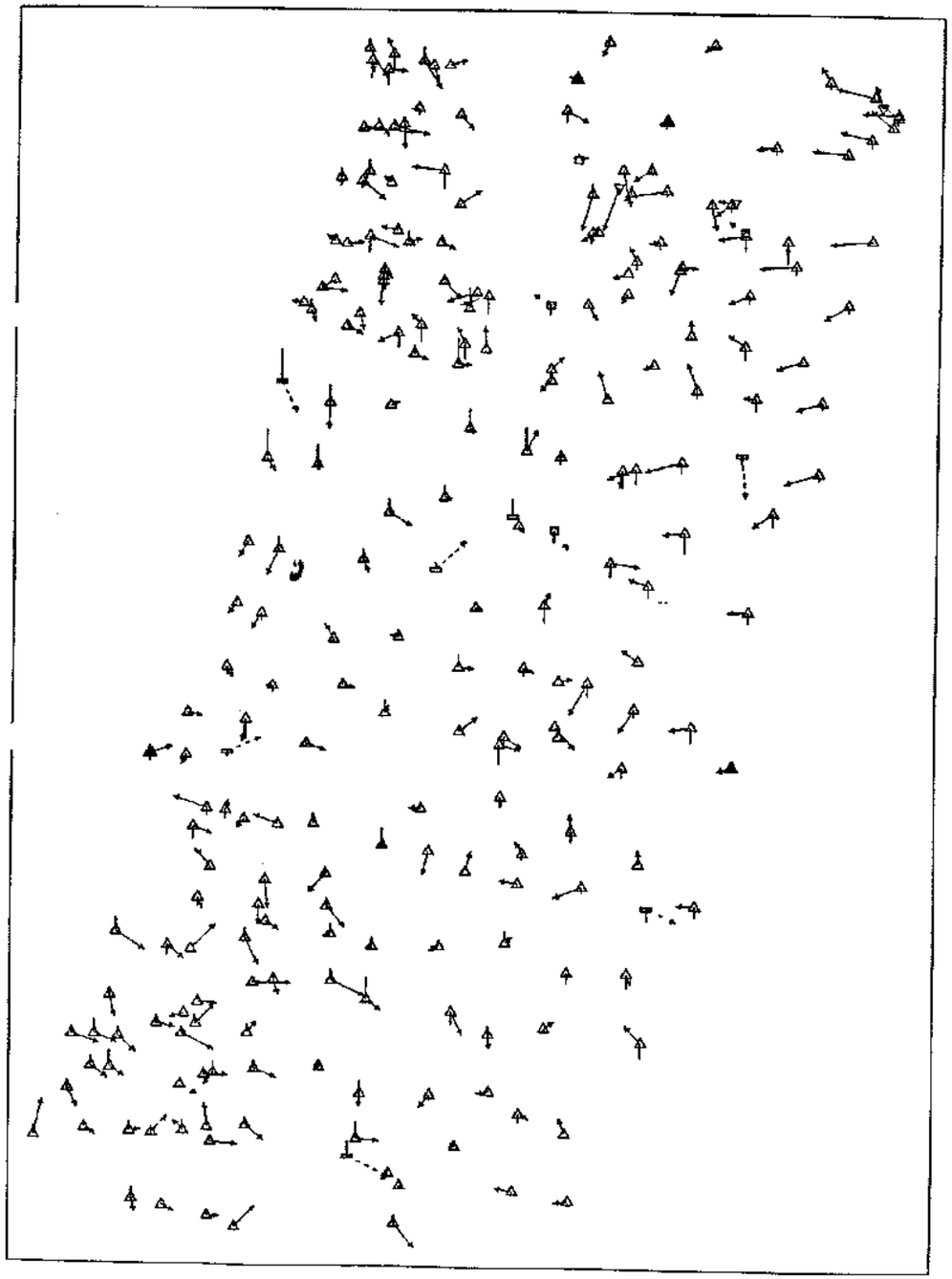

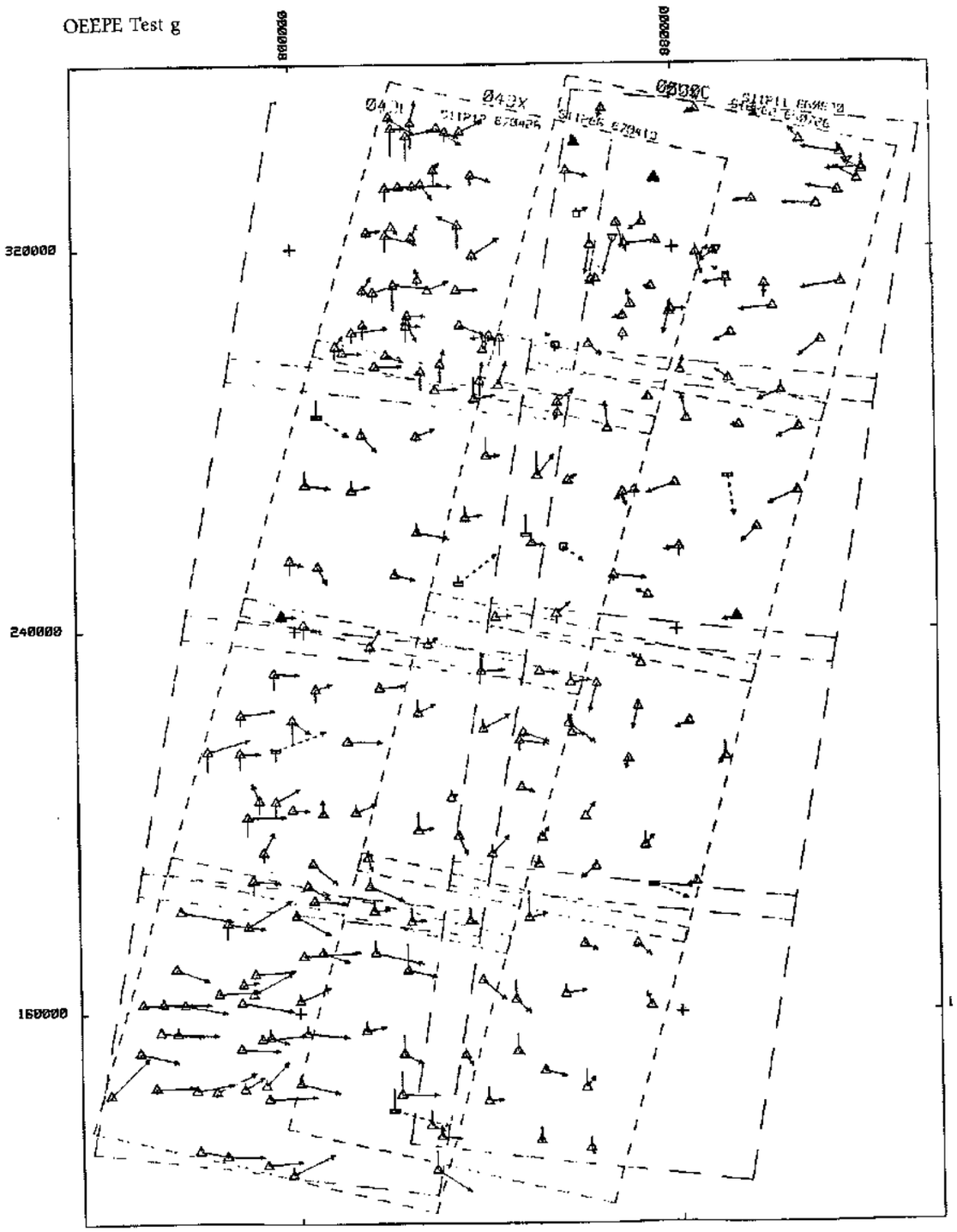

Contribution of the 'Politecnico di Milano' to the OEEPE test on triangulation with SPOT data

Auke de Haan
Istituto di Topografia, Fotogrammetria e Geofisica
Piazza Leonardo da Vinci 32, 20133 Milano, Italy
Bitnet address: geopoli@imiclvx

Abstract

In bundle adjustments with SPOT data, the simple central projection geometry of traditional photogrammetry has to be extended to take into account the effects on the imagery of the satellite's motion in its orbit, the attitude of its platform and the characteristics of the onboard optical instrument.

In the Instituto's approach, the *satellite's orbit* is described by a dynamic model, which allows for the reconstruction of the orbital arc with six parameters, *the attitude of the satellite's platform* is described by 3 cubic splines, which describe pitch, roll and yaw as functions of time, while *the projection geometry of the optical instrument* is described by four detector look angles and the focal length. In the bundle adjustment, successive images of a pass are treated as a single image, and relevant auxiliary data (the satellite's position and velocity vector, pitch roll and yaw velocities and detector look angles) are included as pseudo observations.

The precision of point positioning in bundle adjustments with SPOT data depends on the *precision of the image measurements*, the *geometry of the intersecting imaging rays* and the *precision of the knowledge of the imaging geometry*. The standard deviation of the image measurement of well defined and clearly visible points can be smaller than 0.25 pixel in both directions. With the intersection geometry of the imaging rays of a 21°W/21°E SPOT stereopair this results in a positioning precision of 3 m in planimetry and 4.5 m in height, when the imaging geometry is known perfectly. The treatment of successive images as a single image and the use of auxiliary data and orbital mechanics significantly reduces the need for ground control: with a modest number of ground control points, a positioning precision can be obtained, which is close to that, which would be obtained if the image geometry were known perfectly.

The RMSE of the image coordinate measurement of the points of the OEEPE test was on average about 0.5 pixel (not all points were clearly visible and well defined); the obtained positioning precision of the check points was about 7m in planimetry and 10m in height.

1. - Introduction

The Institute's involvement in research on geometric evaluation of SPOT imagery goes back to its participation to the SPOT preliminary evaluation program (PEPS) *(Togliatti and Moriondo, 1988)*. Work on the contribution to the OEEPE project on triangulation with SPOT data was started in October 1988, when the author joined the Institute. After the development of a mathematical model and corresponding software for bundle adjustments with strips of SPOT data in 1989, the OEEPE test data was processed and analysed in 1990. This final report contains a) a description of the Institute's approach to the modelling of SPOT image geometry, b) a summary of the results of the bundle adjustments, which have been carried out with the test data of the OEEPE project and c) an analysis of the accuracy potential of the positioning accuracy obtainable by triangulation with SPOT data.

2. - The Milan approach to the modelling of SPOT image geometry

SPOT imagery is acquired by line scanning from a low (830 km), near circular orbit in an orbital plane, which is inclined 81.3° with respect to the equatorial plane (fig. 1). Successive image rows are imaged while the satellite moves in its orbit. In order to ensure that successive image rows are taken parallel and without gaps or overlaps, the satellite's Orbit and Attitude Control System continuously tries to align the orientation of the satellite's platform (defined by the satellite-fixed triad *(x1,x2,x3)* (fig. 3)) to a predefined target attitude. The latter is defined with the *p(itch)*, *r(oll)* and *y(aw)* axes, the directions of which depend on the satellite's position and velocity vector (fig. 2).

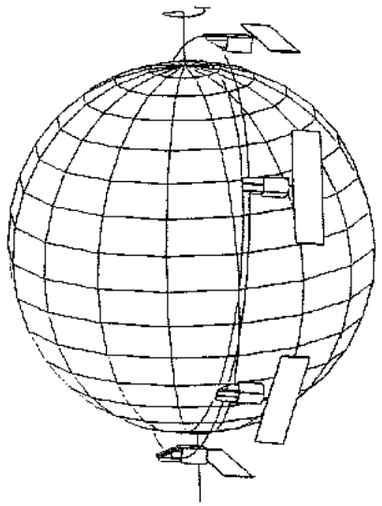

Figure 1 - SPOT orbit.

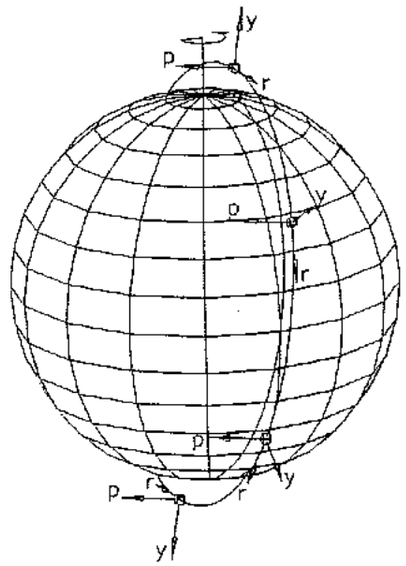

Figure 2 - The satellite's target attitude.

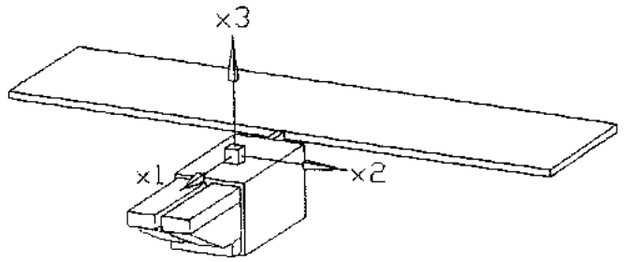

Figure 3 - Attitude of the satellite's platform.

The image rows are formed by the linear array(s) of CCD sensors in the focal plane of the optical instrument. In the panchromatic mode, which offers the highest spatial resolution, the rows are formed with a frequency of 665 Hz by a linear array of 6000 CCD elements; in about 9 seconds an image of 6000^2 brightness counts is completed. The rows are taken perpendicular to the satellite's velocity vector, in a direction, which depends on the position of the adjustable Strip Selection Mirror at the entrance of the telescope, up to 27° at each side of the nadir.

For the geometric evaluation of SPOT imagery, a reconstruction has therefore to be made of the orbital arc, the attitude of the satellite's platform and the characteristics of the optical instrument for the time interval of imaging.

2.1. - The orbital arc corresponding to the time interval of imaging

Although the SPOT satellites include hydrazine thrusters for orbit correction manoevres, these are never used during image acquisition. Consequently, the satellite's motion during these periods is completely determined by external forces, like the earth's gravitation, the attraction of the sun and the moon, atmospheric drag and solar radiation pressure. The acceleration caused by the predominant force of the earth's gravitation can be split into three different parts, the Kepler term (a about 7.4 m/s^2), the J_2 term (a about 8. 10^{-3} m/s^2) and the other harmonic terms (a about 1. 10^{-4} m/s^2). The accelerations caused by the other forces are smaller than 1. 10^{-5} m/s^2.

The knowledge of the forces which accelerate the satellite allows for the complete determination of its trajectory from its position and velocity at an initial time t_0 by (numerical) integration *(Kovalevsky, 1989)*: while the time derivative of the satellite's position vector equals its velocity vector, the time derivative of its velocity vector equals its acceleration vector, which is provided by the force model. When the integration is carried out in an earth-fixed reference system, the accelerated motion of the coordinate system has also to be taken into account.

Accepting a modelling error effect of 1m in the reconstructed orbital arc, which seems reasonable when taking into account the 10x10m pixel size, a force model which includes only the Kepler - and the J_2 term of the earth's gravitational field is sufficient for the reconstruction of an orbital arc corresponding to up to 11 successive SPOT images. This model has been implemented; orbit integration is carried out numerically with a simple single step Runge-Kutta algorithm. Integration is carried out in a geocentric reference system with axis fixed in space.

The use of the knowledge of the earth's gravitational field reduces the problem of the reconstruction of an orbital arc to the problem of the determination of the six elements of the satellite's initial position and velocity vector.

These elements are provided in the available auxiliary data, which includes ephemeris data from post orbit processing of telemetry and tracking data. The ephemeris data is however not perfectly known (for SPOT-1 the positional accuracy is in the order of a few hundred metres). In the bundle adjustment their determination can be improved considerably. The given elements of the initial position and velocity vector are therefore included in the bundle adjustment as pseudo-observations.

2.2. - The attitude of the satellite's platform during image acquisition

While the satellites trajectory during image acquisition is completely determined by external forces, the orientation of the satellite's platform is the result of torques, which are applied by the satellite's Orbit an Attitude Control System (AOCS) to keep the platform aligned to the target attitude. Torques have to be applied to counteract disturbing torques and to perform a rotation once per revolution about the pitch axis.

The AOCS includes rate integrating gyros for the determination of attitude by integration, and earth and sun sensors for the correction of gyro drift by earth and sun sightings. With the data provided by the gyros and the sun and earth sensors, the AOCS determines the torques, which have to be applied to align the spacecraft's platform to the target attitude, i.e. *x3* parallel to the *y* axis in the direction of the satellite's position vector, and *x2* parallel to the *r* axis, perpendicular both to the satellite's position and its velocity vector.

The small residual misalignments between the *(x1,x2,x3)* and *(p,r,y)* axes are described by the error attitude angles pitch, roll and yaw, which correspond to the angles of the three rotations about the *p*, *r* and *y* axes which are needed to align *(x1,x2,x3)* and *(p,r,y)*. The AOCS is able to keep the error attitude angles very stable: the ground effect of variations in error attitude are limited to about 10m. The absolute precision of the alignment is however limited, to about 0.05° for pitch and roll and about 0.15° for yaw, due to gyrodrift between successive sightings, the disturbing effect of the earth's atmosphere on earth sightings, and the imperfect knowledge of the satellite's position vector.

Pitch, roll and yaw velocities, which are determined by the satellite's AOCS are sent down together with the image data. The auxiliary data includes pitch, roll and yaw velocities for every 0.125s. Although these provide no information on the (relatively large) constant in

the values of pitch, roll and yaw, they do provide a detailed description of the variations of those angles during the time interval of image acquisition.

From the large time series of error attitude velocity data a continuous function must be obtained for the description of error attitude as a function of time. In the Institute's approach, each error attitude angle is described by a cubic spline. Cubic splines consist of a number of cubic polynomial segments joined smoothly end to end (at the joints a discontinuity is allowed only in the third derivative). The flexibility of spline functions allows for the description of complicated function patterns with relatively few parameters *(Schumacher, 1981)*. Spline functions can be expressed as a linear combination of a number of shifted B-splines. Fig. 4 shows six cubic B-splines, linear combinations of which define cubic splines on the interval $[t_0,t_3]$.

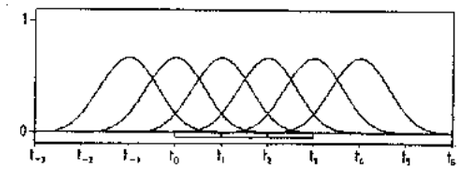

Fig. 4 - The definition of cubic splines as a linear combination of (cubic) B-splines.

At any time t, the function value is determined by only four coefficients, as only four B-splines differ from zero. The pitch, roll and yaw velocities are introduced in the bundle adjustment as pseudo-observations; they correspond to the first derivative of the approximating cubic splines, and can therefore be expressed as a linear combination of first derivatives of four B-splines. The unknown constant error angle and a possible slow drift, which the AOCS was unable to determine, has to be determined from the other observations (especially ground control and image coordinates) in the bundle adjustment.

2.3 - The optical instrument

The linear array of CCD sensors in the focal plane of the optical instrument collect the sunlight, which is reflected by the imaged ground strip, and produce image rows at a 665 Hz frequency. Although the incoming imaging rays are reflected several times by mirrors, first by the Strip Selection Mirror (SSM), then by the two mirrors in the optical system of the folded Schmidt telescope, and finally by the dispersive optics which lead the incoming light to the different CCD arrays, the total effect of the light path from ground strip to CCD array can be assumed to be that of a central projection.

The geometry of this central projection depends on the setting of the SSM, the focal length of the telescope, and the exact position of the CCD array in the focal plane. The auxiliary data includes calibration parameters, which define the central projection

geometry with respect to the *(x1,x2,x3)* triad. These consist of four look angles, which define the look directions of the two end detectors (fig. 5). The precision of the angles with respect to the *x1*-axis (RMSE about 0.008°) is better than that of those with respect to the *x2*-axis (RMSE about 0.018°), due to the imperfect knowledge of the position of the SSM *(Spotimage, 1988)*. The focal length, which must be known very precisely considering the in-flight focal length adjustments with 0.01mm steps, is not given. However, a value, which is compatible with the image measurements can be found with the four detector look angles and the detector spacing (0.013mm).

The given four end detector look angles and the computed value for the focal length are introduced as pseudo observations in the bundle adjustment, in order to be able to allow for improvements in the look angle estimates and to benefit from the precisely known focal length.

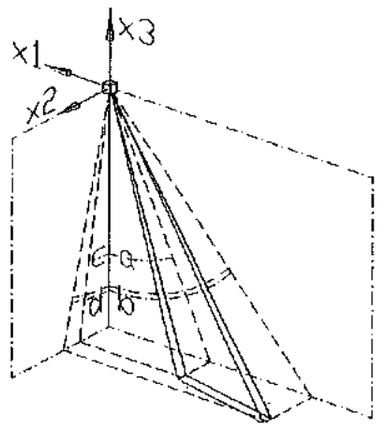

Fig. 5 - The look angles of the end detectors *a,b,c* and *d* define the central projection geometry.

2.4 - The extended bundle formulation for measured image points

In traditional photogrammetry collinearity equations are used to relate measured photocoordinates to the ground coordinates of the measured point and to the parameters, which describe the (central) projection geometry. They express the fact that, at the time of imaging, the imaged point on the film, the projection centre and the ground point lay on a straight line, the so called imaging ray. Using the fact that the imaging rays of a point, measured in two or more photos, intersect eachother at the ground point, ground coordinates of a set of points can be determined together with the parameters

which describe the projection geometry of the photos in a bundle adjustment with collinearity equations and additional ground control data.

The same technique can be applied to relate image coordinates of points in SPOT images to their ground coordinates and to the parameters describing the dynamic image geometry. The central projection model has to be extended however, to include the effect of the satellite's orbit, its attitude and the characteristics of the optical instrument. The modelling of the three aspects of the image geometry, which has already been discussed in sections 2.1 to 2.3, are resumed in table 1.

	Aspects of image geometry		
	Orbit	Attitude	Optical instrument
Model	Dynamic model: Acceleration caused by the Kepler term and J_2 term taken into account. Orbit determined by integration.	Data fitting: Cubic spline functions describe pitch, roll and yaw.	Central projection: Each row is the result of a central projection which is fixed with respect to the satellite's platform.
Parameters	The satellite's position and velocity vector at the initial time t_0.	B-spline coefficients of the 3 cubic splines.	Look angles for the end detectors and focal length.
Pseudo-observations from auxiliary data	The satellite's position and velocity vector at the initial time t_0.	Velocities for pitch, roll and yaw at 0.1s intervals.	Look angles for the end detectors and focal length.

Table 1 - The mathematical model for the image geometry and the use of auxiliary data

Image coordinate measurements provide the row and column number *(r,c)* of an imaged point. As well-defined points can be located with sub pixel accuracy, *r* and *c* are expressed as real numbers. The row *r* of a point determines the time of imaging, the column *c* the position of the imaging detector in the CCD array. The time of imaging *t* is obtained from *r* with the time of imaging of the centre line t_{3000} (given by SPOT) and the row sampling interval (1.504 ms): $t = t_{3000} + (r-3000)*1.504\ ms$. The distance from the centre of the CCD array follows from *c* and the detector spacing (0.013mm): $x = (c-3000.5)*0.013mm$.

Collinearity equations are now written to express the fact that, at the time of imaging, the vector pointing from the projection centre to the imaging detector *((x,y,-f)* in the instrumental reference (fig. 6)) and the vector pointing from the projection centre to the ground point $(X_p - X_s(t))$ in the geocentric reference frame) lay at the same straight line (fig. 7): $(x\ y\ -f)^t = k\ R_{ia}\ R_{ao}\ R_{og}\ (X_p - X_s(t))$. The first two coordinates of $(x\ y\ -f)^t$ are used as the observed quantities, while *t* is kept fixed. With three successive rotations, the vector $(X_p - X_s(t))$ is expressed in the instrumental reference frame: by the first rotation R_{og} it is expressed in the orbital reference *(p,r,y)*, by a second rotation R_{ao} in the attitude

reference *(x1,x2,x3)* after which a final rotation R_{ia} leads to the expression in the instrumental reference *(x,y,z)*. The triad *(p,r,y)* is defined by the satellite's position and velocity vector at time *t*, and therefore the elements of R_{og} can be expressed as a function of the satellite's initial position and velocity vector. The elements of the rotation matrix R_{ao}, which transforms from *(p,r,y)* to *(x1,x2,x3)* can be written as functions of the coefficients of the spline functions for pitch, roll and yaw, which describe the misalignment between *(p,r,y)* and *(x1,x2,x3)*. Finally, the elements of R_{ia} are functions of the detector look angles, which describe the orientation of *(x,y,z)* with respect to *(x1,x2,x3)*.

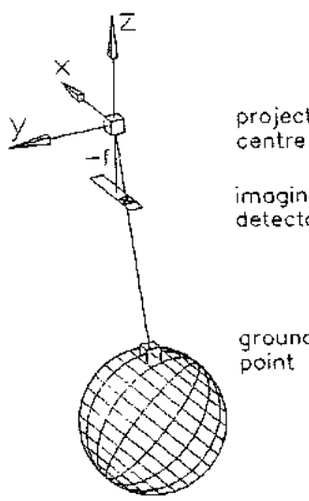

Fig. 6 - The instrumental reference system.

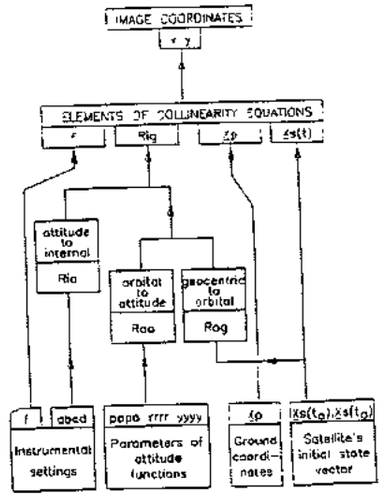

Fig. 7 - Elements of the collinearity equations.

3. - The OEEPE test on triangulation with SPOT data

The Institute participated with five other research centres to the project on triangulation of SPOT data of the OEEPE (European Organisation for Experimental Photogrammetric Research). The other participants were University College London (which acted as pilot centre), the University of Hannover, l'Institut Géografique National (IGN) (Paris), Canada Centre for Mapping (Ottawa, Canada) and the Queensland Department of Geographic Information (Brisbane, Australia). Each research centre independently processed the test data and carried out bundle adjustments, each applying its own approach to the modelling of the imaging geometry.

3.1 - The test data

The data of the OEEPE test consisted of a) four sets of four successive SPOT images from different passes over a 110x200 km area in the South East of France, b) the corresponding auxiliary data, and c) a set of about 200 ground control points, visibile in the imagery and determined by IGN from surveying, aerial photogrammetry and maps. Table 2 and figure 8 summarize the characteristics of the imagery and the types of auxiliary data, which were introduced in the bundle adjustments.

	STRIP 1		STRIP 2	
Instrument	HRV2	HRV1	HRV1	HRV1
Date	28 7 86	30 8 86	19 4 87	26 4 87
Start of image acquisition	10:58:01.4	10:23:18.2	11:00:39.8	10:25:57.3
End of image acquisition	10:58:35.8	10:23:52.0	11:01:14.2	10:26:31.1
Image size (rows x columns)	22858 x 6000	22462x 6000	22872x 6000	22470x 6000
Look angle a (1st detector	18.5°E	24.4°W	20.6°E	23.8°W
Look angle b last detector	22.6°E	20.3°W	24.7°E	19.7°W
Cloud cover (cc) (# of quarter scenes)				
0% < CC < 10%	16	11	9	13
10% < CC < 25%	0	2	3	0
25% < CC	0	3	4	3

	STRIP 1		STRIP 2	
Orbital elements	6	6	6	6
Pitch velocities	275	270	273	269
Roll velocities	275	270	273	269
Yaw velocities	275	270	273	269
Look angles + focal length	5	5	5	5
Image points measured				
by Wild in hard copies	83	83	106	106
by IGN in soft copies	100	100	—	—

Table 2 - Characteristics of the imagery data; image measurements and auxiliary data.

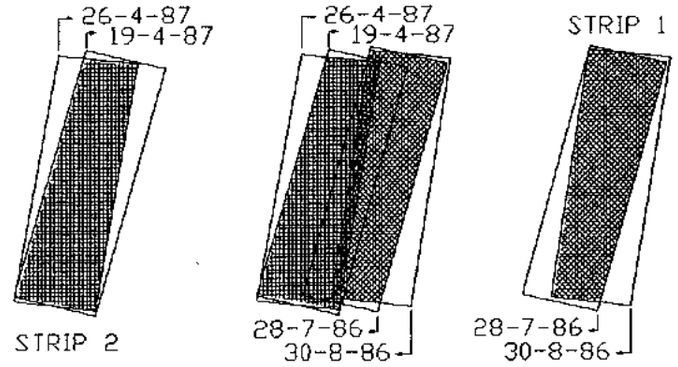

Figure 8 - Coverage of the test area by the imagery of the four passes.

Basically, the imaged area consists of two North-South strips, each of which is covered in oblique viewing from two satellite passes. The imagery was not completely cloudfree, and therefore not all available ground control could be used. The total number of lines per pass is somewhat smaller than 4x6000, because adjacent images have a small overlap. The

imagery was available both in the form of soft copies (i.e. computer compatible tapes with the brightness counts of the 6000^2 pixels of each image) and in the form of hard copies. These, film diapositives of 174x150mm, had been produced by IGN, with a stretched pixelsize (29x25 micron) to compensate for the length distortion in the across track direction due to the oblique viewing. Each diapositive contained eight collimating points to allow for the conversion from photo coordinates to pixel coordinates.

With the Zeiss PK-1 monocomparator of the Institute the image coordinates were measured of 83 control points on the imagery of strip 1, and of 106 points on the imagery of strip 2. In addition, measurements were available, which had been obtained by IGN directly from the digital data, consisting of the pixelcoordinates of 100 ground points in the imagery of strip 1. The ground control points consisted various topographic elements visible in the imagery, like cross-road centres, edges of fields and woods, confluences of rivers, bridges, etc. While their approximate location in the imagery was indicated on paper prints, their exact definition was provided by sketches.

3.2. - The bundle adjustments

The pilot centre of the project had prescribed 10 different control point configurations (fig. 9) to investigate the effect of changes in the number and distribution of ground control on the quality of the results.

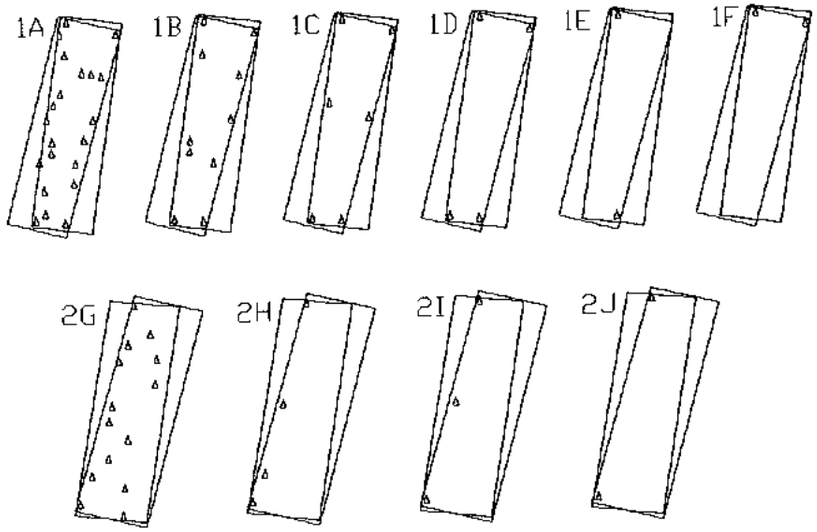

Figure 9 - Control point configurations for the bundle adjustments with the data of strip 1 and 2.

Sixteen bundle adjustments were carried out, ten with the Institute's PK-1 measurements in the imagery of strip 1 and 2, and six with the IGN measurements in the imagery of strip 1. In the bundle adjustments, each set of four successive images was treated as a single image: instead of four different orbital arcs and four different functions for pitch, roll and yaw for each image, a single orbital arc and a single function for pitch, roll and yaw were determined. The observations consisted of a) the observed image coordinates, b) relevant auxiliary data and c) the coordinates of the ground control points. The unknowns consisted of the ground coordinates of the measured image points and the parameters describing the image geometry. After the adjustments, the estimated ground positions of the points, which had not been used as ground control, were expressed in geographic coordinates, and were compared to the values given by IGN. The RMS differences for the sixteen bundle adjustments are presented in table 3.

	Milan bundle adjustment of Milan measurements on diapositives									
Control configuration	1A	1B	1C	1D	1E	1F	2G	2H	2I	2J
Nr of checkpoints	60	70	74	76	78	78	89	99	100	101
RMS_N	10.6	11.5	11.0	10.8	11.5	15.7	9.0	8.5	8.3	8.3
RMS_E	11.7	11.9	12.2	12.2	12.1	15.5	10.3	13.9	11.9	14.2
RMS_H	13.1	12.5	12.9	12.7	13.3	11.2	11.4	12.0	12.0	12.3
RMS_{vector}	20.5	20.7	20.9	20.6	21.3	24.4	17.8	20.3	18.9	20.5

	Milan bundle adjustment of IGN measurements in digital imagery						
Control configuration	1A	1B	1C	1D	1E	1F	$RMS_{di} = \sqrt{\frac{\sum_{i=1}^{n} di^2}{n}}$
Nr of checkpoints	75	85	89	91	93	93	
RMS_N	9.5	9.3	9.2	9.3	10.6	10.8	N: nord
RMS_E	11.1	13.2	12.4	13.8	12.2	19.7	E: east
RMS_H	14.8	13.6	13.5	15.1	18.1	14.7	H: height
RMS_{vector}	20.8	21.1	20.5	22.5	24.3	26.8	

Table 3 - RMS values of the differences between the checkpoint coordinates, determined in the bundle adjustments, and those, determined by IGN from maps, surveying and aerial photogrammetry.

The results of the bundle adjustments are analysed in the next section, where they are placed in the broader context of the determination of the accuracy potential of bundle adjustments with SPOT data.

4. - The accuracy potential of triangulation with SPOT data

The objective of the OEEPE project on triangulation with SPOT data was to determine the positional accuracy, which can be obtained for triangulated points from a strip covered by stereo SPOT data, the number of control points necessary, and the use, which

can be made of auxiliary data. These questions are dealt with in the following, from a theoretical point of view as well as from the results of the processing of the test data.

The precision of point positioning by bundle adjustments wit SPOT data depends on three factors: a) the precision of the image coordinate measurements, b) the precision of the knowledge of the imaging geometry, and c) the geometry of the imaging rays, which intersect at the ground point.

4.1. - The geometry of the imaging rays

The ground position of a point, measured in SPOT imagery from two (or more) different passes, is located at the intersection point of the two (or more) imaging rays (fig. 10).

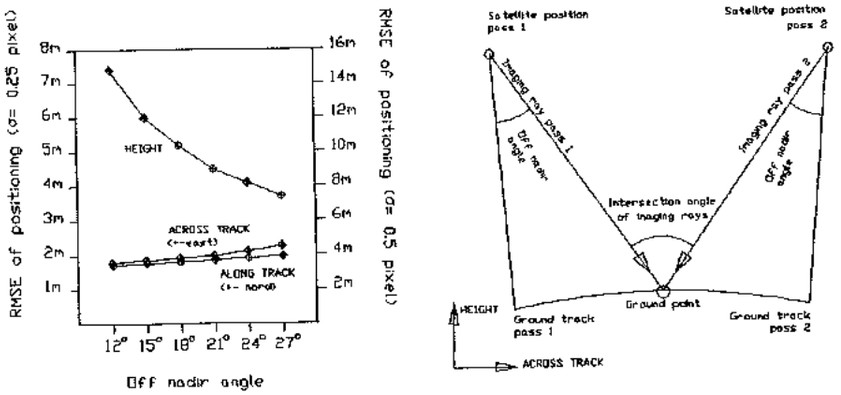

Figure 10 - Geometry of the imaging rays and the resulting positioning precision (perfect knowledge of imaging geometry assumed).

If the imaging geometry were perfectly known, the precision of the ground coordinate estimates would be determined directly by the precision of the image coordinate measurements and the intersection geometry. In practise the imaging geometry will, of course, never be known perfectly. However, it is worthwhile to start with this assumption, in order to determine the precision limits, which would be obtainable with an infinite number of control points.

Due to the characteristics of the orbit of the SPOT satellites, different satellite passes and the scanlines obtained from them are both practically parallel. The parallellity of the scanlines results in a remarkable separation between the positioning contributions of the row and column measurements of a point in the (oblique) imagery of two passes: while the row measurements determine the ground point's along track position with one degree

of redundancy, the two column measurements provide just enough information to determine its across track position and height.

The planimetric precision only weakly depends on the off-nadir angle: it deteriorates only slightly for large off-nadir angles. The standard deviation of the height estimate is larger than that of the along and across track direction, due to the sharp intersection angle of the imaging rays. Considerable improvements are obtained by increasing the off-nadir angle.

4.2 - The precision of image coordinate measurements

It goes without saying that the precision of point positioning from imaging ray intersection directly depends on the precision, with which the ground point can be located in the imagery. The obtainable precision of image coordinate measurements, expressed in terms of pixels, depends on many different factors. One of the decisive factors is the local image contrast in the neighbourhood of the imaged point. This not only depends on the terrain characteristics, but also on illumination conditions, e.g. the presence of shadows, haze or cloud shadow.

The quality of the points in the data set of the OEEPE test was very inhomogeneous: while some points could be identified easily and located precisely, other points could only be recognized with effort and located only (relatively) approximately, due to poor local image contrast, the presence of shadows, or unclear point definitions. A number of points were remeasured in order to determine the precision of the image coordinate measurements. The results showed that well defined points can be measured with an RMSE below 0.25 pixel for both row and column position. The same value was obtained by Westin in a test, where the ground control points had been chosen with care *(Westin, 1990)*. For the set of points of the OEEPE test, the RMSE for the row and column measurements was about 0.5 pixel.

In addition, a comparison was made between the IGN soft copy measurements and the Institute's hard copy measurements. For the imagery of both passes of strip 1, a substantial mean difference was found for both row measurements (mean(IGN-Milan): +0.5 pixel) and column measurements (mean(IGN-Milan): -1 pixel). With respect to these mean values, the RMS difference was about 1 pixel for both row and column. The mean differences indicate a systematic error in either the measurements of the Institute (erroneous pixel values for the collimating points ?) or those of IGN. These systematic errors are probably easily absorbed by the image orientation parameters. The RMS of 1 pixel in the differences is somewhat higher than the value which would be expected (0.7 pixel) with the assumption of an RMSE of 0.5 pixel for the measurements. This could be

due to deformations introduced during film printing. The results of the adjustments with both sets of measurement data show however that a possible degradation of image quality during film production did not have a significant effect on the results.

4.3 - The knowledge of the imaging geometry

Due to the inevitably imperfect knowledge of the imaging geometry, the precision limits, which were derived in section 4.2, will never be reached: the standard deviations of the coordinate estimates for the ground points will therefore be somewhat larger than the derived lower limits.

The number of ground control points, which has to be added to keep the effect of the uncertainty about the imaging geometry within reasonable limits, can be reduced by a) the use of auxiliary data and the knowledge of the gravitational field, and b) by the processing of successive images of a pass as a single image. The ephemeris data and the knowledge of the forces, which govern the satellite's motion, would be sufficient for an accurate reconstruction of the orbital arc, if the position data would be more accurate: for an adequate estimate of the orbital arc ground control is only needed to improve the position data. The attitude angle velocities allow for a description of variations of pitch, roll and yaw during image acquisition: ground control is (only) needed for the determination of the unknown constant in the three angles. The end detector look angles provide a complete description of the central projection geometry of the optical instrument: here ground control is not strictly necessary but can contribute to a further improvement of the knowledge of the look angles. Thanks to the precise knowledge of the force field and the availability of dense series of attitude velocity data, the reconstruction of the orbital arc and of the three attitude angle functions corresponding to multiple successive images requires (practically) the same number of ground control as that required for a single image.

The check point differences for the different control point configurations (tab. 3) only slowly increase as the number of ground control points decreases from 20 to 2 for strip 1 and from 14 to 2 in strip 2. The same trend is shown by the mean standard deviations of the checkpoint coordinate estimates, obtained (from variance propagation) in the bundle adjustments (tab. 4).

The RMSE of the ground control and the image measurements have been estimated by the application of a method for variance estimation proposed by Kubik *(Kubik, 1970)* to bundle adjustments, in which all ground control coordinates had been introduced as observations. The estimated RMSE for the image coordinates confirmed the previuously found value of 0.5 pixel, the ground control coordinates had an estimated RMSE of about

6m. Because of the large number of observations per group (300 ground coordinates and 400 image coordinates) and the high redundancy of the observations (between 40% and 70%) these estimates can assumed to be significant.

	1F	1E	1D	1C	1B	1A	
# gcp	2	2	4	6	10	20	∞
$RMSE_N$	6.9	6.9	5.7	5.2	4.8	4.5	3.9
$RMSE_E$	7.0	6.9	5.8	5.4	5.0	4.8	4.2
$RMSE_H$	12.5	12.3	11.0	10.4	10.0	9.7	9.0
RMSE vector	15.9	15.7	13.7	12.8	12.2	11.7	10.6

Table 4 - The mean standard deviations of the checkpoint coordinate estimates in the bundle adjustments with the IGN data, and in the hypothetical case of known image geometry. Assumptions: RMSE image measurements 0.5 pixel, RMSE ground coordinates 6m.

5. - Aknowledgements

The author wishes to express his gratitude to the OEEPE, IGN and the Commision of the European Communities for their contribution to the research of Institute on triangulation with SPOT data. He thanks IGN for providing the test data, the OEEPE for sponsoring the project, and the Commission of the European Communities for partial funding of the reasearch.

References

Chevrel M., Courtois M., Weill G. (1981), The SPOT satellite remote sensing mission. Photogrammetric Engineering and Remote Sensing, volume XLVII, nr. 8, August 1981.

Förstner W. (1985), The reliability of block triangulation, Photogrammetric Engineering and Remote Sensing, volume LI, nr. 6, August 1985.

Friedmann D., Friedel J., Magnussen K., Kwok R., Richardson S. (1983), Multiple scene precision rectification of spaceborn imagery with very few control points. Photogrammetric Engineering and Remote Sensing, volume XLIX, nr. 12, December 1983.

Kubik K. (1970), The estimation of weights of the measured quantities within the method of least squares. Bulletin Géodésique, nr. 95, 1970.

Kovalevsky J. (1989), Lecture notes in celestial mechanics. In: Sansò F., Rummel R. (Eds) (1989), Theory of Satellite Geodesy and Gravity field determination. Lecture notes in earth sciences, nr. 25, Springer Verlag, Berlin, 1989.

Schumacher L. (1981), Spline functions, basic theory, Wiley and sons, New York.

Spotimage (1988), SPOT User handbook. CNES and Spotimage, Toulouse.

Togliatti G., Moriondo A. (1988), Evaluation métrique et sémantique des images SPOT. Bulletin d'Information de l'Institut Géografique National, nr. 58, December 1988.

Westin T. (1990), Precision rectification of SPOT imagery, Photogrammetric Engineering and Remote Sensing, volume LVI, nr. 2, February 1983.

Triangulation of SPOT Imagery at the Department of Lands, Queensland[1]

Russell J Priebbenow[2]

Abstract

A mathematical model is developed to describe the relationship between SPOT image coordinates and ground coordinates, for a strip of SPOT imagery acquired from a single orbit pass. The model, based on that developed by the author for single SPOT images, uses orbital equations to model the satellite path, while variations of the satellite attitude with time are modelled using low order polynomials and the on-board attitude velocity measurements. This model is used to test four strips of four images over a region in south-eastern France, with coordinates of control and check points provided by IGN, France. The results verify the model and show that triangulation of SPOT imagery is an effective means of reducing the ground control requirement for a block of SPOT imagery.

1. Introduction

During 1989, the OEEPE (Organisation Européenne d'Etudes Photogrammétriques Expérimentales) sponsored a research project to investigate the triangulation of strips of images from the French satellite SPOT. The test involved four strips of four images, with each strip acquired from a single orbit pass. The sixteen images formed eight stereo pairs over part of south-eastern France. The principal aim of the experiment was to determine whether triangulation is a valid technique for reducing the ground control requirement for strips of SPOT imagery. The behaviour of a number of triangulation algorithms developed by the participants in the project was assessed using a number of different configurations of ground control points.

The laboratories involved in the experiment were each provided with the set of sixteen images, and sketches of the locations of a number of control and check points. The image coordinates of these control and check points were not provided with the imagery, but instead were to be determined by each researcher. Using the ground and image coordinates of ten combinations of

[1]Presented at the OEEPE Workshop on the Triangulation of SPOT Data, University College London, Sept 27-28, 1989. Revised 30th May 1990.

[2]Russell J Priebbenow PhD (Qld), B Surv (Hons) (Qld), Specialist Technical Advisor, Sunmap Remote Sensing Centre, Division of Information, Queensland Department of Lands, PO Box 40, Woolloongabba Qld 4102, Australia.

ground control points, the ground coordinates of the check points were then to be determined. A subsequent test was also carried out with one pair of image strips using a set of image coordinates determined by IGN. This paper presents the model used by the author for this experiment, the procedure used by him to carry out a number of tests with the data, and the results of these tests.

2. Mathematical Model

In order to calculate ground coordinates from image coordinates, it is necessary to use a mathematical model which describes the relationship between these two sets of coordinates. This model is subsequently referred to as the image ground model. The model used for this experiment is based on that presented by Priebbenow and Clerici (1987), and is presented in Equations 1.1 and 1.2.

$$\begin{pmatrix} 0 \\ y' \\ -f' \end{pmatrix} = \lambda \cdot M \cdot \begin{pmatrix} X_m - X_s \\ Y_m - Y_s \\ Z_m - Z_s \end{pmatrix} \quad \ldots\ldots (1.1)$$

$$x' = k \cdot t \quad \ldots\ldots (1.2)$$

The various components of these equations are now described.

- x' and y' are the observed image coordinates, defined with respect to a rectangular coordinate system with the x' axis perpendicular to the image lines and the origin at the centre of the central line of the image.
- f' is the focal length of the SPOT HRV (the SPOT sensor system), scaled so as to be compatible with the image line length. This value is calculated using the detector look angles provided with the image auxiliary data. In subsequent discussion, the coordinates y' and f' also correspond to coordinates in the HRV coordinate system.
- k is a scale factor which defines the relationship between the image x' coordinate and time t.
- t is the relative imaging time, and is defined with respect to an origin t_0 which is equal to 0 at $x' = 0$ in the first image of a strip of images acquired from a single orbit pass.
- λ is a scale factor.
- X_m, Y_m, Z_m are the coordinates of the ground point, in a cartesian coordinate system referred to as the model coordinate system. The model coordinate

system is defined with respect to the GRS80 coordinate system. Its origin is on the surface of the GRS80 ellipsoid at the mean of the nominal scene centres, as determined from the auxiliary image data. The geodetic (GRS80) coordinates of the model origin are designated (λ_0, Φ_0) and the geocentric coordinates of this point are designated (X_{e0}, Y_{e0}, Z_{e0}). The Y_m axis is in the mean flight direction of the satellite, as determined from the scene orientation angles provided with the image auxiliary data. The azimuth of the Y_m axis is $(\pi+H)$. Figure 1 shows the relationship between the geocentric and model coordinate systems.

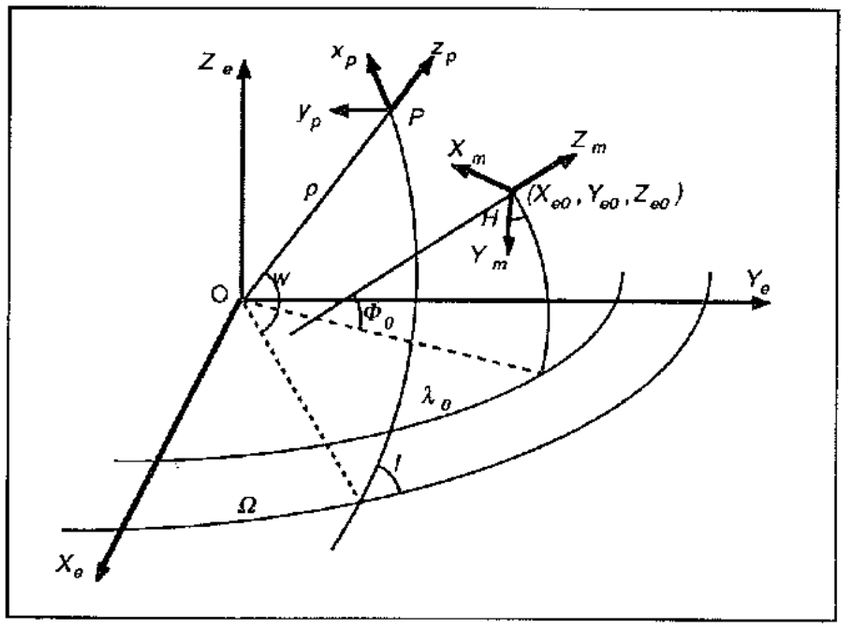

Figure 1 Model coordinate system (X_m, Y_m, Z_m), ideal platform coordinate system (x_p, y_p, z_p), and satellite orbit parameters (ρ, I, Ω, w), showing their relationship to the GRS80 geocentric coordinate system (X_e, Y_e, Z_e).

Ground coordinates, based on a local geodetic datum, can be transformed to the GRS80 datum in two steps. Firstly, geoidal heights are corrected for the separation between the geoid and ellipsoid. For this experiment, the geoid ellipsoid separation over the test area was approximated, to an accuracy of better than 0.5 m, by a ten parameter polynomial in Easting and Northing. Secondly, the coordinates are transformed from the local datum to the GRS80 datum using parameters such as those provided in DMA (1987). The effect of any small inaccuracy in these transformation parameters is negated, since the

same parameters are used to transform ground control coordinates to the model coordinate system for determination of the image ground model, and subsequently in the reverse procedure to determine the ground coordinates of unknown points using the resulting image ground model.

- X_s, Y_s, Z_s are the coordinates of the perspective centre of the HRV, in the model coordinate system. These parameters vary with time, and are expressed in terms of the osculating orbital parameters $(\rho, I, \Omega, w, e_x, e_y)$ each of which varies with t. Only the variation with time of these parameters as described by Keplerian motion, perturbed by the V_{20} term of the earth's gravitational harmonic series, is considered. Figure 1 shows the first four of these parameters with respect to the GRS80 geocentric coordinate system (X_e, Y_e, Z_e).

  The definition of these six osculating parameters is:

  ρ geocentric distance to the satellite,
  I inclination of the orbit plane, with respect to the equatorial plane,
  Ω longitude of the ascending node, with respect to a geocentric coordinate system,
  w angular distance of the satellite from the ascending node, in the orbit plane, equivalent to the sum of the argument of the perigee ω and the true anomaly f,
  e_x $e \cdot \cos \omega$, where e is the orbit eccentricity,
  e_y $e \cdot \sin \omega$.

  The variation of these parameters with time is described using Lagrange Planetary Equations, which are given in Toutin (1985). The value of each parameter at any time t is calculated from its value at an initial time (t_0-5) using numerical integration. The values of the parameters at this initial time are designated $(\rho, I, \Omega, w, e_x, e_y)(t_0-5)$.

- $\boldsymbol{M}$ is an orthogonal matrix which rotates model coordinates into a system parallel to the HRV coordinate system. This matrix varies with time t. It can be expressed as the product of a series of rotations, by

$$\boldsymbol{M}^T = \boldsymbol{R}_Z(\pi/2-H) \cdot \boldsymbol{R}_Y(\Phi_0) \cdot \boldsymbol{R}_X(\lambda_0-\Omega) \cdot \boldsymbol{R}_Z(\pi/2-I) \cdot \boldsymbol{R}_Y(-w) \cdot \boldsymbol{R}_Z(\kappa_p) \cdot \boldsymbol{R}_Y(\phi_p) \cdot \boldsymbol{R}_X(\omega_p) \cdot \boldsymbol{R}_Y(\phi_m) \cdot \boldsymbol{R}_X(-\omega_m) \cdot \boldsymbol{R}_Z(\kappa_m) \quad \ldots\ldots (2)$$

  where

  - rotations of the form $\boldsymbol{R}_a(\theta)$ denote rotations of the angle θ about the 'a' axis;

  - Φ_0, λ_0, and H are angles used to define the model coordinate system, as described above, and are treated as fixed parameters of the image ground model;
  - Ω, I and w are osculating parameters which vary with time, as defined above;
  - the product $\boldsymbol{R}_Z(\pi/2-H) \cdot \boldsymbol{R}_Y(\Phi_0) \cdot \boldsymbol{R}_X(\lambda_0-\Omega) \cdot \boldsymbol{R}_Z(\pi/2-I) \cdot \boldsymbol{R}_Y(-w)$ defines the angular relationship between the model coordinate system and the ideal platform coordinate system;
  - ω_p, ϕ_p and κ_p are angles of rotation which define the angular relationship between the ideal and actual platform coordinate systems. The ideal platform coordinate system (x_p, y_p, z_p) is shown in Figure 1, and approximates the mean actual platform coordinate system whose axes are parallel to the Roll, Pitch and Yaw axes of the platform. These angles are small and vary with time. They consist of two components: polynomials as functions of time, expressed using the parameters $(\omega_0, \omega_1, \omega_2, \phi_0, \phi_1, \phi_2, \phi_3, \kappa_0, \kappa_1, \kappa_2)$; and estimates of the variation of the satellite attitude as derived from an integration of the on-board attitude velocity measurements, designated as $Yaw(t)$, $Pitch(t)$ and $Roll(t)$. The angles ω_p, ϕ_p and κ_p are thus given by Equation 3.

$$\begin{aligned} \omega_p(t) &= \omega_0 + \omega_1 \cdot t + \omega_2 \cdot t^2 + Roll(t) \\ \phi_p(t) &= \phi_0 + \phi_1 \cdot t + \phi_2 \cdot t^2 + \phi_3 \cdot t^3 - Pitch(t) \\ \kappa_p(t) &= \kappa_0 + \kappa_1 \cdot t + \kappa_2 \cdot t^2 + Yaw(t) \end{aligned} \quad \ldots\ldots (3)$$

  - ω_m, ϕ_m and κ_m are angles of rotation which define the angular relationship between the HRV and actual platform coordinate systems, and are derived from the detector look angles provided with the satellite auxiliary data. These angles are treated as fixed parameters of the image ground model.

The above image ground model is expressed in terms of a number of known and unknown parameters. The values of the unknown parameters are to be determined using the observed image coordinates and ground coordinates of a set of ground control points, and in some cases, also using the observed image coordinates of additional parallax points. The unknown parameters of the model are:

- The satellite orbital parameters $(\rho, I, \Omega, w)(t_0-5)$. In the least squares solution of the image ground model parameter values, the parameters $(e_x, e_y)(t_0-5)$ are not treated as unknown. Rather, the values of these parameters are

derived from the satellite ephemeris records provided with the auxiliary image data. Priebbenow (1989) shows that that the treatment of these parameters as unknown does not enhance the accuracy of ground coordinate determination, and increases the number of model parameters and thus the minimum ground control requirement. Approximate values for $(\rho, I, \Omega, w)(t_0-5)$ are derived from the ephemeris data, and, in the least squares solution of the parameter values, are given the standard errors ±85 m, $\frac{\pm 85}{\rho}$ rad, $\frac{\pm 85}{\rho}$ rad, and $\frac{\pm 170}{\rho}$ rad respectively (Priebbenow, 1989).

- The attitude angles $(\omega_0, \omega_1, \omega_2, \phi_0, \phi_1, \phi_2, \phi_3, \kappa_0, \kappa_1, \kappa_2)$. The program which is used to calculate the image ground relationship allows the order of the ω_s, ϕ_s and κ_s polynomials to be selected, thus varying the number of attitude parameters of the model. For a single scene, it was shown (Priebbenow, 1989, p.119) that it was sufficient to use a zero order polynomial for ω_s and κ_s and a first order polynomial for ϕ_s, with a further improvement being achieved in some cases using a second order polynomial for ϕ_s. However, it is likely that higher order polynomials will be needed for a strip of images to account for low frequency attitude variations not described by the on-board attitude velocity measurements. In the least squares parameter solution, all of these parameters are initially assigned the approximate values of zero, with the following standard errors: ω_0, ϕ_0, κ_0 (±0.02°); ω_1, κ_1 (±0.0001°/s); ϕ_1 (±0.0005°/s); ω_2, κ_2 (±0.00005°/s²); ϕ_2 (±0.0001°/s²); ϕ_3 (±0.00005°/s³).

3. Observation of Image Coordinates

Prior to the commencement of the SPOT triangulation tests, it was necessary to determine image coordinates for control and check points. This section describes the process used to obtain these image coordinates.

The imagery supplied for this series of tests was in the form of second generation film positives, preprocessed to Level 1A. The size of the pixels in the *y'* direction (along line) had been scaled to minimise the 'sloping model' effect which occurs with a stereo pair consisting of two oblique images acquired with different view angles. In spite of a local contrast enhancement having been applied to this imagery, its clarity was not as good as that of other SPOT imagery which has been used by the author. This is possibly due to a combination of poor atmospheric clarity and the use of second generation copies of the images.

The image coordinates of control and check points were determined using a Zeiss Planicomp C100. An image orientation, used to determine the relationship between the image and Planicomp coordinate systems, was firstly carried out by calculating an affine transformation based on measurements of the eight reference marks on the image.

Following the image orientation, the image coordinates of each point occurring in the image were determined. Wherever possible, image coordinates were measured while viewing overlapping images stereoscopically. Where a point occurred in more than two images, its image coordinates in the third image (and subsequent images) were measured using a stereo pair consisting of the new image and one of the images in which the point had previously been measured, such that the stereo pair comprised one 'left view' image and one 'right view' image. The measuring mark was placed at the previously measured position, and the point measured in the new image by removing x and y parallax using the measuring mark in that image. In this way, the interpretation of the position of a point was common to all images.

Priebbenow (1989, p.152) showed that the observation of additional parallax points can improve the accuracy of the image ground model, and serves to reduce the overall residual y parallax in the stereo model. The image coordinates of a grid of 16 parallax points (4×4) were therefore observed in each stereo pair in Test Area A and Test Area B. Parallax points were also observed in the common area between Test Areas A and B, by stereoscopically viewing a 'left view' image from Test Area A and a 'right view' image from Test Area B, and vice versa. In these cases, the number of parallax points observed depended on the amount of overlap occurring.

Before executing the standard set of tests required for the OEEPE experiment, a further step was carried out to eliminate any gross errors, and to assist in the identification of a number of check points. Using the observations of all ground control points whose coordinates were provided, and of all parallax points, the values of the image ground model parameters were determined for the four strips of imagery. Using these parameters and the known ground coordinates of the check points, the image coordinates of all points were calculated. Any point which had calculated image coordinates which differed from observed coordinates by more than 50 µm, and any point which had not been previously located, was reobserved using these calculated image coordinates. However, unless there was clear evidence of an incorrect interpretation of the point

diagram, or of an error in the diagram or control print, the point was measured as shown in the point diagram. The points for which new image coordinates were derived as a result of this procedure are listed below in Table 1, together with the reason for the new measurement.

Point Number	Reason for Measurement of Point with Assistance of Calculated Image Coordinates
Test Area A	
029	Point not marked on control prints.
1041	Ground coordinates used to assist in correct identification of point.
1047	Ground coordinates used to assist in correct identification of point.
3005	No point diagram provided.
3041	No point diagram provided.
3043	No point diagram provided.
9002	Point not marked on control prints.
9029	Point not marked on control prints.
Test Area B	
21	Large difference between calculated and given ground coordinates. Point diagram is incorrect. New measurement at the correct intersection.
41	Large difference between calculated and given ground coordinates. Point diagram is incorrect. New measurement at the correct intersection.
1115	Large difference between calculated and given ground coordinates. Point diagram is incorrect. New measurement at the correct intersection.
1027	Ground coordinates used to assist in correct identification of point.
1047	Ground coordinates used to assist in correct identification of point.

Table 1 Check points whose image coordinates were measured using their ground coordinates to assist in their identification.

Ground coordinates were provided for 129 check points in Test Area A and for 132 check points in Test Area B. However, it was not possible to provide calculated ground coordinates for all of these points for a variety of reasons. For example, a large number of points - 17 in Area A and 4 in Area B - were measured in one image only, and ground coordinates could not be computed. Table 2 shows the points for which ground coordinates were not calculated, with the associated reason for each point. Two of the points which occur in only one image in Area A are points which are used as control points for the standard OEEPE tests: Point 026, which occurs in control distributions 'a' and 'b'; and Point 3036, which occurs in control distributions 'a' to 'd'.

The image ground model described in Section 2 treats each strip of images as a single image. It was therefore necessary to determine the line numbers of corresponding lines in successive images in each strip. This was done by

observing pairs of successive images stereoscopically, measuring the image coordinates of five points in the image overlap area, and computing the mean difference between corresponding pairs of x' image coordinates. This mean value was then rounded to the nearest 0.025 mm (one line width), from which corresponding image line numbers could be determined.

Point Numbers	Reason for which Ground Coordinates not Calculated
Test Area A 009 026 029 109 1041 1075 1124 3005 3014 3026 3028 3036 3041 3043 3046 3052 98	Points only measured in one image.
1020 1022	No point diagram provided, point not measured.
1122	Couldn't see stereo sufficiently well to measure. (Point is the peak of a mountain.)
9054	Couldn't locate the point in the images.
Test Area B 1024 1027 1029 1032	Points only measured in one image.
8	Large difference between calculated and given ground coordinates at this point (120 m E, 45 m N) so point was deleted.
89	No point diagram provided, point not measured.
1023	Couldn't locate the point in the images.
1035 1050	Couldn't locate the point in the images, even with the assistance of the given ground coordinates.

Table 2 Check points for which ground coordinates were not calculated, and the associated reason for this.

4. Test Results

The object of this study is to assess the suitability of the image ground model described in Section 2 for the triangulation of SPOT imagery. This assessment, which is described in this section, was made using five groups of tests. Firstly, a preliminary analysis of the image coordinates of ground control points was used to detect erroneous measurements. A group of tests which used the image coordinates measured by the author was then carried out to investigate some refinements to the image ground model. Thirdly, the standard set of tests for the OEEPE experiment was carried out, again using the image coordinates measured by the author. This set of tests was repeated for Test Area A using

image coordinates determined by IGN. Finally, a number of additional tests were carried out to assess a number of alternative ground control configurations to those used in the OEEPE experiment. This involved a simultaneous triangulation of the four strips of images using ten different control configurations. These five groups of tests are now described. Except where otherwise indicated, these tests use the image coordinates which were determined by the author from hard copy images.

4.1 Image Coordinate Assessment

An initial assessment of the control point data in each test area was made, to attempt to detect any erroneous observations of the image coordinates of these points. This assessment involved a determination of the image ground model parameters using all control points in the test area, and an analysis of the image coordinate residuals using the *Tau test* (Pope, 1976). In Test Area A, two control points were identified as having unacceptably high residuals, based on an initial assumption of image coordinate observations with a standard error of ±0.012 mm. Consequently, large standard errors were assigned to the image coordinates of these points for all of the tests, as follows: Point 45, ±0.05 mm; Point 3036, ±0.1 mm. (As stated above, Point 3036 occurs only in one image.) No control points in Test Area B were identified as having unacceptably high image coordinate residuals.

4.2 Image Ground Model Refinement

The image ground model proposed in Section 2 permits the choice of the order of the attitude polynomials (see Equation 3). The purpose of these polynomials is to account for low frequency attitude variations not described by the on-board attitude measurements which are supplied with the imagery. This section described a series of tests which were carried out to ascertain the most appropriate order of polynomial to use for strips of imagery such as those supplied for this experiment.

In this and all subsequent tests, the procedure used in each test is as follows:

- Calculate the parameters of the image ground model for the relevant images, using a set of ground control points.
- Use the resulting parameters to calculate ground coordinates corresponding to the observed image coordinates of the check points.

- Compute the difference between the calculated and known ground coordinates of the check points, and thus the mean and RMS difference.

This set of tests was carried out using (i) a block comprising all 16 images in the study area, using the control points from configuration 'a' (Figure 2) and configuration 'g' (Figure 3) as control for this block; (ii) Test Area A using control configuration 'a'; and (iii) Test Area B using control configuration 'g'. Earlier studies by the author (Priebbenow, 1989, p.119) indicated that, for a single scene, it was sufficient to have polynomials of order 0 for ω_s, and κ_s and that the polynomial for ϕ_s should be at least of order 1, with a potential improvement in accuracy in some cases where a second order polynomial is used for ϕ_s. This set of tests therefore uses 0, 1 and 0 as the minimum orders for polynomials in ω_s, ϕ_s and κ_s respectively. Table 3 shows the results obtained using a number of different orders of attitude polynomials.

Order of Attitude Polynomial ω_s	ϕ_s	κ_s	Coordinate Differences E Mean	E RMS	N Mean	N RMS	h Mean	h RMS
(i) Area A+B, Configuration 'a+g'								
1	1	1	-0.8	9.3	0.8	7.8	1.3	5.1
0	2	0	-0.5	9.3	1.0	7.9	1.6	5.7
1	2	1	-0.7	9.2	1.0	7.9	1.2	5.0
2	2	2	-0.6	9.3	1.0	8.0	1.2	5.0
0	3	0	-0.7	9.3	1.1	8.0	1.3	5.7
1	3	1	-0.7	9.2	1.1	8.0	1.2	5.0
2	3	2	-0.6	9.3	1.1	8.1	1.3	5.0
(ii) Area A, Configuration 'a'								
0	2	0	0.1	9.8	0.5	8.0	2.8	7.6
1	1	1	-0.7	9.7	0.6	8.0	1.3	5.1
1	2	1	-0.7	9.7	0.6	8.0	1.3	5.1
(iii) Area B, Configuration 'g'								
0	2	0	-0.1	8.9	2.3	9.5	0.7	4.3
1	1	1	-0.1	8.9	2.0	9.4	0.7	4.3
1	2	1	-0.1	8.9	2.3	9.4	0.7	4.3

Table 3 Mean and RMS differences on check points for a variety of orders of attitude polynomials, over Test Areas A and B using the control points from configurations 'a' and 'g'.

A comparison of the RMS coordinate differences in part (i) of Table 3, using an *F test* with a 95% level of significance, shows no significant difference between the results. However, it was noted that in both cases where the orders of the ω_s and

κ_S polynomials were 0, the RMS h value was 0.6 m to 0.7 m higher than in the remaining cases. These results suggest that there may be an improvement in height accuracy with the inclusion of first order terms for ω_s and κ_S, but that there is no further improvement in accuracy in E, N or h with the inclusion of higher order terms for these parameters. Similarly, there appears to be no advantage in using a ϕ_S polynomial of order greater than two.

Further tests were carried out over Test Areas A and B separately, as shown in parts (ii) and (iii) of Table 3, to verify these conclusions. The three tests in part (ii) of Table 3 show: no significant difference in planimetric accuracy in any of the three tests; a significant improvement in height accuracy with the use of first order polynomials for ω_s and κ_S; and no improvement in accuracy with the use of a second order polynomial for ϕ_S. The three tests in part (iii) of Table 3 show no significant difference in planimetric or height accuracy in any of the three tests.

For subsequent tests, first order polynomials were therefore used for ω_s, ϕ_s and κ_S, except in cases where there was insufficient ground control to justify the inclusion of first order terms. For example, the effect of the first order term in the ϕ_s polynomial is equivalent to a scale change in the along-track direction, and if control is not distributed in this direction, such as in configuration 'f', the inclusion of such a term could worsen rather than improve the accuracy of determination of ground coordinates. Also, the adjusted values of the first order ϕ_s and κ_S parameters have a correlation of approximately 90%. Therefore, where there are low numbers of ground control points, the first order κ_S parameter has been omitted.

4.3 OEEPE Experiment

The official OEEPE experiment involved a triangulation of the SPOT images using each of the ten specified control configurations shown in Figures 2 and 3. The attitude polynomials used for ω_s, ϕ_s and κ_s in these tests were of order 1, 1 and 1 respectively, where there were sufficient ground control points to justify the use of first order parameters. Table 4 shows the results of these tests, and the order of the attitude polynomial used in each case. In Test Area A, 108 check points were used to obtain the results shown, while in Test Area B, 123 check points were used.

Comparisons of the RMS differences in Table 4 were made using an *F test*, at a significance level of 95%, to indicate whether differences between RMS values

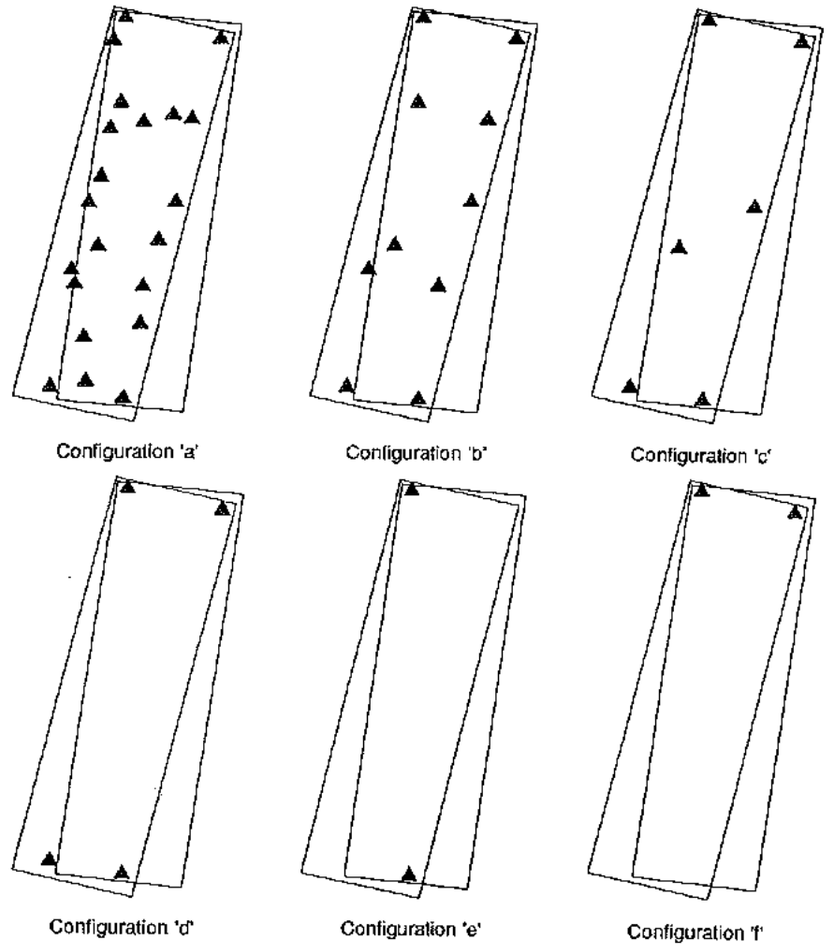

Figure 2 Control configurations 'a' to 'f' used for standard OEEPE tests in Test Area A.

are significant. A comparison of the values in Test Area A shows that in h, none of the RMS differences are significantly different from that obtained for control configuration 'a', while in E and N, only the RMS difference for control configuration 'f' is significantly larger than that obtained for control configuration 'a'. The only conclusion which can be drawn from this is that there is no significant decrease in the accuracy of ground coordinate determination as the number of ground control points decreases from 21 to 4, but as the number of points decreases below 4, there may be a significant loss in accuracy.

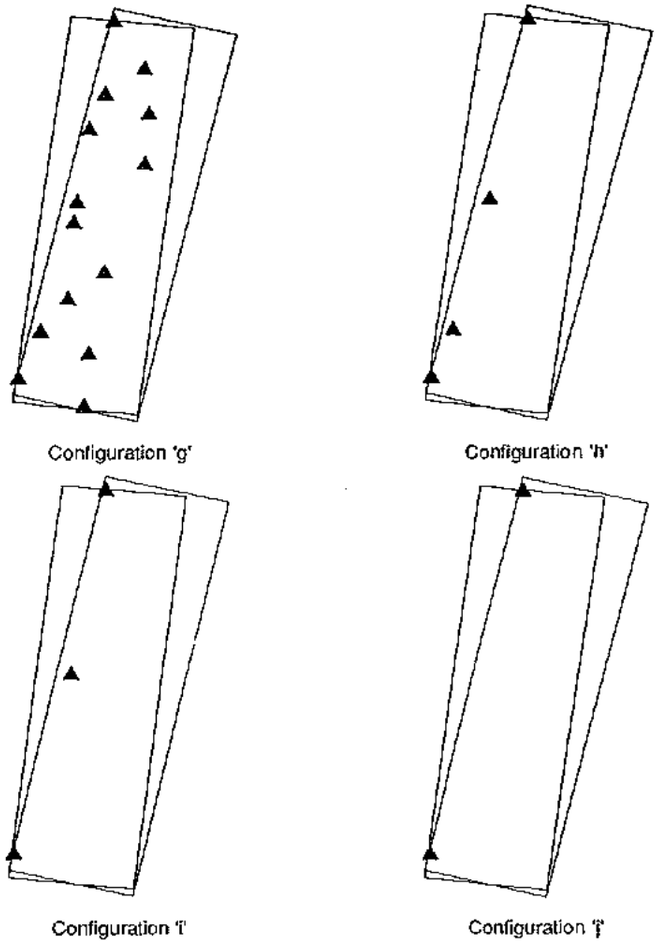

Figure 3 Control configurations 'g' to 'j' used for standard OEEPE tests in Test Area B.

A similar comparison of the values in Test Area B shows that none of the RMS differences are significantly different from those obtained for control configuration 'g', in *E*, *N* or *h*. It is therefore concluded that in this case there is no significant decrease in the accuracy of ground coordinate determination as the number of ground control points decreases from 14 to 2. This conclusion is not incompatible with that made for Test Area A. Rather, it demonstrates that, for low numbers of ground control points, good accuracy may be achievable but cannot be assured.

Configuration	No of GCP's	Order of Attitude Polynoms.	Coordinate Differences E Mean	E RMS	N Mean	N RMS	h Mean	h RMS
Test Area A								
a	21	1 1 1	-0.7	9.7	0.6	8.0	1.3	5.1
b	10	1 1 1	-0.3	10.4	0.3	8.3	0.0	6.8
c	6	1 1 1	-0.6	10.6	-0.6	8.9	1.1	5.8
d	4	1 1 1	-5.0	11.1	2.2	8.9	2.7	6.0
e	2	1 1 0	-3.9	10.4	0.2	8.1	2.7	6.0
f	2	1 0 0	-13.6	17.0	8.0	12.3	0.4	5.9
Test Area B								
g	14	1 1 1	-0.1	8.9	2.0	9.4	0.7	4.3
h	4	1 1 0	-7.0	11.6	-6.2	12.4	-1.4	4.1
i	3	1 1 0	-4.9	10.3	1.6	12.8	-0.3	3.8
j	2	1 0 0	-5.1	10.4	-4.8	11.1	2.8	5.2

Table 4 Mean and RMS differences on check points for the standard OEEPE tests.

4.4 Triangulation Using IGN Image Coordinate Observations

In order to enable a comparison to be made between the image ground models used by the various research groups involved in this study, a set of image coordinates derived by IGN was processed by each of the research groups. These image coordinate observations were monoscopic observations of the control and check points, using the digital SPOT images. The image coordinates of a total of 102 control and check points were observed. This section describes the results obtained by the author from that data set.

Initially, the image coordinate data was analysed to attempt to detect any gross errors in the observations. A triangulation which used the 21 points of configuration 'a' as control identified two check points (1124 and 9028) which appeared to have been identified differently in the left and right images, and were thus influencing the adjustment process. The image coordinate observations of these two points were therefore assigned low weights for the tests. In addition to these two points, three other check points (025, 1122 and 2016) have ground coordinate differences larger than 30 *m*. These five points have been excluded from the ground coordinates used to derive the data presented in Table 5.

This experiment involved a triangulation of the SPOT images in Test Area A using each of the six specified control configurations shown in Figure 2. The attitude polynomials used for ω_s, ϕ_s and κ_s in these tests were the same as those

Configuration	No of GCP's	Order of Attitude Polynoms.	Coordinate Differences E Mean	E RMS	N Mean	N RMS	h Mean	h RMS
a	21	1 1 1	-0.8	10.1	-0.8	8.9	2.5	10.7
b	10	1 1 1	-2.0	11.5	-0.1	8.7	1.0	10.1
c	6	1 1 1	-3.3	11.8	1.0	8.7	-0.2	10.0
d	4	1 1 1	-8.2	13.6	5.9	10.7	1.9	10.2
e	2	1 1 0	-5.9	12.0	5.4	10.5	5.3	12.0
f	2	1 0 0	-26.5	29.6	11.2	15.1	-5.4	13.3

Table 5 Mean and RMS differences on check points for the tests using image coordinates observed by IGN in Test Area A.

used for the corresponding control configurations in the test described in Section 4.3 (see Table 4). Table 5 shows the results of these tests. A comparison was made between the RMS differences of configurations 'b' to 'f' and those of configuration 'a' using of an *F test*. The results for configurations 'b' to 'e' are not significantly different from those obtained for configuration 'a' in *E*, *N* or *h*. However, the RMS differences in *E* and *N* for configuration 'f' are significantly larger than those for configuration 'a'.

A comparison of the RMS differences for configurations 'a' to 'e' with the corresponding results in Table 4 shows that the RMS differences in *E* and *N* are on average 13% larger in Table 5, while the RMS differences in *h* are 78% larger on average. This larger difference in *h* is due to the fact that the image coordinates used to derive Table 5 were observed monoscopically, and there is no correlation between corresponding pairs of image coordinate observations of the left and right images. The author (Priebbenow, 1989, p.132) has investigated the stereoscopic observation of control points in SPOT imagery, and noted correlations as high as 80% in the *y'* (height determination) direction. It can be shown that such a correlation corresponds to an improvement in the accuracy of height determination.

4.5 Additional Tests - Block Triangulation

In addition to the standard set of tests required for the OEEPE experiment, the author carried out a further series of tests to investigate the application of the image ground model to two overlapping strips of stereo pairs. These tests are now described.

This series of tests involved the triangulation of all sixteen images using the 9 different ground control configurations shown in Figure 4. The results of these tests are shown in Table 6. The results obtained for configurations 'k' to 's' are compared with those obtained for configuration 'a+g', using an *F test* as described above. In Easting, the RMS differences for configurations 'q' and 'r' are significantly higher than that for configuration 'a+g'. In Northing, the RMS differences for configurations 'q' and 's' are significantly higher than that for configuration 'a+g'. However, in height none of the RMS differences for configurations 'k' to 's' are significantly different from that for configuration 'a+g'.

Configuration	No of GCP's	Order of Attitude Polynoms.	Coordinate Differences E Mean	E RMS	N Mean	N RMS	h Mean	h RMS
Test Area AB								
a+g	35	1 1 1	-0.8	9.3	0.8	7.8	1.3	5.1
k	18	1 1 1	0.1	9.3	2.2	8.3	0.9	5.6
l	9	1 1 1	1.2	9.4	2.4	8.1	0.5	5.7
m	6	1 1 1	-3.8	10.1	2.3	8.6	0.1	5.1
n	6	1 1 0	-2.8	10.2	3.6	9.5	-0.4	5.0
o	6	1 1 0	-1.9	10.2	1.0	8.1	-1.0	5.5
p	4	1 1 0	-4.4	10.3	4.0	9.2	0.6	5.3
q	4	1 1 0	7.3	12.7	16.1	21.5	0.7	5.9
r	4	1 1 0	7.5	13.0	2.4	8.5	-0.9	5.6
s	4	1 1 0	4.8	10.6	-2.6	10.3	2.2	6.1
a+g (no Δ)	35	0 1 0	-0.2	9.5	0.4	8.0	1.2	5.8

Table 6 Mean and RMS differences on check points for a number of control configurations over the eight stereo models comprising Test Areas A and B.

On the basis of the results presented in Table 6, it is concluded that, for such a number of stereo models, no fewer than four control points should be used, and that where only four points are used, they should be in the four corners of the block. The use of more than four well distributed control points does not significantly improve the accuracy of ground coordinate determination, but may serve to improve the reliability of the results. The use of six control points distributed as shown in configurations 'n' and 'o' gives acceptable results over the entire four strips, in this case. However, the maxim used in photogrammetry that measurements should not be made outside of the area included by the ground control should also apply to SPOT imagery, due to the lower reliability outside of the extent of the control.

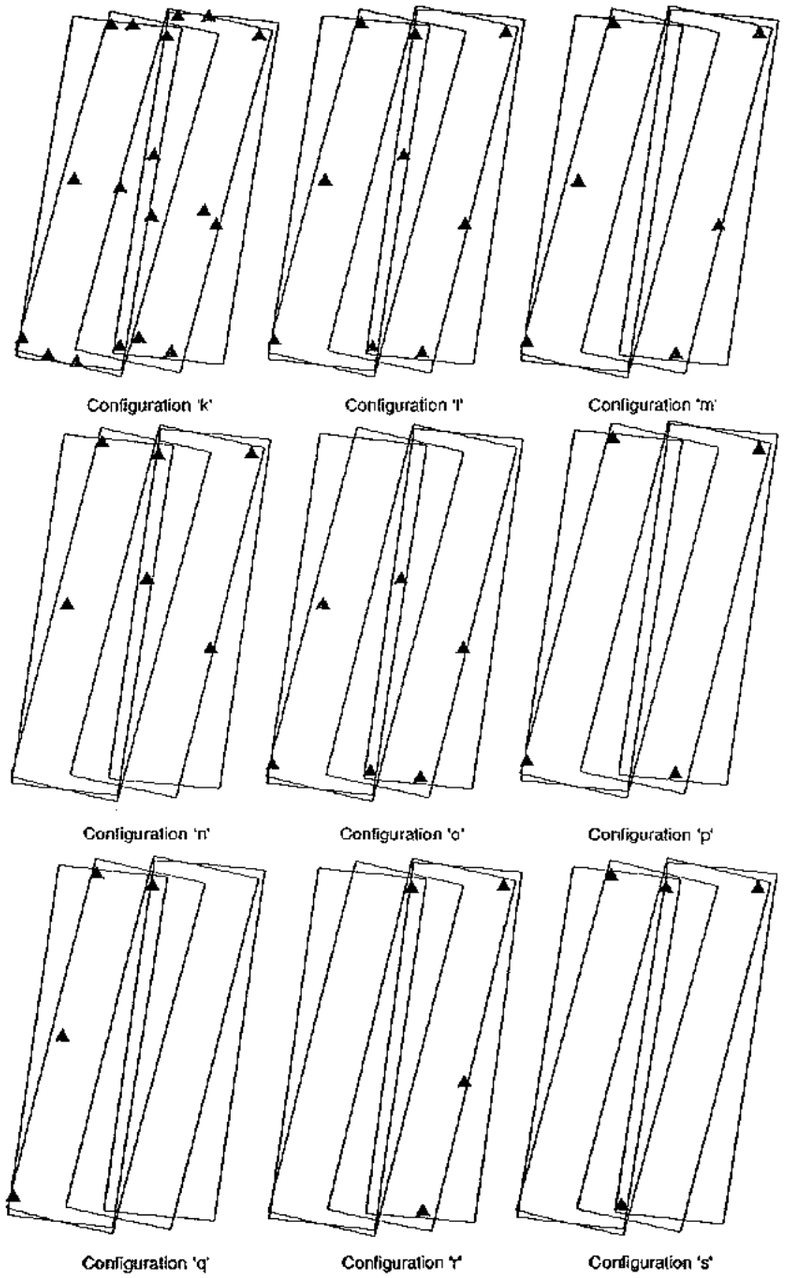

Figure 4 Control configurations 'k' to 's' used for additional tests in Test Areas A and B together.

The issue of reliability is particularly important if one considers that the image ground model for each strip of images is described by nine 'unknown' parameters (with attitude polynomials of order 1 1 0) whose values are determined during the triangulation process. If only four ground control points are used, the values of these parameters are being determined using eight image coordinate observations of the ground control points, the *a priori* estimates of the values of the parameters, and if observed, the image coordinates of additional parallax points. The likelihood of detecting erroneous image coordinate observations in such a situation is very low. For the sake of reliability, it is therefore recommended here that the minimum ground control requirement for such a block of images is six points distributed along the eastern and western edges of the block, such as in configuration 'm'.

Also shown in Table 6 (last line) are the results of an image ground model determination with no triangulation - an image ground model was determined for each of the 16 images - using the ground control configuration 'a+g'. It is noted that each of the RMS differences is slightly larger than for the same control configuration using triangulation, although these differences are not statistically significant. This result indicates that there are no significant systematic errors introduced by applying the model described in Section 2 to a strip of images.

5. Conclusions

The results of the above tests show that the triangulation of SPOT imagery is an effective means of reducing the number of ground control points required to permit the precise determination of ground coordinates from stereoscopic SPOT imagery. Whereas earlier studies by the author recommended a minimum of six control points per stereo pair, this study recommends that a minimum of six ground control points be used for a block of up to 16 images acquired in four strips of four images. These points should be distributed evenly along the eastern and western sides of the block. The image coordinate measurements of the control points should be supplemented by the observation of additional parallax points.

The above results also verify that the mathematical model proposed by the author for triangulation of SPOT imagery is appropriate. Tests of this model show that the path of the satellite can be described using four unknown parameters, and that its variation in attitude can be described using the four path parameters and an additional five or six attitude parameters.

These conclusions should be qualified by stating that they apply only where nothing unusual occurs to the orientation of the satellite during image acquisition. Generally, the attitude variations of the satellite are constrained to be small, and in such a case, the model which has been proposed should be capable of describing them. In the event of unusual attitude variations occuring, an indication of their occurence would be expected from either the on-board attitude velocity measurements or from the image coordinate residuals of additional parallax point observations.

Acknowledgements

The author wishes to thank OEEPE for sponsoring the experiment, IGN, France for providing the test data, and SPOT Image for supplying the imagery. The use of the Zeiss Planicomp at QUT for measurement of the images is also acknowledged.

References

DMA, 1987. Department of Defense World Geodetic System 1984 - Its Definition and Relationships with Local Geodetic Systems, DMA Technical Report DMA TR 8350.2, Defense Mapping Agency, Washington DC.

Pope, A.J., 1976. The Statistics of Residuals and the Detection of Outliers, NOAA Technical Report NOS 65 NGS 1, National Oceanic and Atmospheric Administration, U.S. Department of Commerce, Rockville, Md.

Priebbenow, R.J., 1989. Development of an Analytical Restitution Method for SPOT Imagery with Application to Topographic Mapping in Australia, Doctoral Thesis, University of Queensland.

Priebbenow, R.J., Clerici, E., 1987. Cartographic Applications of SPOT Imagery, Proceedings of SPOT 1 Image Utilization, Assessment, Results Symposium, Paris, November 23 - 27, pp. 1189 - 1194.

Toutin, T., 1985. Analysé mathématique de possibilités cartographiques du système SPOT, Thèse du doctorat, Ecole Nationale des Sciences Géographiques, Paris.

Strip orientation of SPOT imagery with an orbital model.

D J Gugan
Laser-Scan Limited
Cambridge Science Park
Milton Road
Cambridge CB4 4FY
UK

1 INTRODUCTION.

Work on the orientation of SPOT imagery was started in 1983, when the author was employed as a research assistant at University College London. This work was reported by Gugan (1987) and Gugan and Dowman (1988).

In 1988 the author joined Laser-Scan, who have been involved with the development of the SPOT geometric model via the Alvey MMI-137 project in collaboration with University College London (Muller, 1989). Part of this work has been the investigation of techniques for the orientation of strips and blocks of SPOT imagery.

2 THE SPOT ORBITAL MODEL.

The SPOT orbital model used as a basis for this work is described by Gugan (1987). The primary components of the dynamic motion of the satellite as an image is acquired can be modelled by the eulerian orbital parameters - the orbit ellipse shape (semi-major axis, a, and eccentricity, e), the orientation of the orbit plane with respect to the earth (inclination, i, longitude of the ascending node, Ω), the position of the ellipse within the plane (argument of the perigee, ω) and the position of the satellite within the orbit (true anomaly, F). Two of these parameters (ω and e) are held as constants because of correlation with other parameters due to the low orbit eccentricity. These parameters are shown in figure 1. Parameters F and Ω vary according to the nominal orbit period of the satellite and rate of earth rotation.

Due to orbit perturbations, the satellite attitude is also modelled by three rotations about the satellite axes, and three rates of change of the rotations.

This model was originally developed for use with photogrammetric

---

Paper presented at the OEEPE Workshop on Triangulation of SPOT Data, University College London, UK, September 27-28th 1989.

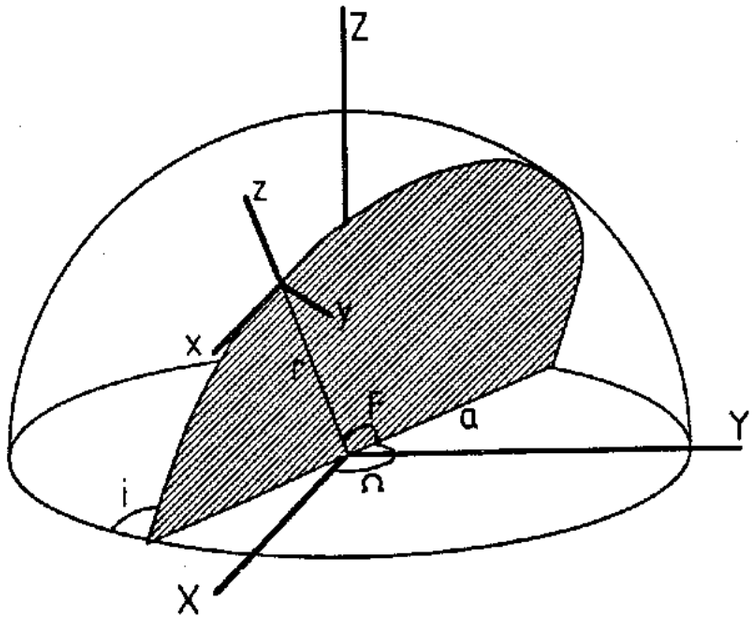

Figure 1. Orbital parameters of the SPOT geometric model.

analytical plotters, and has been implemented on Kern DSR and DSP systems, and on Wild BC2 systems. It therefore makes no use of information contained in the header, such as the position/velocity data or rates of change of attitude. The only information needed by the software is the mirror look angle, which can easily be obtained from the SPOT Image on-line data base if required.

Results of image orientations using this geometric model on the Kern DSR stereoplotter are described by Gugan and Dowman (1988). About 6 control points are required to form a stereo model, and accuracies of about 9m in plan and 4m in height are attainable with high quality control.

This software package is marketed by Kern, and has been installed in the UK, Sweden, Finland, India and Spain. The Ordnance Survey (GB) was the first organisation in the world to use SPOT imagery for a production mapping task, using this system (Hartley, 1988, Murray, 1988).

3 RESULTS WITH THE OEEPE STRIP.

The OEEPE test data for the south of France (4 strips of 4 contiguous images) were received in March 1989. These images are:

Strip A:	050-259/050-260/050-261/050-262	28th July 1986	-20.5°
	050-259/050-260/050-261/051-262	30th August 1986	22.3°
Strip B:	049-259/049-260/049-261/049-262	19th April 1987	-22.8°
	049-259/049-260/049-261/049-262	26th April 1987	21.6°

The original intention was to investigate the suitability of the orbital model described above for:

- o the orientation of long strips of data
- o modification for block adjustment using tie points

Other priorities have unfortunately limited the amount of work that has been carried out on the second objective. Preliminary work was carried out to modify the single model program to use tie points (i.e points for which ground coordinates were unknown) in the solution. The orbit model was found to be very unstable, and the results using no tie points were not improved upon. This approach was therefore deemphasised, and work concentrated on the use of the orbit model for strip-image orientation. Strip A alone was used for these tests.

3.1 Image measurement.

The image coordinates of the 8 strip A images were measured using a the Kern DSR stereoplotter. 121 control points provided by IGN were measured. These were categorised according to point quality:

'Very good'	17 %	(points measured to better than half a pixel)
'Good'	38 %	(points measured to about 1 pixel accuracy)
'Average'	22 %	(points with some doubt as to exact position)
'Poor'	17 %	(poorly defined points and/or poor image quality)
'Very poor'	6 %	(very poor image quality, e.g. haze, deep shadow)

The control point quality was a function of the quality of the ground point (for instance, sharp road junctions are much better points than hill tops), and the image quality (such as the contrast with the surrounding area). In addition, the control was derived from a number of sources - aerial survey to 1:25,000 map sheets - giving accuracies between 2 and 10m.

Overall, this exercise emphasised the need for post-acquisition selection and measurement of ground control, as preselected points may be difficult to identify on the imagery due to low local contrast or cloud/haze.

3.2 Image orientation.

The images were first orientated as single models to obtain base-line figures for the accuracy of the whole strip. 6 or 7 control points were used for each stereo pair, and between 11 and 36 check points

were used for the results below:

Image vector error range: 16 - 44 microns
Ground plan error range: 11.5 - 33.7 metres
Ground height error range: 8.1 - 11.1 metres

Overall plan error (78 check points): 22.0 metres
Overall height error (78 check points): 9.8 metres

These figures largely reflect error caused by poor control point accuracy and poor image quality (resulting in poor measurement accuracy). It should also be noted that height measurements made with a stereoscopic model set up are significantly better than measurements made in comparator mode, listed here.

At this stage the image orientation program was modified to allow the input of multiple data files with image coordinates from a contiguous strip. Figure 2 shows the strip configuration and positions of the 10 control points used. 79 points were used as independent check points giving the following results:

Image coordinate residuals		Ground residuals (estimated)	
Left	Right	Plan	Height
29 microns	27 microns	(23m)	(10m)

Unfortunately, the limited time available prevented the generation of ground residuals, so the plan and height residuals here have been estimated from comparable results.

These results show the ability of the orbital model technique to model the motion of the satellite during image acquisition. There is little or no degradation in the orientation quality caused by the modelling of four images together. It is considered that high quality control points with high precision ground measurements would produce considerably improved orientation results.

4 FUTURE DEVELOPMENTS.

Laser-Scan are primarily involved with the development of geographical information systems (GISs) and data capture systems. This includes a direct interface to Kern DSR and DSP stereoplotting instruments, geometric rectification of SPOT imagery and the generation of digital elevation models (DEMs).

Laser-Scan are currently planning further development of the Alvey-developed DEM generation system. This will include the integration of SPOT stereo model orientation software with image stereo matching. It is anticipated that the system will make full use of the attitude data available in the image header data, and will optimise the use of control/tie points in the solution. It is likely that the model described here will be superceded during this development.

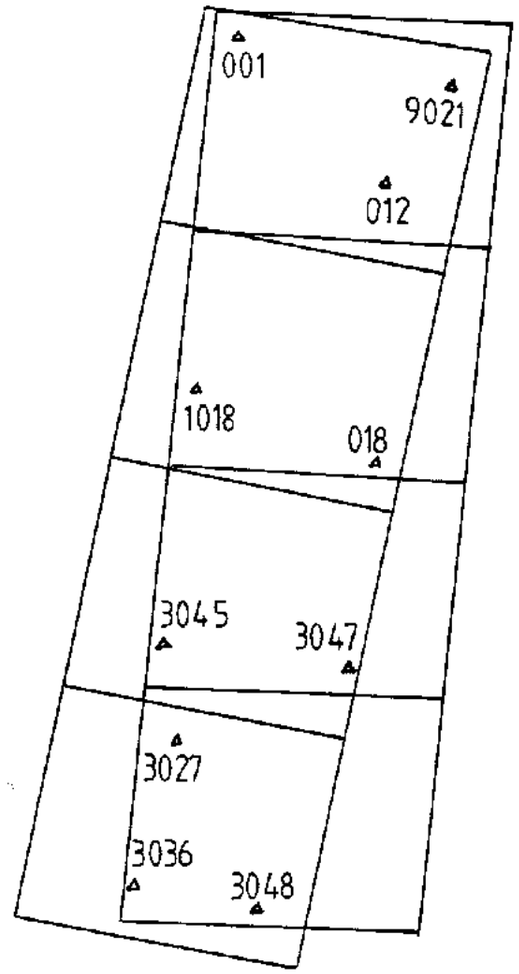

Figure 2. Configuration of control points in Strip A.

5 CONCLUSIONS.

The work described here clearly shows that a simple orbital model can be used for the orientation of long strips of SPOT image data with little or no degradation in the orientation quality attainable with a single model. It would be expected that the use of attitude data from the image header would become of increasing use with longer image strips, maintaining orientation quality.

Laser-Scan are continuing to develop systems for the extraction of topographic data from satellite imagery, and will continue to be involved in this subject area in the future.

6 REFERENCES.

Gugan, D. J., 1987. Practical aspects of topographic mapping from SPOT imagery. Photogrammetric Record, 12(69):349-355.

Gugan, D. J. and Dowman, I. J., 1988. Accuracy and completeness of topographic mapping from SPOT imagery. Photogrammetric record, 12(72):787-796.

Hartley, W. S. 1988. Topographic mapping using SPOT-1 data: a practical approach by the Ordnance Survey. Photogrammetric Record, 12(72):833-846.

Muller, J-P. A. L., 1989. Real-time stereo matching and its role in future mapping systems. Paper presented at 3rd UK National Land Surveying and Mapping Conference, Warwick, UK, 17-21st April, 1989.

Murray, K. J., 1988. The application of SPOT imagery to small scale line mapping. Photogrammetric Services internal report, Ordnance Survey, Southampton.

TRIANGULATION OF SPOT DATA AT UNIVERSITY COLLEGE LONDON

by

Francelina Neto and Ian Dowman

Background

The test area is the European test site extending from Marseille to Grenoble (France). The area of 240 Km in a north-south direction and 100 Km east-west, is covered by eight SPOT models in two strips.

Control has been fixed by IGN (Institut Géographique National - France). The control in strip A consists of 80 points from triangulation and aerial photography and 30 points fixed especially in the field. In strip B there are further 105 points from 1:25,000 maps and 1:60,000 photography.

This report covers four aspects of the test. First the orientation of the strips according to the OEEPE specification. Second, an assessment of the type of control used. Third, block adjustment using Schut's polynomial method and fourth the results fo adjustment of digital data provided by IGN.

Method of triangulation

The models were set up and observed in the Kern DSR1 analytical stereo plotting instrument. The method of orientation was that described by Gugan(1988). The software allows the orientation of a sequence of SPOT images (strip), provided that they were acquired continuously. But there are some precautions to take when performing this type of orientation.

As the images are continuous, a different inner orientation must be done for each of them. When the images are printed on film, a slight overlap is allowed between them to avoid losing information, which may cause problems. This overlap has to be measured and allowed in the inner orientation. It is usually different for each image join.

Determination of overlap of imagery joins

The overlap between two images are determined using the image coordinates. The coordinates of the image are as shown in figure 1.
As the images of one strip (left and right) have been registered continuously, the y coordinate of any point common to two images is the same. Identifying common points of two images and measuring their x coordinates in each of the two image coordinate systems, allows the calculation of the overlap (figure 2).

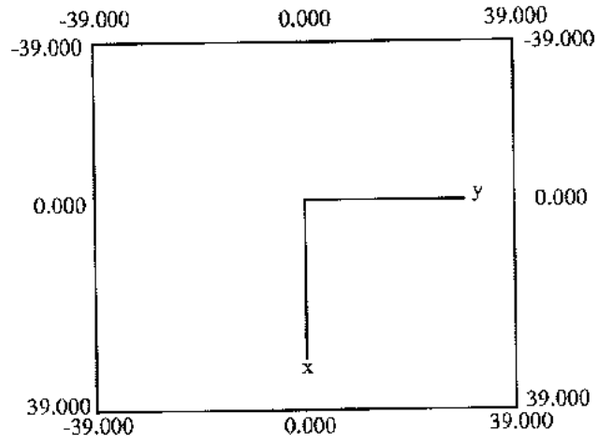

Fig 1 - Image coordinates

Consider a point P in the overlap zone as shown in figure 2, whose coordinates in the first image system are (x_1, y) and in the second image system are (x_2, y). The overlap of that join can be determined by

$$ov = (39.000 - x_1) + (39.000 - |x_2|)$$

As x_2 is always negative for P, it is

$$ov = 78.000 - x_1 + x_2$$

In order to minimise errors of measurement and to identify errors of identification, more than one point is measured in each join. The overlap of each join will then be considered as the medium value of the various values obtained for that particular join.

When a point is in the model currently set up, measuring its coordinates is not difficult. Using the mathematical model computed to set up that stereomodel, and driving the analytical stereoplotter to the correct position, they are instantaneously recorded. But it can happen that the image coordinates of one point are needed in another image coordinate system. In figure 2, one example is to know the coordinates of point Q in the coordinate system of image 1. The distance between the centres of the two images is

$$d = 2 \text{ X } 39.000 - ov$$

If the coordinates of point Q in the image 2 are (x_2, y), in image 1 they will be (x_1, y) where

$$x_1 = d + x_2$$

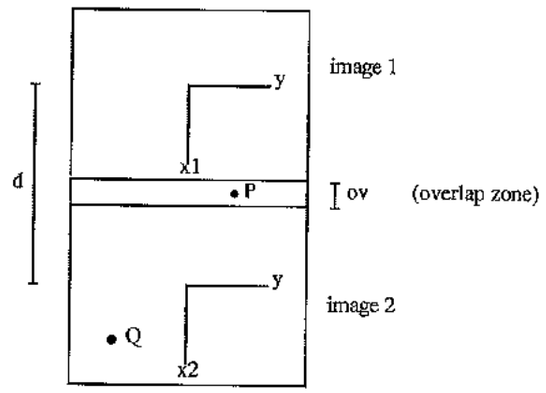

Fig 2 - Image coordinates of the same point in the two images coordinate system

After the first model of the strip has been set up, it is replaced by subsequent models, remeasuring the inner orientation. For the strip to be orientated, all the control points of the strip have to be input in one only continuous system of image coordinates. This system of coordinates is chosen to be the northern image coordinate system. So, when remeasuring the inner orientation of each model of the strip, the coordinates of its corners should be input in the northern image reference system. The current software will not deal with this situation. The solution for this problem is to translate all the already measured coordinates into the system of coordinates of the image currently in the instrument plates. After all control points of the strip have been added, the exterior orientation is re-computed and the strip is orientated.
The orientation obtained is independent of the image coordinate system actually being used. In other words, the orientation does not change if only the image coordinate system used is changed, adopting any of the several models of the strip. The orientation will change when new control points are used to orientate the strip.
As rates of changes are only linear, a greater number of images orientated simultaneously will result in a progressively poorer orientation.

Ground Control Used

The accuracy of each type of control is shown in table 1.

Orientations have been carried out using the OEEPE designation to specify them. The control points used in these cases have been previously indicated by OEEPE for the proposed test (table 2).

Although other sets of control points have been specified by OEEPE, it has been impossible to use all of these. In some cases, less than 5 control points were specified to set up the strips, which is impossible with the software used, without using on-board recorded data. In another case, the 6 control points used to set up strip A, it has not proved possible to perform a good orientation of the model. An unstable orientation was obtained resulting very big y-parallaxes, making it impossible to see all the strip stereoscopically.

Type of point	Accuracy in (m)	
	planimetry	altimetry
1: 25,000 topographic maps	5	2
1: 30,000 aerial stereopairs	2	2
1: 60,000 aerial stereopairs	4	2
computed by field stereopreparation	3	2

Table 1 - Accuracy of data provided for test

Strip	number of control points	control points
A	18	46, 45, 501, 504, 514, 518, 522, 528, 1018, 1047, 2001, 2002, 2009, 3002, 30027, 3040, 3045, 3053
	10	501, 504, 514, 518, 526, 528, 1078, 2002, 3036, 3040
B	14	6, 19, 25, 39, 48, 58, 73, 78, 104, 105, 1017, 1028, 1036, 1046
	6	6, 58, 73, 78, 1028, 1036

Table 2 - OEEPE control points configuration.

In order to analyse the variation of the residuals, the two strips of SPOT models have also been orientated using different type and number of control points.All types of control points described by IGN exist in strip A but points chosen from 1:60,000 aerial stereopairs and from 1:25,000 topographic maps are the only types of ground control available in strip B. Strip B has been orientated using only these two type of control points. Strip A has been orientated with control points chosen from:

- 1:25,000 topographic maps
- computed by field stereopreparation, and
- 1:30,000 + 1:60,000 aerial stereopairs.

It can happen that one orientation has to be made using more than one single type of control points.

In strip A, points chosen from 1:30,000 aerial stereopairs only appear in the northern area, while points chosen from 1:60,000 aerial stereopairs only exist in the southern region. This is the reason why one of the orientations has been made using these two types of control points simultaneously.

Residuals of the two Strips

After each of the orientations have been performed, all check points in the strip have been measured. The measured coordinates of the check points have been compared with their known Lambert grid coordinates. For each orientation, the rms of the residuals obtained are presented in table 3. Graphs 1 - 7 present residuals of table 3.

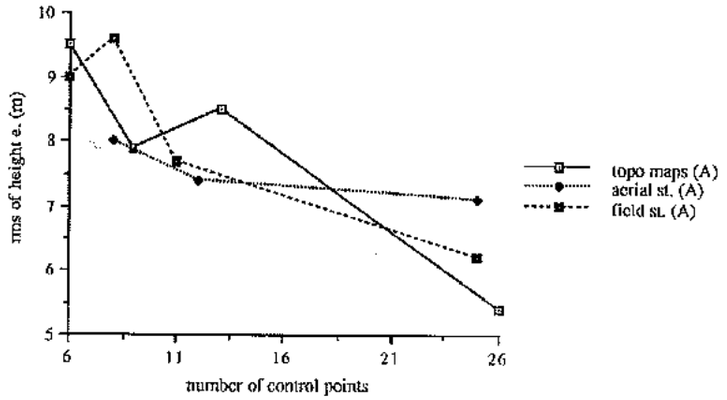

Graph 1 - rms of height residuals for strip A using different control

Type of point chosen to set up model	number of control points	number of check points	rms (m)		
			height e.	plan e.	vector e.
STRIP A					
1:25,000 topographic maps	26	104	5.4	9.1	10.6
	13	106	8.5	16.9	18.9
	9	106	7.9	18.5	20.1
	6	106	9.5	19.1	21.3
1:30,000 aerial stereopairs + 1:60,000 aerial stereopairs	25	105	7.1	14.2	15.9
	12	106	7.4	15.3	17.0
	8	105	8.0	14.6	16.6
computed by field stereopreparation	25	105	6.2	10.2	11.9
	11	106	7.7	14.9	16.7
	8	106	9.6	16.1	18.7
	6	106	9.0	20.5	22.4
OEEPE	18	106	7.3	15.6	17.2
	10	106	7.3	16.1	17.7
STRIP B					
1:60,000 aerial stereopairs	13	133	8.0	10.4	13.2
	7	135	7.6	16.3	18.0
1:25,000 topographic maps	12	134	5.9	10.4	12.0
	7	134	6.2	11.8	13.3
OEEPE	14	135	8.4	12.6	15.2
	6	136	8.9	14.1	16.6

Table 3 - Residuals obtained from setting up strips with different type of control points.

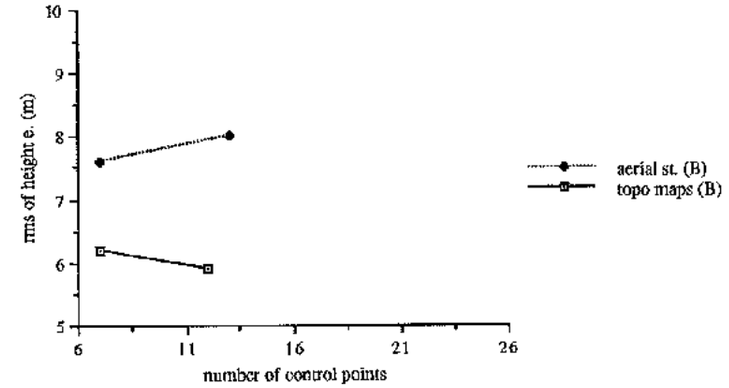

Graph 2 - rms of height residuals for strip B using different control

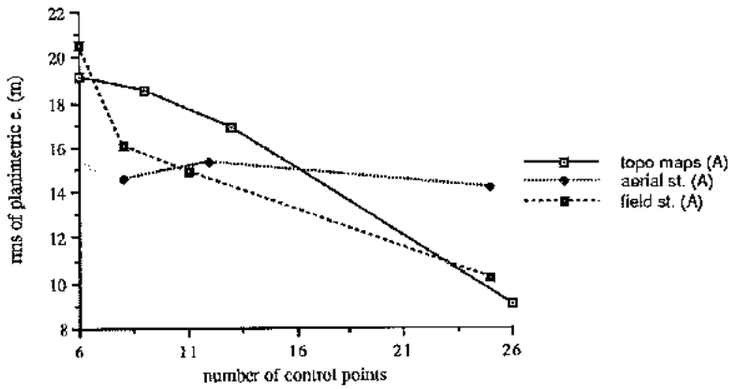

Graph 3 - rms of planimetric residuals for strip A using different control

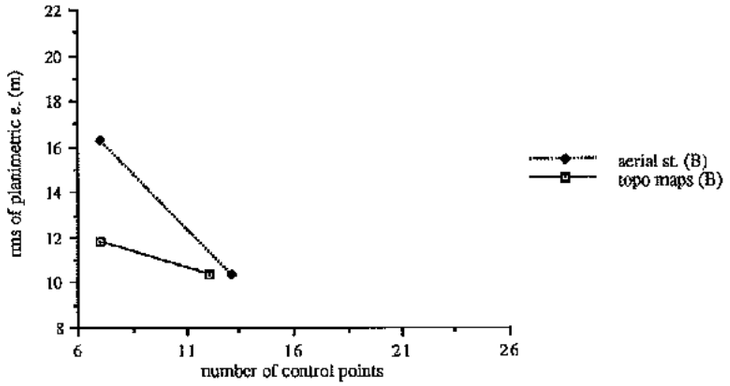

Graph 4 - rms of planimetric residuals for strip B using different control

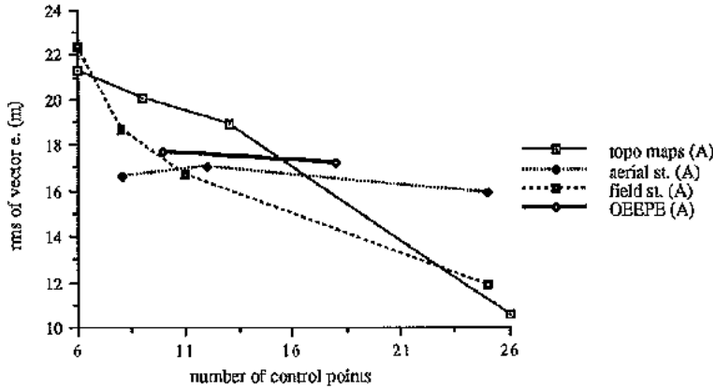

Graph 5 - rms of vector errors for strip A using different control

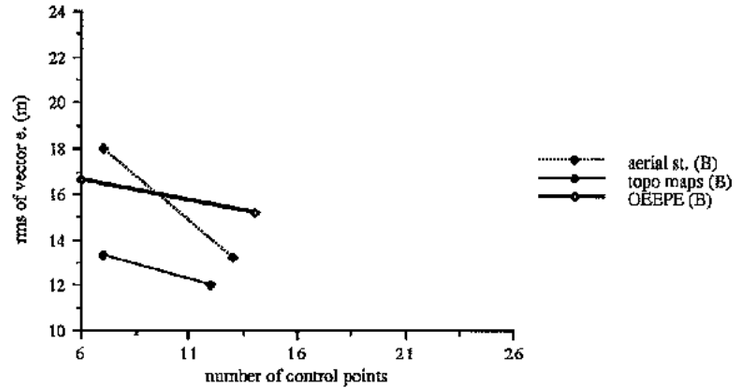

Graph 6 - rms of vector errors for strip B using different control

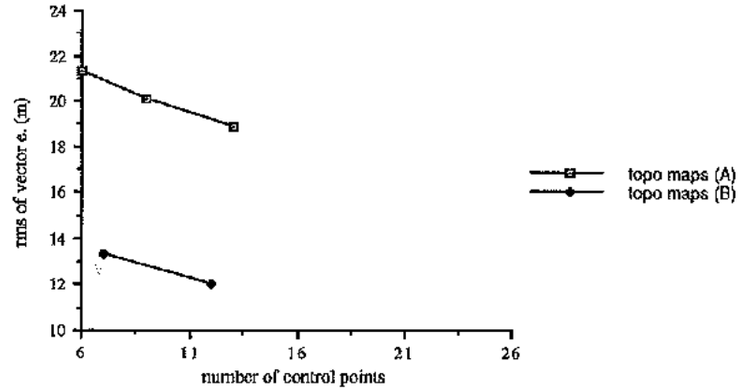

Graph 7 - rms of vector errors for strip A and B using same type of control

Analysis of the Results

Comparison of results for one model orientation

In order to compare strip results with those for a single model results from the latter are summarised in table 4.

Type of point chosen to set up model	number of control points	number of check points	rms (m)		
			height e.	plan e.	vector e.
1:25,000 topographic maps	10	42	9.4	10.8	14.3
1:30,000 aerial stereopairs	11	42	4.6	9.8	10.9
computed by field stereopreparation	9	43	6.6	13.0	14.6

Table 4 - Residuals obtained setting up model with three different type of control points

Comparing the information given by table 4 and table 3 for one model and strip residuals, and considering for each orientation the cases where about the same number of control points has been used, bigger residuals are found in the strip. Values of rms of vector error are about 10.9 to 14.6m for one stereomodel and 16.6 to 20.1m for the strip (four models oriented simultaneously). As rates of changes taken are only linear, a greater number of images orientated simultaneously results in progressively poorer orientation. This is the reason why bigger residuals are found in strip A than in its northern model, when the latter is orientated separately.

When the number of control points to set up the strip is increased, values of the residuals found for the strip do not differ very much from those found in one model. When 25 or 26 control points are used to orientate strip A, the rms of vector error varies from 10.6 up to 15.9m. As the strip is composed of four image models, 25 control points to the whole strip means around 6 to 7 control points for each image of the strip. So, if these values are compared with those of table 4, and considering the number of control points used to orientate the northern model, the results obtained are about the same order of those found for one single model.

Analysis of results for different type of points

From the results shown in table 3, various points can be sorted out. A systematic result is that the errors increase when smaller number of control points are used to set up the strip.

In general, smaller rms of the residuals are found for strip B than for strip A. This may be due to its bigger base to height ratio which improves essentially the height. Another aspect that can contribute to this is that more check points exist in strip B, and that smaller variations

on ground height occur in strip B. Strip A covers a small part of the Alps, and big variations on terrain altitude are registered. If approximately the same variability of the residuals occur in the measured points, higher number of check points leads to smaller values of rms of residuals. But this is not the case as variations are not the same in both strips.

The residuals vary with the type of control points used (table 3). When more control points are used, points chosen from 1:25,000 topographic maps or computed by field stereopreparation give better orientations. But when fewer control points are used, better accuracy is obtained for strip A with points chosen from 1:30,000 and 1:60,000 aerial stereopairs. In strip B, the residuals always keep smaller for orientations using points chosen from 1:25,000 topographic maps. A possible justification for these facts is given in the next paragraphs.

There are all types of ground control in strip A. But their distribution within the area varies. Points chosen from 1:25,000 topographic maps or computed by field stereopreparation cover, in general, regions all about at the same altitude or at least without a continuous or smooth inclination of the terrain. Points chosen from 1:30,000 aerial stereopairs all appear concentrated in one region of very high altitude, in the Alps, and where differences of height up to more than 1,000 meters are registered. Points chosen from 1:60,000 aerial stereopairs are essentially concentrated in an almost flat region, in the south of strip A. For this reason, they are the type of points that better represent the lower regions of the model. When a combination of control points chosen from 1:30,000 and 1:60,000 aerial stereopairs is used, better coverage of the variations of the terrain is obtained. The orientation model will be closer to the real ground variations and smaller residuals will be obtained. The other types of control points do not cover the ground variations so well, specially when less control points are used. In this case, bigger residuals should be expected. When more control points are used to orientate the strip, and in order to obtain a good control distribution, points chosen from aerial stereopairs have been added to the other types. This gives a better representation of the ground variations and a better model is obtained. On the other hand, points chosen from 1:60,000 aerial stereopairs are not so accurate as the other ones. This justifies smaller residuals for strip A set up with 25 or 26 points chosen from 1:25,000 topographic maps or computed by field stereopreparation.

In strip B, the different types of points cannot be connected to a well defined characteristic of the region like it happens in strip A. But points chosen from 1:25,000 topographic maps are all concentrated in the far north and in the far south of the model. And all the points chosen from 1:60,000 aerial stereopairs are in the middle of the strip. When an orientation is set up with points from 1:60,000 aerial stereopairs, the representation of the ground is worse than when points from 1:25,000 topographic maps are used, as the latter are far better distributed along strip B.

Higher rms of errors have been found for the orientations using the OEEPE control points. Difficulties with y-parallax appeared in both strips, which contributed to problems of measurement and worse results. This may be due to the fact that sometimes there has been difficulties in finding exactly the control points. Although the good quality of the imagery, some of the control points were not the easiest to identify nor to define. Higher residuals obtained may also be due to different distribution of the control points. This fact has been proved to be influential in the results obtained by Gugan (1987a).

From the overall results obtained, rms of errors in planimetry are more sensitive to variations of the number of control points and even of their type than rms of errors in height. The residuals in height suffer bigger variations with a variation in the base to height ratio. But the rms of errors in planimetry, and in height, decrease with higher base to height ratio models.

Analysis of distribution of residuals

It can be observed that when fewer control points are used the residuals are larger in planimetry and in height. But, in the average, the vector errors do not change direction. This indicates that using less control points, the orientation of the strip will be poorer, increasing the model deformation. In these models, and especially for the 6 point orientation, planimetric residuals present in general a systematic shift towards west. Some small regions in the north present a shift towards the north. On the other hand, height residuals are in the average positive in the northern zone of the model and negative from half of the model to south.

In strip B, both types of points present the same residuals patterns in height. In both orientations considered, a negative systematic error is found for all the strip. In planimetry, check points from 1:60,000 aerial stereopairs show random errors. But check points from 1:25,000 topographic maps present well-defined patterns. In the case of strip B orientated with points chosen from 1:25,000 topographic maps, the residuals of the check points only present a defined pattern in the northern model. They appear random in the rest of the strip. This may be due to the fact that when the strip is set up with the same type of control points and of check points more sensitive to the model deformation, the effect decreases.

Conclusions and general comment on ground control

The accuracy of one strip orientation depends on the number of control points used. In this work, using the software implemented at UCL and not using on-board recorded data, the following rms of errors have been found:

n° of control points		B/H	n° of check points	rms height (m)	rms plan (m)
(A)	25 to 26	0.78	106	5.4 to 7.1	9.1 to 14.2
(A)	6 to 8	0.78	106	8.0 to 9.5	14.6 to 20.5
(B)	6 to 7	0.81	134	6.2 to 8.9	11.8 to 16.3

It has been confirmed that the residuals depend on the base to height ratio of the stereomodel. When the orientation is changed, rms of plan accuracy suffer bigger variations than rms in height.

Different results have been obtained when different types of control points were used to set up the strip. It has been found that residuals are also dependent on the type of check point used. The distribution, either of the control points and of the type of check points, affect the residuals obtained.

If one intends to orientate a strip of SPOT imagery for systematic use, some considerations have to be made. It has been shown that the type of control point affects the precision of the orientation. In case the terrain suffers high variations of altitude, a better model is obtained if the control points are representative of very sudden slopes. From the types of points provided by IGN, points chosen from 1:30,000 and 1:60,000 aerial stereopairs or points chosen and computed by field stereopreparation resulted in better models. A better model is obtained when using more accurate control.

The type of control is very important, and sometimes it is more important than the model itself. Almost similar precision can be obtained with different types of control applied to different base to height ratio models. This does not apply if the difference of the base to

height ratio of the models is very big. The quality of the imagery is also very important as it conditions the choice of the control points.

Besides the orientation technique used in this study, complementary studies should be carried out, and the orientation precision evaluated.

Better precision may be obtained using the 13 parameter solution, for which a minimum of 7 control points are needed. In this case, the 13 parameter considered would be better than the 10 parameters, plus the second order rates of change of the satellite attitude. Gugan (1987a) tested the 13 parameters in one model, without success relatively to the results obtained with the 10 parameter solution. But as one strip covers four models, bigger variations of the satellite attitude should be expected, and a better orientation obtained using the 13 parameters solution. If on-board registered data is used, less control points are needed to orientate the model.

Block Adjustment of OEEPE SPOT Data

Since no suitable bundle adjustment was available, Schut's polynomial adjustment program was used for strip and block triangulation. Schut's adjustment does not use the geometry of the imagery to perform the triangulation. For this reason it can be applied to the adjustment of various kind of imagery. Schut's program computes a polynomial transformation of the measured coordinates, using some control and some tie points. The transformation parameters are found such that control points will have their 'true' ground coordinates (residual nil) and such that tie points will have the same coordinates in both strips (images or blocks) being considered.

Schut's polynomial adjustment can be performed using different sets of parameters. The operator can define the use of a translation and two rotations. The order of the polynomial for each of the parameters can also be defined, as well as the number of iterations. For the case being considered in this work, it was found that first order polynomials in all parameters and a 6 iterations solution gave the same kind of precision as higher degree polynomials and a bigger number of iterations. If first order polynomials are used a minimum of 3 control points per strip is needed, and a solution can be found using only 1 tie point. If a second order solution is used for all the parameters, a minimum of 6 control points per strip (or image) is needed.

The results of block adjustment using the OEEPE data is shown in table 5. The results obtained for each strip using Gugan-Dowman's model are first presented, followed by the residuals obtained considering all the data for both strips adjusted using the same control points that were used to orientate each strip seperately. Then some independent adjustments were carried out.

The distribution of the control points used for the adjustments are shown in figure 3. Nine points were common to both strips, being considered as tie points in all cases. These are very well distributed along the overlapping region.

Conclusions on the block adjustment

From the results presented in table 5, the following points can be concluded:

- Schut's polynomial adjustment program can be used for adjustment of blocks of SPOT imagery, giving fairly good results;
- the points chosen as control should not be all simultaneously tie points;
- at least one tie point should be used as control point; and
- the control points should be very well distributed both along line and sample directions.

Following the rules given above, the adjusted block gives smaller residuals than each of the strips separately.

control	rmse (m)		
	height	plan	3D
Strip A	8.7	18.9	20.8
Strip B	9.2	14.6	17.3
Strip A+B	6.2	14.0	15.3
Adj1 6CPs	23.5	13.2	26.9
Adj2 8CPs	5.7	11.6	13.0
Adj3 7CPs	6.7	13.4	15.0
Adj4 4CPs	7.3	12.2	14.2
Adj5 5CPs	7.2	14.0	15.7
Adj6 3CPs	119.5	17.2	120.7
Adj7 5CPs	6.4	11.3	13.0

Table 5 - Accuracy of block adjustment by Schut's program

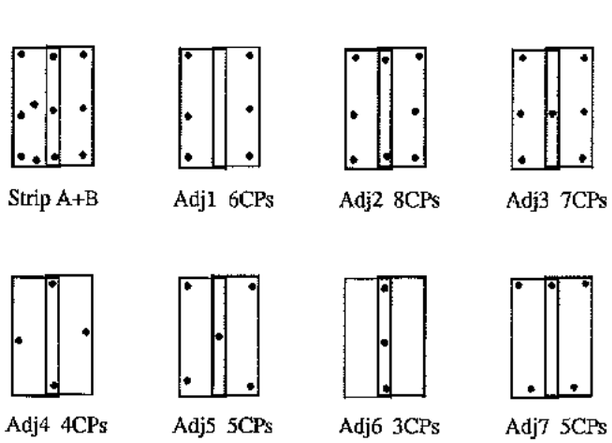

Fig 3 - Control configuration used in the block adjustment

Test on IGN Data

On the OEEPE workshop on block triangulation of SPOT imagery, IGN presented better results than any other participant. This fact may be due either to better identification and measurement of the control and check points, or due to the use of a better model to model SPOT imagery. IGN sent to the pilot centre (UCL) the measured coordinates of the points. These coordinates were used to model strip A of OEEPE test using Gugan-Dowman's model. Then the results were checked and compared with those obtained using the UCL measurements.

In the next pages the method os processing the IGN data be used by Gugan's space resection program is described, the results obtained are presented and a final comment is given.

Preparation of IGN data

IGN supplied data in the form of line and sample measurements of each point in each single image. A transformation of the data has been required as the space resection program does not accept measured data in the form of line and sample. And also because all the data has to be in the same image system of coordinates.
In a first step IGN line and sample measurements were transformed into mm and the origin considered at the scene centre, using the following expressions:

$$x = \text{line} * 78 / 6{,}000 - 39{,}000$$
$$y = \text{sample} * 78 / 6{,}000 - 39{,}000$$

The second step consisted in translating all the coordinates of the different images of the strip to the plate system of coordinates of the top model. This was done considering the overlap between images already evaluated in UCL.

After all the transformations were performed, Gugan's program was run and the residuals computed.

Results

In table 6 the residuals obtained using IGN data and Gugan-Dowman's approach to model the OEEPE SPOT strip are presented in the first two lines. Accordingly to OEEPE test requirements, two orientations were performed and specified as a and b. The original results presented by UCL on the OEEPE workshop, and some results obtained later using the VAX are also presented in the same table. This allows further comparisons and some comments can be made about the results obtained.

Comment

From the results presented on table 6, it can be seen that using the same model, IGN data measurements gave worse results than UCL measurements. And the differences are relatively bigger for rms in height than in plan. If better results were obtained using IGN data, one would conclude that this was due to better measurements made by IGN. In the present case, better results were obtained using UCL measurements. Not forgetting the fact that both data have been used in a similar way by the same program. This leads to the conclusion that the better results presented by IGN on the OEEPE workshop result from the use of a better orientation model. The better results of IGN may either be due to the approach itself used by

them, or due to the use of conjugate points to improve the solution.

	control	check	rms height	rms plan	rms 3D
IGN	a	94	11.4	15.6	19.3
	b	93	11.0	16.1	19.5
UCL VAX	a	105	6.4	10.6	11.4
	b	104	6.3	12.9	11.0
UCL original	a	106	7.3	15.6	17.2
	b	106	7.3	16.1	17.7

Table 6 - rms in meters of residuals found using Gugan-Dowman model to orientate SPOT / OEEPE strip A with IGN and UCL measured data

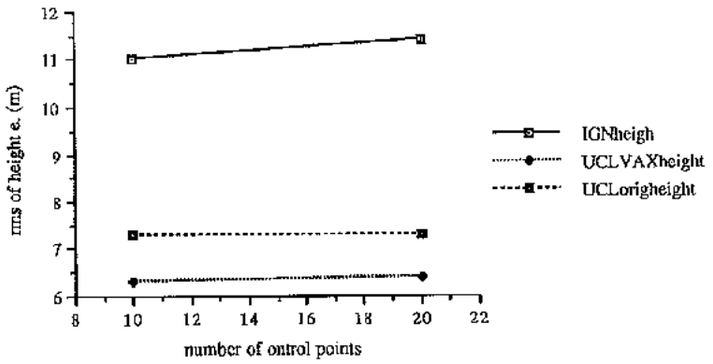

Graph 8 - rms of height residuals of IGN data processed at UCL and UCL data

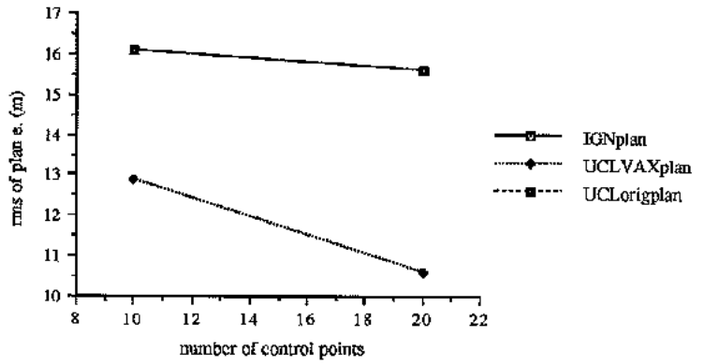

Graph 9 - rms of plan residuals of IGN data processed at UCL and UCL data

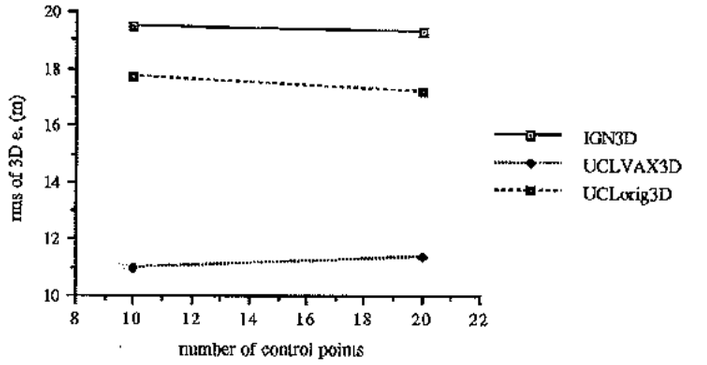

Graph 10 - rms of 3D residuals of IGN data processed at UCL and UCL data

References

Gugan, D.J., 1987a. PhD. Thesis. University of London.

Gugan, D.J., 1987b. Practical aspects of topographic mapping from SPOT imagery. Photogrammetric Record, 12(69): 249-355.

A NEW CAMERA MODEL FOR THE ORIENTATION OF SPOT DATA AND ITS APPLICATION TO THE OEEPE TEST OF TRIANGULATION OF SPOT DATA

By

Mark O'Neill and Ian Dowman
University College London

Introduction.

The O'Neill-Dowman SPOT camera model was implemented under the aegis of the Alvey MMI-137 Real Time 2.5D Vision project at University College London. The camera model was designed to provide an accurate method of transforming SPOT imagery from image space to object space and vice versa, using the minimum amount of ground control to orient the models. Furthermore the model works accurately with both single SPOT-1 stereo-pairs and strips ,which are contiguous swaths of SPOT imagery up to several hundred kilometres in length.

Design Considerations of the O'Neill-Dowman Camera Model.

The three basic design considerations for the O'Neill-Dowman Camera model were:

(a) To use all available auxilliary information in order to reduce the number of ground control points which have to be used to set up the model.

(b) Functional simplicity - the use of simple, easily understood algorithms where ever possible to achieve the desired result. In spite of using this approach, the model is quite complex: This is because the satellite telemetry data is of poor quality, which means that complex relaxation and orbit reconstruction are required to achieve a tolerably accurate model. An accurately parameterised orbit would permit a more concise algorithm.

(c) A modular code structure. This facilitates experimentation with the camera model. Modular code in the form of shared libraries also makes certain general routines available for other applications.

An Overview of the O'Neill-Dowman Camera Model

Setting up a stereo model using the O'Neill-Dowman camera model is a two stage process:

(a) Setting up a relative model using the SPOT-1 header.

(b) Orienting the relative model to an absolute coordinate system using a small number, typically 3, ground control points.

Computing the Relative Model.

In the first stage of the process an approximate orientation matrix, $\underline{R}_o$, valid for the whole extent of the imagery being considered, is derived from the splined orbital position data given in the header.

A correction to this matrix, $\underline{R}_c$ is then determined from the splined satellite attitude data. The relative orientation matrix, $\underline{R}_{rel}$, may then be calculated;

$$\underline{R}_{rel} = \underline{R}_c \cdot \underline{R}_o \qquad (1)$$

The processes described above are performed for each camera position required.

Computing the Absolute Model.

The second stage of the modeling process is to orientate the model to a known co-ordinate system, using N ground control points [GCP's]. The GCP's are used to compute a correction to the attitude matrix $\underline{R}_g$; the amended attitude matrix for a given look becomes:

$$\underline{R}_a = \underline{R}_g \cdot \underline{R}_{rel} \qquad (2)$$

Where:

$\underline{R}_a$ is the absolute orientation matrix.

It is also sometimes necessary to introduce a shift of the orbit path for a given look.

Computing the Space Intersection.

For a pair of ray vectors r_1, r_2 the point of space intersection used by the model is defined to be the mid point of that vector M which is perpendicular to both ray vectors, at their point of closest approach. We will call this position vector S.

The Optimisation Process.

The rotation $\underline{R}_g$, for the absolute correction to the camera model orientation is computed using a numerical optimisation process based upon the Powell direction-set algorithm.

The RMS magnitude of the error vector is reduced using a suitable optimisation algorithm. Parameters with respect to which the optimisation takes place include vector shifts of the orbit tracks of each look and rotation of the line elements of the camera about their respective perspective centres. The optimisation scheme is set up in such a way that it is easy for additional constraints, for example temporal correction of the sensor tracks, to be added without gross changes to the algorithm.

The camera model currently uses a Powell direction set minimiser [Powell, 1964]. Extensive testing has shown this to be the best choice of optimisation algorithms in terms of both the speed of the relaxation process, and of the ease with which the parameter set and cost function may be changed.

It is also possible to optimise the relative orientation by minimising ray-ray skewnesses using conjugate points obtained from an appropriate source such as the Otto- Chau stereo matcher, [Otto and Chau, 1989] with respect to a similar parameter space to that used in the case of the absolute model.
The Back Transformation

Because the SPOT-1 camera model has a linear geometry, with many perspective centres, the back transformation, must be accomplished dynamically using an optimisation process. Currently, the error vector is minimised, with respect to the line and sample position within the image space for a given look. This approach works well but is slow, due to the extensive computation in the optimisation process.

A detailed description of the O'Neill-Dowman Camera Model.

Having briefly looked at how the model is set up, we shall now look at the individual stages of model formation in more detail.

SPOT header data.

In order to produce a refined camera orientation, the first problem which must be solved is the computation of an accurate initial estimate of the SPOT HRV sensor position over the time period in which the image was acquired. This initial phase of the computation is accomplished using th e SPOT header data.

The SPOT header is a condensation of the satellite telemetry data, for a time frame within which the corresponding SPOT image was acquired. The O'Neill-Dowman Camera Model uses the following items from the header file:

(a) The scene centre time.
(b) The nominal size of a pixel on the ground [nadir view].
(c) The satellite position data.
(d) The inertial velicity data.
(e) Theuniversal time data.
(f) The attitude data .
(g) The absolute time when each item of attitude data was acquired , this may be found using the absolute scene centre time, and the known time step between the acquisitions of successive lines within the SPOT scene [1.504 ms PAN; 3.08 ms XS].
(h) The ϕ_x and ϕ_y which give the nominal look angles for the first and last sensors in the SPOT pushbroom sensor array.

Splining the SPOT header position and velocity data.

An orbit segment for the sensor about the image acquisition period may be generated by interpolating the position data. The process of splining permits the expression of orbit position vector P, as a vector function of the absolute time, t:

$$\vec{P}(t) = \vec{f}(x,y,z,t) \qquad (3)$$

The velocity vector V, is similarly splined using natural boundary conditions to yield a [numerical] vector function of time:

$$\vec{V}(t) = \vec{f}(x,y,z,t) \qquad (4)$$

Computation of approximate satellite reference axes.

The velocity and position vectors may now be used to define a third vector, el(t) which is parallel to the pushbroom sensor. The vector triad, $\vec{P}(t)$, $\vec{V}(t)$, $\vec{el}(t)$, form a good approximation to the satellite, and hence, the sensor reference axis system at time t:

$$\hat{g}(t) = \hat{P}(t) = \text{vunit}(\vec{P}(t)) \quad (5)$$
$$\hat{t}(t) = \hat{V}(t) = \text{vunit}(\vec{V}(t)) \quad (6)$$
$$\hat{el}(t) = \hat{g}(t) \times \hat{t}(t) \quad (7)$$

Where:

vunit signifies the operation of taking the unit vector in the direction of the argument vector.

$\hat{g}(t)$ is a sensor attitude reference axis unit vector in the direction of the satellite position vetor,

$\hat{t}(t)$ is a sensor attitude reference axis unit vector in the direction of the sensor track,

$\hat{el}(t)$ is a sensor attitude axis reference unit vector in the direction of the sensor pushbroom array.

The prescription given in equations (5) - (7), makes the assumption that the satellite is pointing in the same direction as the velocity vector.

Computation of the rough attitude matrix, $\underline{R}_o$

The approximate satellite attitude matrix, $\underline{R}_o(t)$, may be computed from the vector triad [t(t), el(t), g(t)]. The rough orientation matrix $\underline{R}_o(t)$ transforms the satellite orientation from a reference space, in which the satellite reference axes are parallel to the vectors [1.0,0.0,0.0], [0.0,1.0,0.0] and [0.0,0.0,1.0] to an approximation to the object space. The components of the matrix $\underline{R}_o(t)$ may be described in terms of the triad $[\hat{t}(t), \hat{el}(t), \hat{g}(t)]$:

$$\underline{R}_o(t) = \begin{matrix} \hat{t}[1](t) & \hat{el}[1](t) & \hat{g}[1](t) \\ \hat{t}[2](t) & \hat{el}[2](t) & \hat{g}[2](t) \\ \hat{t}[3](t) & \hat{el}[3](t) & \hat{g}[3](t) \end{matrix} \quad (8)$$

Computation of direction of an arbitrary ray in object space.

Transformation of a ray vector, emergent from pixel position [l,s] via the perspective centre which corresponds to line l, image at time t, may be accomplished by first considering the ray in reference space and then transforming it, using the matrix $\underline{R}_o(t)$:

$$\vec{r}_o(t) = \underline{R}_o(t) \cdot \vec{r}_{ref}(t) \quad (9)$$

Where:

$\vec{r}_{ref}(t)$ is the unit direction vector of a ray in the reference space.

$\vec{r}_o(t)$ is the unit vector of the transformed ray in the sensor-ground system space.

$\underline{R}_o(t)$ is the rough transformation ma trix for time t, defined in (8) above.

The explicit inclusion of the time parameter t, is a reminder of the dynamical nature of the SPOT-1 sensor.

Computation of position vector of ray in reference space.

The position of a ray whose line and sample co-ordinates in the image plane are [l,s] may be determined by linear interpolation of the supplied look angles for the first and last CCD elements in the sensors, $\phi_{x1}, \phi_{y1}, \phi_{x2}$ and ϕ_{y2}. This will yield a pair of rotation angles ϕ_x and ϕ_y which correspond to the pixel at [l,s] on the image plane. The reference ray [0.0,0.0,-1.0] is then rotated about the X and Y axes of the reference axis, giving the position vector of the ray in the reference space:

$$\phi_x = \phi_{x1} + \frac{(s-1).(\phi_{x2} - \phi_{x1})}{i_s} \quad (10)$$

$$\phi_y = \phi_{y1} + \frac{(s-1).(\phi_{y2} - \phi_{y1})}{i_s} \quad (11)$$

$$r_{ls} = \underline{R}_y \cdot \underline{R}_x \cdot r_{ref} \quad (12)$$

Where:

$\phi_{x1}, \phi_{y1}, \phi_{x2}$ and ϕ_{y2} are the nominal look angles for the first and last sensors along the pushbroom supplied in the SPOT header.

s is the sample position.

i_s is the number of pixels along the pushbroom array [6000 PAN; 3000 XS].

$\underline{R}_y, \underline{R}_x$ are rotations about the X and Y reference axes of amounts ϕ_x and ϕ_y respectively.

Computing the space intersection.

Equations (3) to (12) may be used to establish the position and orientation of the satellite within a time period ∂t, within which the respective images were acquired. These complementary orientations and positions may then be intersected to yield a set corresponding geocentric ground vectors, $\vec{S}(t_1, t_2)$.

The ground intersection is accomplished by finding the shortest vector $\vec{m}$, perpendicular to the ray vectors, $\vec{r}_1, \vec{r}_2$. Since this vector is perpendicular to both of the ray direction vectors, it is simple to find a unit vector in the direction of $\vec{m}$:

$$\vec{m} = \vec{r}_1(t_1) \quad (13)$$

The desired intersection point may then be found by solving a set of linear equations.

The use of ground control points to refine the absolute attitude.

If ground control points are available, they may be used to refine the absolute attitude calculated using equations (3)-(13) above. Typically, the zero order camera model gives ground positions which are related to a set of corresponding check points on the ground by a linear vector shift [to first order]:

$$\vec{G}_i = \vec{S}_i + \vec{E}_i \qquad (14)$$

Where:

$\vec{S}_i$ is the ith ground position generated by the camera model.

$\vec{G}_i$ is the corresponding ith check point ground position.

$\vec{E}_i$ is the ith error or residual vector.

Refinement of the absolute orientation is accomplished by minimising E_i for a set of ground control points $\vec{G}_i$ iteratively, with respect to a parameter space consisting of sensor position and orientation, and possibly additional parameters introduced as a result of experimentation. The position and orientation of the camera is known, as a function of t. Its derivative with respect to t is not known, and not readily computable. Given a stereo image co-ordinate, [l, s, l', s'], experimentation has shown that the set of error vectors E_i of minimum magnitude corresponding to a set of ground control points $\vec{G}_i$ and optimised correction parameters, is likely to be a global minimum of the parameter space. Therefore, the best form of optimiser is clearly a multivariate global minimiser which does not require derivatives. The Powell Direction Set Method, originally described by Powell, [1964], but refined by other workers since then.

Selection of Parameter Space.

In the simplest case, the parameter space which is optimised consists of a an uncorrelated pair of global rotations $[R_{x1}, R_{y1}, R_{x2}, R_{y2}]$ for each position respectively.

The Cost Function.

The optimisation algorithm thus finds the set of of rotations, $[R_{x10}, R_{y10}, R_{x20}, R_{y20}]$ which minimise a global cost function of the form:

$$C = \left[\frac{\sum_{i}^{N_g} |S_i - G_i|^2}{N_g} \right]^{\frac{1}{2}} \qquad (15)$$

Where:

C is the scalar cost,

$\vec{G}_i$ is the ith ground control point,

$\vec{S}_i$ is the corresponding ith space intersection.

N_g is the number of ground control points.

The optimal parameter values are used to implicitly correct the rotational parameters $\phi_{x1}, \phi_{y1}, \phi_{x2}$ and ϕ_{y2} for an object space ray emerging from a given pixel, producing a modified transform between the sensor reference space and object space:

$$\vec{R}_{x1'} = \vec{R}_{x10} \cdot \vec{R}_{x1} \qquad (16)$$
$$\vec{R}_{y1'} = \vec{R}_{y10} \cdot \vec{R}_{y1} \qquad (17)$$
$$\vec{R}_{x2'} = \vec{R}_{x20} \cdot \vec{R}_{x2} \qquad (18)$$
$$\vec{R}_{y2'} = \vec{R}_{y20} \cdot \vec{R}_{y2} \qquad (19)$$

Extending the Optimised Parameter Space.

In addition to the rotational parameters described, an uncorrelated pair of position shift parameters for each orbit, $\vec{\Delta P}_1, \vec{\Delta P}_2$ may also be introduced. The parameter set optimised in this case is $[\vec{R}_{x1}, \vec{R}_{y1}, \vec{\Delta P}_1, \vec{R}_{x2}, \vec{R}_{y2}, \vec{\Delta P}_2]$.

Extension of the Cost Function to Include Conjugate Data.

The cost function for the minimisation process may be readily extended to include a relative component in addition to the absolute component described above. The cost function then becomes:

$$C = W_{abs} \cdot C_{abs} + W_{rel} \cdot C_{rel} \qquad (20)$$

W_{rel} and W_{abs} are the weighting factors for the relative and absolute contributions to the cost function.

C_{abs}, the absolute component of the cost function is defined in (15).

C_{rel}, the relative part of the cost function is defined:

$$C_{rel} = \left[\frac{\sum_{i}^{N_c} |m_i|^2}{N_g} \right]^{\frac{1}{2}} \qquad (21)$$

Where:

N_c is the number of conjugate points;

$|m_i|$ is the ray-ray skewness of a pair of conjugate rays r_{c1}, r_{c2}, emergent from camera positions 1 and 2 respectively.

The conjugate points used by the cost function (15) are obtained from the output of an appropriate stereo matcher, for example the Otto-Chau stereo matcher [Otto and Chau, 1989]. The weighting factors have been introduced into the cost function so that irrespective of the number of conjugate points or ground control points used in setting up the model, the effective contribution to the overall cost function of each term is equal. This avoids a combination of the weak geometry of the SPOT HRV instruments, and large numbers of conjugate points giving rise to spurious orientations.

Extensions to the basic model

There are a number of refinements to the model, some of which have been implemented and others which have yet to be developed.

The parameter set for the minimisation is still subject to investiagaion and the cost function itself could probably be improved. It has been shown that the incorporation of the attitude data gives an improvement to the relative orientation, this has been done by splining the data in the header and then calculating a purturbation matirix for the points required. Later tests have indicated that the improvement is only marginal and it does not appear that the use of attitude dat gives a significant improvement.

The model has also been extended to handle strips and data can be extracted from individual header files and put together to form a continuous strip, the co-ordinates systems of individual models can also be joined by automatic calculation of the along track overlap using the scene centre time for each scene.

Speeding up the model

A number of techniques have been used to speed up the peformance of the algorithm. The major improvement in speed has come from blocking the orbit and assuming linear change between the points for which the attitide matirices have been computed. In addition the algorithm can be speeded up by optimisation of the code and the use of specialised hardware. These aspects are discussed further in O'Neill (1991).

The back transformation

Although the absolute orientation has been expressed as a function of absolute time it may also be expressed as a function of line and sample position. A relationship can be developed between the image, the sensor and a point on the ground and the shortest perpendicular distance between a point on the ground and the ray emanating from an image point can be minimised with resepect to the image co-ordinates.

Results

The model has been tested with a number of different data sets and full results are described in O'Neill (1991). Tests have indicated that the method is robust and gives results comparable to other methods of orienting SPOT data. The notable feature of the method is that a good relative model can be formed without any control points and that there is very little improvement when more than 3 points are used and that the accuracy in independent of strip length.

The results with the OEEPE data from S. France are given in Tables 1 and 2 for the control configuration in figure 1.

Figure 1. The control configurations for the tests of the O'Neill Dowman model.

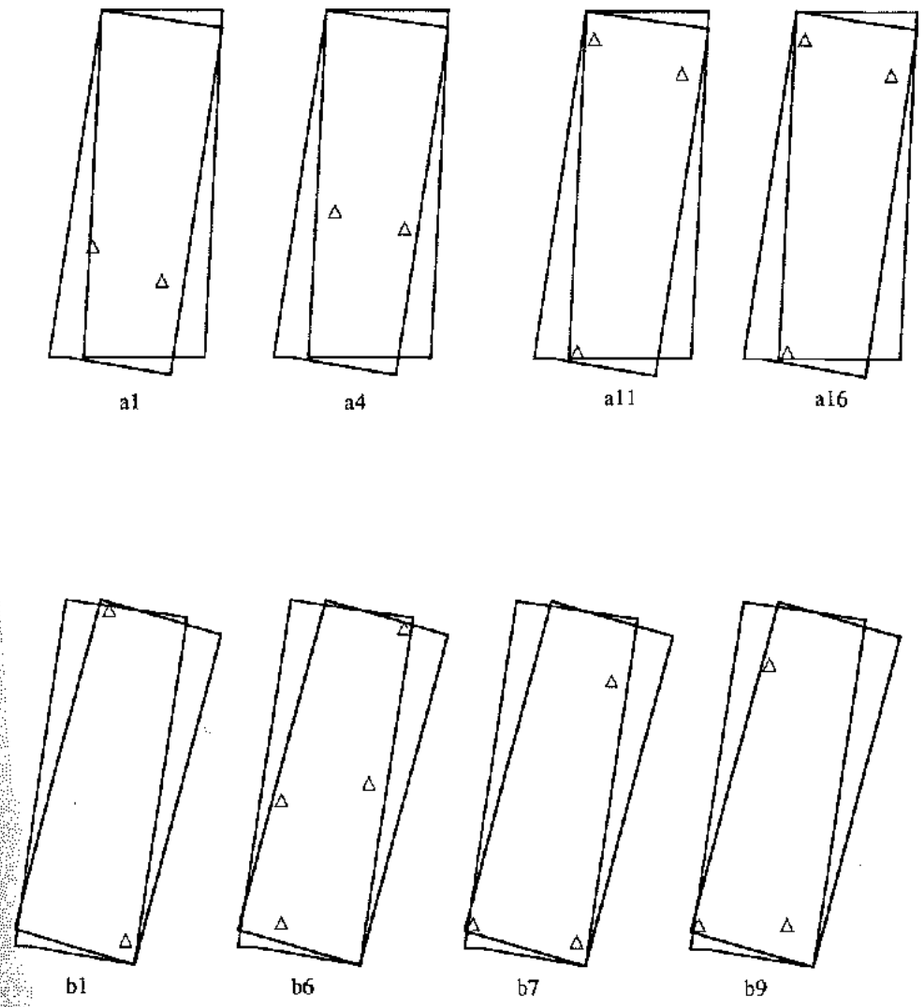

Table 1. Results of Test with OEEPE strip A.

Config.	No Control pts	No Check pts	RMSE Plan m	RMSE Ht m	RMSE Vector m
a1	2	102	31.8	12.1	34.1
a4	2	93	21.6	11.4	24.5
a11	3	94	13.8	10.2	17.1
a16	3	93	13.5	10.5	17.1

Table 2. Results of Test with OEEPE strip B.

Config.	No Control pts	No Check pts	RMSE Plan m	RMSE Ht m	RMSE Vector m
b1	2	130	21.8	14.8	26.4
b6	4	130	15.3	8.6	17.6
b7	3	130	16.1	10.9	19.5
b9	3	120	15.5	7.9	17.4

Conclusions

The work with the block of data for the OEEPE test of triangulation of SPOT data has shown that a method of orientation using orbit and attitude data from the SPOT header can be used to give good results over strips of four models with as few as 2 or 3 control points. The method can be used with no control points to give a relative model which, when used with an automatic stereo matcher can produce a relative DEM for whole SPOT models.

Acknowledgements

The camera model described in this paper arises out of the Alvey MMI-137 project on Real Time Stereo 2.5D Vision Systems funded by SERC. The project is a collaboration between University College London , Departments of Photogrammetry and Surveying and Computer Science, Laserscan Laboratories Ltd, Cambridge, Thorn EMI Central Research Laboratories, Hayes, Middlesex and the Royal Signals and Radar Establishment at Malvern.

The SPOT data was provided for the OEEPE project 'Triangulation of SPOT data' by SPOT Image through IGN (France).

The authors would like to thank all who have contributed to the project in OEEPE and the department of Photogrammetry and Surveying at UCL.

References

O'Neill, M.A., 1991. A Dynamic model for SPOT data. PhD thesis submitted to University of London.

Otto, G.P. and Chau, T.K.W., 1989. 'Region-growing' algorithm for matching of terrain images. Image and Vision Computing, 7(2):83-94.

Powell, M.D.H., 1964. A method to compute the minimum of a function of several variables without using derivatives. Computing Journal 7(4):303-307.

SIMULTANEOUS BLOCK TRIANGULATION OF THE OEEPE SPOT DATA SET

Prepared by:

TRIFID Corporation
744 Office Parkway, Suite 224
St. Louis, MO 63141 USA

(314) 991-3095

September 20, 1989

ABSTRACT

This paper outlines the methods and results of the block triangulation performed by TRIFID Corporation in support of the SPOT Triangulation Workshop run by the Organisation Europeenne D'Etudes Photogrammetriques Experimentales (OEEPE). The workshop was held at the University College London on September 27 and 28, 1989.

The block triangulation is a unified least squares bundle adjustment capable of simultaneously processing up to 300 SPOT images using rigorous photogrammetric projective equations and orbital constraints. By introducing the concept of imaging events, the method reduces the amount of required control, allows the extension of geopositioned imagery into uncontrolled regions, and improves the relative positioning along orbital passes. Final absolute accuracies commensurate with the accuracy of the input control are readily obtainable.

INTRODUCTION

The SPOT remote sensing system was launched in 1986. It has continually provided high quality images with a real potential for many mapping and positioning applications. With a panchromatic resolution of 10 meters, and a multispectral band resolution of 20 meters, the SPOT sensor collects reasonably detailed images over large areas of the earth at regular temporal intervals. Using an adjustable mirror, stereoscopic coverage with excellent base to height ratios is easily collected from orbital passes.

One of the major shortcomings of the system is the ability to derive from the imagery accurate object space positions of geographic features. This problem is usually not significant for small geographic areas (3600 km² or less), where one monoscopic image or one stereomodel is all that is required; it is often easily solved by using an abundance of accurate photo identifiable ground control points. However, for large cartographic projects (particularly in areas of sparse control) the problem is much more significant. The derived object space positions between image boundaries will contain discontinuities, and a multitude of ground control points will be required. This can limit the use of SPOT data in large mapping projects over sparsely controlled terrain, unless special measures are taken.

TRIFID Corporation has developed a simultaneous least squares bundle adjustment for the block triangulation of SPOT data for applications where the following conditions exist:

- multiple SPOT monoscopic or stereoscopic coverage is available,
- either minimal photo identifiable control is available or cost considerations require minimizing the use of available control,
- the desired object space accuracy (both absolute and relative) is to be consistent with 1:24000 and 1:50000 U.S. National Map Accuracy Standards.

This software was developed from a mathematical model derived by TRIFID Corporation which defines the operational characteristics of the SPOT sensor system. The software embodies a least squares optimum estimation process which is based on the collinearity condition equations and is augmented and strengthened with parameter constraints. Of significance is the application of the orbital constraint to enforce the condition that each image point from a single imaging pass must be referenced to a state vector which defines the sensor trajectory.

The following sections of this paper give a brief description of the mathematical derivations, the computer software, and triangulation operations description. Lastly, the results of test runs with multiple SPOT data sets is documented.

SATELLITE BLOCK ADJUSTMENT

The adjustment of blocks of aerial photographs acquired with conventional mapping cameras is a mature technology which is routinely used for mapping applications. Conceptually, this technology could be applied to images acquired from satellite platforms.

There are, however, significant differences which must be considered in formulating the mathematical model and parameter estimation technique for SPOT satellite images. These differences are caused by 1) the imaging sensor 2) the orbital dynamics and 3) the use of auxilliary sensor information.

The SPOT imaging sensor is very different from an aerial frame camera in complexity, recording media, imaging format, and calibration requirements. One of the main differences is the dynamic nature of the linear array CCD sensor. Each line of imagery collected by the sensor will have a unique exposure station position and orientation. These positions and orientations are related through time, allowing a single set of parameters to describe these exterior orientation elements. It is critical for the math model to accurately relate the timing data to the sensor dynamics.

SPOT sells and distributes images defined as 6000 elements by 6000 lines, even though the sensor may have actually recorded 6000 elements by 36000 lines while in operation. The images defined for the adjustment process are called an "imaging event", that is, all lines of imagery between the first line on the first image to the last line on the last image. The use of imaging events more closely describes the actual imaging process, reduces the number of parameters which must be estimated by the solution, eliminates the need for measuring points at each north/south image overlap, and removes any resulting north/south data inconsistencies.

For conventional aerial triangulation it is difficult if not impossible to derive mathematical expressions for the aircraft line of flight. For satellite imagery the mathematical expressions of celestial mechanics are precise definitions of the physical laws of orbital motion. Knowledge of the sensor platform orbit provides added information to the overall adjustment process. The exposure station position can be precisely computed given accurate system time and the position therefore becomes highly correlated, adding strength to the overall solution.

For the SPOT sensor there are a number of auxilliary sensors which produce data describing the operation of the system (timing, orientation rate data, etc.). This data is used to derive initial estimates of the

unknown parameters. These onboard clocks and gyroscopes are sources of data independent of the pixel data contained within the imagery. Therefore, these data sources are used to augment the block triangulation by generating additional observation equations within the least squares solution.

SENSOR MATHEMATICAL MODEL

The following ground to image projection equation is used to compute the sensor coordinates for a given ground point from Level 1A imagery.

$$\bar{r}_a = s \; M_A \, M_L \quad (\bar{R}_j - \bar{R}_i)$$

where:

- $\bar{R}_j$ ground point coordinate vector in Earth Centered Fixed (ECF) coordinate system
- $\bar{R}_i$ instantaneous sensor position vector in ECF system
- M_A rotation matrix from a Local Vertical System (LVS) to an Adjustable Image System (AIS) (a function of imaging event parameters and time)
- M_L rotation matrix from the ECF system to LVS (a function of imaging event parameters)
- $\bar{r}_a$ image coordinate
- s scale factor.

The projective equation is modified to include the six imaging event orientation parameters

ω bias and rate,
φ bias and rate,
ϰ bias and rate,

and the six imaging event position parameters for the state vector

X position and velocity (ECF),
Y position and velocity (ECF),
Z position and velocity (ECF).

The resulting standard linearized form is,

$$v + \dot{B}\,\dot{\Delta} + \ddot{B}\,\ddot{\Delta} = \varepsilon$$

where:

- $\dot{B}$ is the matrix representing the partial derivatives of the projective equations with respect to imaging event parameters,
- $\ddot{B}$ is the matrix representing the partial derivatives of the projective equations with respect to ground coordinates,
- $\dot{\Delta}$ is a vector representing the adjustments to imaging event parameters,
- $\ddot{\Delta}$ is a vector representing the adjustments to ground coordinates,
- v is a vector representing residuals, and
- ε is a vector representing discrepancies.

Additional observation equations are generated from a-priori values for the adjustable parameters $\dot{\Delta}$, $\ddot{\Delta}$. A-priori estimates for imaging event parameters result in:

$$\dot{v} - \dot{\Delta} = \dot{\varepsilon}$$

and a-priori estimates for ground point values give:

$$\ddot{v} - \ddot{\Delta} = \ddot{\varepsilon}$$

where the ε vectors represent discrepancies between the current estimate of the parameter and the initial value.

The normal equations are formed by computing the partial derivatives of the rigorous ground to image projection equation. This requires a proper accounting for the relatively complex and dynamic nature of the sensor's state vector and orientation parameters. These normal equations take the form:

$$N = \begin{bmatrix} \dot{N} & \bar{N} \\ \bar{N}^T & \ddot{N} \end{bmatrix}$$

where

$$\dot{N} = \begin{bmatrix} \dot{N}_1 + \dot{W}_1 & & \emptyset \\ & \ddots & \\ \emptyset & & \dot{N}_m + \dot{W}_m \end{bmatrix}$$

$$\ddot{N} = \begin{bmatrix} \ddot{N}_1 + \ddot{W}_1 & & \emptyset \\ & \ddots & \\ \emptyset & & \ddot{N}_n + \ddot{W}_n \end{bmatrix}$$

$$\bar{N} = \begin{bmatrix} \bar{N}_{11} & \cdots & \bar{N}_{1n} \\ \vdots & & \vdots \\ \bar{N}_{m1} & \cdots & \bar{N}_{mn} \end{bmatrix}$$

The subscript m is total number of imaging events, and the subscript n is the total number of ground points in the block. An individual imaging event is identified by the subscript i (i = 1, m) and individual ground points are identified by the subscript j (j = 1, n).

The matrices $\dot{W}_i$ and $\ddot{W}_j$ are the weight matrices for each of the imaging events and ground points. A weight matrix w_{ij} is formed for each of the image coordinates.

For each imaging event, the $\dot{N}_i$ matrix is formed by summing over all points j the product of

$$\dot{B}_{ij}^T \, w_{ij} \, \dot{B}_{ij} .$$

For each ground point, the $\ddot{N}_j$ matrix is formed by summing over all imaging events i the product of

$$\ddot{B}_{ij}^T \, w_{ij} \, \ddot{B}_{ij} .$$

Each of the $\bar{N}_{ij}$ matrices is formed by the product of

$$\dot{B}_{ij}^T \, w_{ij} \, \ddot{B}_{ij} .$$

The process of computing the products defined above requires the evaluation of the matrices $\dot{B}_{ij}$ and $\ddot{B}_{ij}$ for every point j occurring on every imaging event i.

The vector of constants T has the form

$$T = \begin{bmatrix} \dot{T} \\ \ddot{T} \end{bmatrix}$$

where

$$\dot{T} = \begin{bmatrix} \dot{T}_1 \\ \vdots \\ \dot{T}_m \end{bmatrix} \quad \text{, and } \ddot{T} = \begin{bmatrix} \ddot{T}_1 \\ \vdots \\ \ddot{T}_n \end{bmatrix} .$$

Each of the $\dot{T}_i$ matrices is formed by summing over all points j the product of

$$\dot{B}_{ij}^T \, w_{ij} \, F_{ij},$$

and each of the $\ddot{T}_j$ matrices is formed by summing over all imaging events i the product of

$$\ddot{B}_{ij}^T \, w_{ij} \, F_{ij}.$$

The matrices F_{ij} are the evaluation of the projection equations for the appropriate i and j values.

The adjustable parameters are contained in the $\dot{\Delta}$ and $\ddot{\Delta}$ vectors. The solution vector is obtained by multiplying the inverse of the normal equations by the vector of constants. The reduced normals are formed by folding the ground point normals into the imaging event normals. A non-linear weighted least squares method requires successive iterations until the solution vector approaches zero. The method of recursive partitioning is used to handle the large matrices in the algorithm.

The inverse of the reduced normals is generated in the least squares solution process. This inverted matrix gives the covariance matrix for the adjusted parameters. This matrix may be used in error analysis. This analysis is dependent upon the accuracy of the data contained within the input variance-covariance matrices.

INPUT DATA

The triangulation process assumes the use of digital imagery and support data with Level 1A processing (other levels of geometric correction would make it very difficult if not impossible to perform a rigorous triangulation). Either panchromatic or multispectral imagery can be used.

In order to perform the triangulation, we require the following data for each image from the leader file:

1. Time of the center scan.
2. Ephemeris data
   - X,Y,Z positions
   - X,Y,Z rates
   - associated times.
3. Mirror position.
4. HRV number (1 or 2).

5. PAN or XS flag (we can triangulate any mixture of panchromatic or multispectral).
6. Pitch rate data (if available).

We use the above data to derive initial starting estimates for the following twelve unknown adjustable terms for each imaging event:

$$\begin{matrix} R(X,Y,Z) \\ \cdot\ \cdot\ \cdot \\ \dot{R}(X,Y,Z) \end{matrix} \quad \text{(initial state vector)}$$

ω, φ, κ (orientation bias)

$\dot{\omega}, \dot{\varphi}, \dot{\kappa}$ (orientation rate)

The initial state vector (R, $\dot{R}$) is obtained from the SPOT one minute ephemeris. The R, $\dot{R}$ closest to the time of the imaging event center is used. The initial omega value is determined from the mirror position and the HRV number. The initial phi value is determined from the latitude of the sensor obtained from R and the PAN / XS flag. The initial kappa value is simply set to zero.

Initial values for omega rate, phi rate, and kappa rate are set to zero. The pitch rate data is optionally integrated and added onto the instantaneous value for phi at any time in the image.

The instantaneous values for position and orientation at any particular time are rigorously derived from the most current estimates as a function of time. The position and rate for any sensor position along the imaging event can be rigorously computed from the state vector. The algorithm rigorously constrains the computed position and rates at any time to lie on the orbit described by the initial state vector.

In addition to the above estimates for the imaging event parameters, we obtain the following data for the block:

1. Line, sample values of all image coordinates (converted to "imaging event" line values).
2. The accuracy of the line, sample coordinates.
3. Ground control values for all points.
4. The reference datum of the ground control and the accuracy (standard deviation or 90% CE, LE) for the control and diagnostic points.

The line and sample values are obtained using software developed on a SUN workstation. The workstation displays the digital SPOT image from the CCT and records the coordinates of the pixel locations selected by the operator.

The adjustment depends on the collection of line/sample values for three types of photo identifiable ground points: tie points, control points, and diagnostic points.

Most of the points in any solution will be tie points. Tie points are simply conjugate image points with precisely known line/sample values which are identifiable on multiple imaging events. The initial ground point coordinates for tie points are very imprecise; the ground coordinate variance-covariance matrix for each tie point is such that the tie point ground value does not affect the solution. Tie points are selected so that all overlapping imagery has measured conjugate image points.

Control points are similar to tie points, except that the ground point coordinates are accurately known and are given appropriate horizontal and vertical weights. They are used to establish the relationship between the sensor and the external three dimensional coordinate system. The absolute accuracy of the triangulation is dependent on the number, distribution, and accuracy of the control points.

Due to the nature of the block triangulation process, not all orbits will require control points. However, control points need to be located around the edges of the block to achieve the best accuracy. While there is no absolute minimum number of control points, the accuracy of the adjustment is improved as more control is added, up to a number where there are diminishing returns.

Diagnostic points are identical to control points. The only difference is that diagnostic points are withheld from the solution, and are used later in an accuracy evaluation procedure to ensure that the triangulation meets accuracy standards. The diagnostic points are most beneficial for accuracy evaluation if well distributed throughout the entire block.

The SPOT CCT does not provide variance-covariance data specific to an individual SPOT image. SPOT has documented the specification accuracies for the mirror positioning, attitude drift rates, and ephemeris positions. Ground control accuracies are derived from the ground control source accuracy. Image coordinate accuracies are determined by the mensuration process. The appropriate variance-covariance matrices for the imaging event parameters, ground point values, and image point values are derived and input into the triangulation math model.

SOFTWARE

All the software is written in FORTRAN on a SUN 3/180 under a UNIX operating system. In anticipation of requests to deliver the software to other systems, it is very modular and was designed to be easily transportable.

The triangulation process uses an iterative least squares technique to converge on a solution for the support parameters. The solution generally converges within four iterations.

The algorithm exploits the sparse matrix conditions of the normal equations to reduce computer time. The actual time required depends on the total number of unknowns in the solution; it is dependent on the number of imaging events and ground points (it is not dependent on the number of images). It takes approximately five seconds per iteration to run a small block containing two or three imaging events. For blocks of 30 imaging events, each iteration may require approximately 90 seconds.

The current array dimensions limit the size of the block to 30 imaging events, with a maximum of 10 images per imaging event. These array dimensions are easily modified for blocks of larger size. The only overlap restriction is that conjugate image points are distributed over the block; if conjugate image points are not contained within any single imaging event, then the software essentially performs a weighted resection for each of the imaging events.

The parameters are adjusted on an imaging event basis. Therefore, 300 images on 30 separate orbits (10 images per orbit, 30 imaging events) can be adjusted as quickly as 30 images on 30 separate orbits (one image per orbit, 30 imaging events).

TRIFID has software modules to generate rational function coefficients from the output of the triangulation. These rational function coefficients have been used in all our real-time applications. They allow for a very simple and straight-forward method of generating consistent mapping products from SPOT imagery. We use these coefficients to generate rectified and orthorectified SPOT images, geocoded onto various map projections. The rational functions have been applied to derive accurate point positions of features on digital monoscopic and stereoscopic workstations.

OEEPE TEST DATA RESULTS

Dr. David Gugan, of Laser Scan Laboratories, graciously provided us with all the data for the OEEPE test area. The data set consisted of four stereopairs collected on two orbital passes. The data was provided in the form of printouts of measured image coordinates, ground control coordinates, and SPOT header data.

It was necessary to preprocess this data to make it compatible with the TRIFID software. The preprocessing consisted of converting the image point coordinates to line and sample values, converting the control from the French Lambert Conformal Conic projection coordinates to geographic coordinates, and entering the appropriate SPOT header data. A subset of points were then selected to be used as control and diagnostic points, with the remainder to be used as tie points (the provided ground control coordinates for the tie points were not used).

The ground control values which were provided were derived from four sources; 1:25000 maps, field surveys, 1:30000 stereophotographs, and 1:60000 stereophotographs. We found each of the sources to be clustered; for example, the 1:25000 map derived points were all grouped together, not distributed throughout the block. (See Figure 1.)

Several of the points were only measured on a single image; these points were not used, as the solution requires conjugate image point pairs. Several of the points were "tie points" to join across a north-south image boundary within a strip. Our concept of imaging events makes a pair of these "tie points" redundant, and one of each pair were dropped.

Two imaging events were adjusted in the triangulation (one event for each orbit). The block triangulation was performed with 16, 12, 6, and 4 well distributed control points to see the effects of control on the adjustment. Each run contained 40 tie points. The coordinates of 41 diagnostic points were computed from the adjusted solution and compared to the values provided.

The results showed a significant bias between the ground points derived from the 1:25000 map sheets and the points derived from the field survey and the photos (see Figure 2). The 1:25000 derived points were deleted from the control and diagnostic sets but were kept in the tie point set; the adjustments were then rerun. The results with several ground point control configurations are shown below. These results compare closely with the values derived through the theoretical error propagation.

Number of control points	Accuracy (90%, meters) CE	LE	Accuracy (RMS, meters) LAT	LON	HT
16	14.0	11.6	7.0	5.3	6.9
12	14.6	11.2	6.7	6.3	6.7
6	16.3	11.7	7.7	7.0	7.0
4	18.0	14.8	9.0	7.6	9.1

Table 1

These results show that the eight images can be accurately positioned with 6 control points. When 4 control points are used, systematic errors appear in the vector plots of the diagnostic points.

Point Distribution

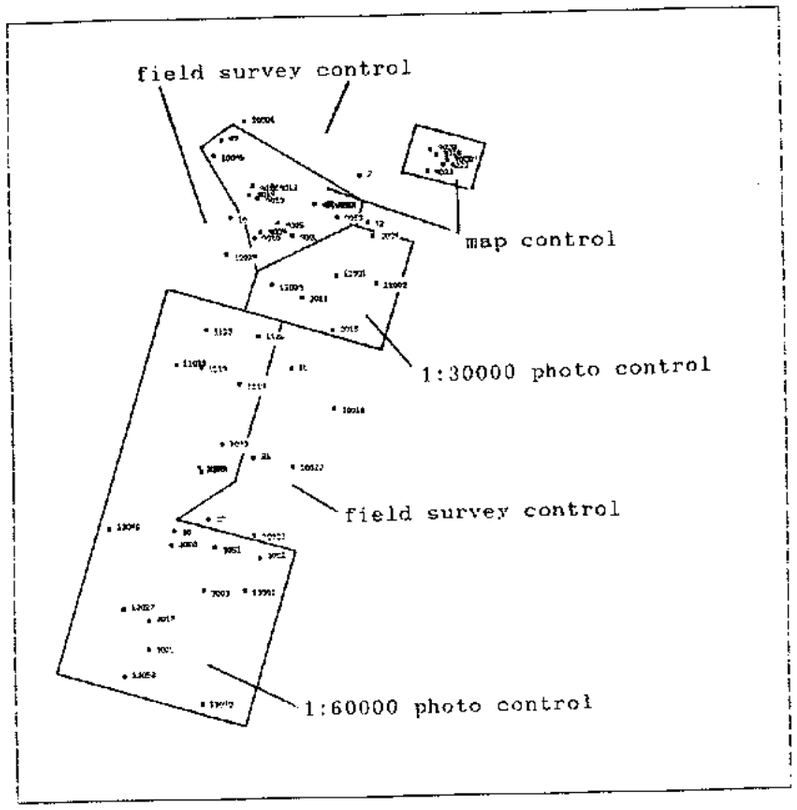

Figure 1.

Horizontal Residual Plot

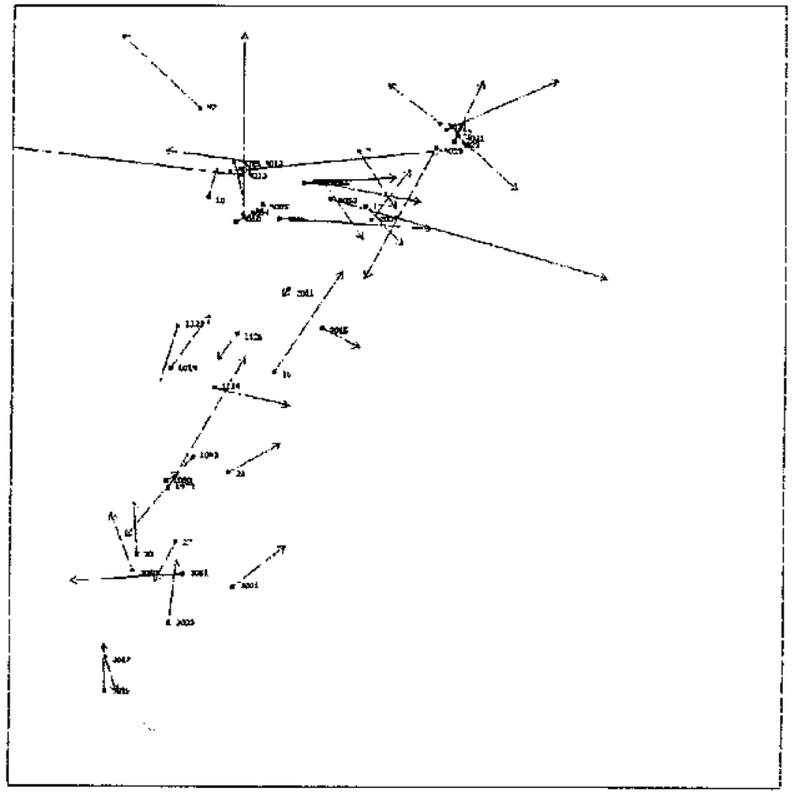

Vector scale : 20.0 meters

Figure 2.

RESULTS OF OTHER TEST DATA

Real data tests have also been performed over other geographic areas; for example, New Mexico and West Virginia in the U.S. For these data sets, the mensuration was performed by TRIFID on a monoscopic digital display using company developed software. TRIFID image processing software was used to radiometrically enhance the digital imagery. A brief description of the results over each area follows.

New Mexico

The New Mexico site consists of three orbits with a total of four images. A large amount of ground control was available with a high degree of absolute accuracy. There were a total of 83 control points to choose from over the two model area, all with an accuracy of 2.1 meters horizontal (90% CE) and 3.3 meters vertical (90% LE) relative to the World Geodetic System 1984 (WGS-84).

Ten points were selected to use as control, and the other 73 were withheld from the solution to use as diagnostic check points. The 10 points were placed in each corner of each model, with 19 additional tie points placed evenly throughout the models to tie the images together. (The algorithm treats tie points and control points identically, of course, the only difference being the variance-covariance matrix associated with the initial estimate of the ground value.) The adjustment converged within five iterations.

Rational functions were computed from the triangulation parameters, and diagnostic point values were derived. The absolute accuracy was of 13.29 meters horizontal (90% CE) and 13.44 meters vertical (90% LE) relative to WGS-84 (RMS 8.6 meters horizontal, 8.1 meters vertical). These values concur with the theoretical error propagation numbers.

The same data was re-triangulated, using only five control points (one in each corner and one in the center of the two model region) and 19 tie points. The 73 diagnostic points were derived in the same manner as above, and produced an absolute accuracy of 12.76 meters horizontal (90% CE) and 15.18 meters vertical (90% LE) (RMS 8.3 meters horizontal, 9.2 meters vertical). Again, the derived diagnostic values agreed with the theoretical error propagation values.

West Virginia

The West Virginia data set consists of a single stereopair. USGS 1:24000 quadrangle sheets were used to derive ground values for 14 points. The accuracy of these values are 12.2 meters horizontal (90% CE) and 6.0 meters vertical (90% LE) relative to NAD 27. Four of the points were used as control (one in each corner) and the other 10 were withheld as diagnostic points. Ten tie points established the relativity between the images.

Subsequent diagnostic comparisons using the rational function coefficients showed an accuracy of 17.88 meters horizontal (90% CE) and 16.11 meters vertical (90% LE) (RMS 11.1 meters horizontal, 9.3 meters vertical). These values agree with the theoretical error propagation values.

SUMMARY

TRIFID Corporation has developed a rigorous simultaneous block triangulation program for SPOT images. The technique uses a unified least squares approach in performing a bundle adjustment. The system is operational and has provided excellent results.

There are several advantages to using this method with SPOT digital imagery:

1. A simultaneous block triangulation will allow for the generation of mapping products over large areas with minimal breaks in the data across image boundaries.
2. A fully weighted, rigorous block triangulation minimizes the need for ground control points.
3. The accuracy of ground positions are adequate for 1:50000 scale applications.
4. Updated image support data (exterior orientation parameters) are created. The images are not resampled.
5. The software variance-covariance output allows for rigorous accuracy estimation of the derived products.
6. There is a low cost-benefit ratio given the costs of adjustment versus the quality of the support data and application data consistency.

Four or five control points are all that are required for triangulating a single stereomodel; however, for analysis purposes, four or five diagnostic points over the stereomodel should also be available. With the imaging event concept, the triangulation of larger blocks reduces the number of control points. If long continuous imaging events are being adjusted, the block triangulation should require an average of only a single control point per individual SPOT model (60 km x 60 km). However, a sufficient number of well-distributed diagnostic points should always be available to perform an accuracy analysis of the adjustment.

The SPOT sensor's relatively high resolution, stereo capability, and wide coverage offers potential for systematic three dimensional mapping of large areas. By rigorously performing a simultaneous bundle adjustment of a block of SPOT images, the true potential of the accurate mapping capabilities of the sensor can be realized.

APPENDICES

Appendix I

1 Instructions for phase 1 of test.

2. Instuctions for phase 2 of test.

OEEPE

ACTION GROUP ON USE OF SATELLITE DATA
TEST ON TRIANGULATION OF SPOT DATA

TEST INSTRUCTIONS

Objective

The objective of the project is to determine:

1. the accuracy which can be obtained when determining control points from a strip covered by stereo SPOT data;

2. the number of control points which are necessary;

3. the use which can be made of auxilliary data provided by tracking the satellite and from on-board instruments;

4. the programs which are available for triangulation of SPOT data and the efficiency which can be achieved by such methods.

Each participant will be provided with test data and will carry out the triangulation using methods available the them. Participants will provide a detailed description of their method for publication with the test results.

Test Area

The test area will be the European test site extending from Marseilles to Grenoble. The area of 240km in a north-south direction and 100km east-west is covered by eight SPOT models in two strips and by control fixed by IGN(F). The control in strip A consists of 80 points from triangulation and aerial photography and 30 points fixed especially in the field. In strip B there are a further 105 points from 1:25 000 maps and 1:60 000 photography.

Participants may work with one strip or both.

Level 1A data will be provided to all centres on magnetic tape or as film positives with header information provided separately.

Material

Participants will be provided with the following materials:

Images - 4/8 SPOT stereo pairs with relevant ephemeris and auxilliary data;

Additional information
- A geoid map with contours relative to the ellipsoid

Control - 110 already selected and co-ordinated by IGN, with description and location marked on marked on photograph. Ground co-ordinates of 20 points will be provided.

Requirements

Participants will provide to the pilot centre ground co-ordinates of the check points of which descriptions are provided with comments on their suitability as control points and the ease of identification. The following control distributions should be used:

STRIP A
a) all points provided;
b) points 001, 004, 014, 2002, 1078, 018, 026, 028, 3036, 3040;
c) points 001, 004, 1018, 018, 3036, 3040;
d) points 001, 004, 3036,3040;
e) points 001, 3040;
f) points 001, 004.
STRIP B
g) all points
h) points 5, 1036, 78, 73;
i) points 5, 1036, 73;
j) points 5, 73.

Co-ordinates of check points must be provided in hardcopy form with comments, and may also be provided in one of the following forms: DEC PDP 5" floppy disk; DEC VAX TK50 cartridge; IBM PC 5" floppy disk; Apple Macintosh 3½" disk. Please consult the pilot centre if there is any doubt over the format or medium to use.

Participants will also provide details of the method used and comments on problems and possible improvements.

The software used should have, as a minimum, the following features:

1. provision for handling strips of SPOT data as a unit with control distributed over the length of the strip;

2. provision for use of the header data from the SPOT tape;

3. output of setting up parameters for each model in the strip and co-ordinates of control points in each model.

4. an additional desirable feature is provision to join strips together.

Project organisation

University College London will act as the pilot centre and will co-ordinate the project which will be overseen by a working group consisting of the participants.

The report on the project will consist of papers describing the method used and the reults obtained, prepared by each of the participants. The papers will be presented at a workshop.

Timetable

July 31st 1989	Completion of work
September 27th 28th 1989	Final Workshop.

DEPARTMENT OF PHOTOGRAMMETRY AND SURVEYING

UNIVERSITY COLLEGE LONDON
GOWER STREET LONDON WC1E 6BT

9th April 1990

OEEPE TEST OF SPOT TRIANGULATION

Dear Colleague

I enclose the image co-ordinates of of the eight scenes in strip A observed by IGN. The units are pixels on the images for which you already have header data and ground control.

Please process this data using your program with the *same control configurations* as used previously for strip A and derive ground co-ordinates of the check points.

If at all possible could you let me have your results by 31st May so that I can report to the Steering Committee meeting in June that the practical part of the test is complete. I will then prepare the final report by September. Please let me have a revised report on your method and on the processing which you have carried out for the test with the results. If I do not receive anything further I will assume that the report which you prepared before still stands.

Many thanks for your co-operation. I hope that we can now draw the test to a speedy conclusion.

Best wishes.

Yours sincerely

Ian Dowman

To: Auke de Haan, Politecnico Milano
Vlad Kratky, Canadian Centre for Mapping
Russel Priebbenow, Dept of Geographic Information, Queensland
Gustav Picht, IPI, Hannover
Isabelle Veillet, IGN
Ian Dowman, UCL

Telephone (+44) 01-380 7225 01-387 7050 Fax (+44) 01-380 0453 Telex 296273 UCLENG G e-mail iah@ph.ac.ucl.ox National Grid Reference TQ 296 822
I A Harley, BSurv, PhD, FISAust, FRICS Professor of Photogrammetry and Surveying Head of Department

FIRS
 4 scenes

 50AA259
S12P82 860728 105805 50259
 41 POINTS
002 2359.1 53.4
001 719.4 470.9
003 4326.7 219.6
004 5479.6 513.3
005 818.1 2769.2
006 1982.3 1668.4
007 3820.6 1660.4
008 4919.4 1466.6
010 1341.6 4029.3
011 3720.8 3406.3
012 4407.1 3333.9
013 3696.4 2949.6
014 1627.4 5375.2
2001 4224.9 5440.9
2002 5222.4 5456.3
2003 5626.2 4232.9
2004 4692.8 3754.8
2005 4105.3 4489.2
2006 2888.1 4345.1
2007 3338.4 5486.4
2008 2196.1 5002.9
9004 2176.6 4360.1
9005 2430.3 3902.3
9006 2896.9 4267.6
9010 2096.8 4631.8
9012 1973.9 2637.1
9013 1759.3 3148.3
9014 1535.3 3083.1
9015 1522.8 2762.3
9020 5044.3 303.3
9021 5480.8 563.7
9022 5483.7 772.6
9023 5221.3 1087.3
9028 5221.6 450.3
9050 3357.8 2896.8
9051 3408.8 2846.2
9052 3058.6 3001.6
9053 3693.9 3345.4
9054 3719.9 3426.4
44 1061.6 5542.4
46 376.8 1921.8

 50AB260
S12P82 860728 105814 50260
 21 POINTS
015 5386.1 2757.9
016 4135.4 3494.6
017 3817.9 4611.9
018 5425.5 4647.5
1018 1568.6 4098.1
1019 2144.9 4026.1
1021 1424.9 3957.4
2009 2915.1 579.1
2011 3684.4 848.1
2012 4622.7 743.6
2013 5682.3 520.8
2014 3794.1 2224.1
2015 4658.4 1839.4
2016 5896.9 1843.1
1114 3143.1 4366.1
1122 1379.1 2710.4
1123 1911.7 2662.7
1124 2359.4 1412.2
1125 2933.6 2649.4
1126 3123.7 2553.6
1048 2330.3 5420.3

 50AC261
S12P82 860728 105822 50261
 23 POINTS
019 3992.8 415.8
021 4146.6 1303.4
022 5074.0 1374.5
023 4228.4 2425.6
024 5856.1 1934.6
025 2527.9 3492.6
027 3759.9 3803.2
028 4894.2 4107.2
030 3120.1 4429.4
1037 2899.6 1134.3
1042 2296.1 1048.4
1043 3335.8 1035.8
1047 1279.6 152.4
1076 1588.9 2476.6
1078 2301.4 2369.4
1079 3134.9 2152.6
1080 3045.9 1967.9
3044 2319.6 4997.9
3045 1630.1 4791.3
3047 5907.7 4629.3
3051 4149.9 4774.1
3001 5208.4 4872.1
3050 3187.9 4995.9

 50AD262
S12P82 860728 105831 50262
 17 POINTS
3002 5201.7 546.9
3003 4320.3 792.7
3024 4208.7 1897.4
3025 5707.6 1739.4
3027 2713.1 2003.6
3029 2221.1 856.1
3017 3379.6 2243.9
3042 4986.7 3720.1
3016 3659.1 3291.9
3040 5332.9 4930.1
3048 4455.9 4997.1
3023 4206.8 3559.3
3004 5237.3 518.7
3035 2682.5 5393.0
3053 3371.6 4436.4
3015 2746.9 3615.9
101 2450.9 5213.9

SECO
 4 scenes

 50BA259
S11P11 860830 102322 50259
 41 POINTS
002 2096.6 123.9
001 514.8 318.9
003 3934.6 553.4
004 5100.8 1007.9
005 356.4 2611.4
006 1587.6 1677.3
007 3256.7 1911.7
008 4397.9 1872.9
010 787.3 3938.7
011 3074.1 3636.9
012 3733.6 3658.4
013 5022.2 3451.1
014 895.4 5313.6
2001 3366.1 5727.8
2002 4256.6 5873.4
2003 4832.7 4717.4
2004 3884.4 4108.6
2005 3237.7 4759.7
2006 2156.4 4455.6
2007 2518.1 5653.1
2008 1441.3 5017.6
9004 1490.4 4379.6
9005 1812.3 3957.8
9006 2170.1 4380.1
9010 1389.4 4635.6
9012 1468.4 2636.6
9013 1246.3 3117.8
9014 1054.6 3023.3
9015 1070.8 2702.8
9020 4688.5 738.8
9021 5099.7 1058.2
9022 5026.2 1262.4
9023 4718.3 1537.8
9028 4835.8 900.2
9050 2765.3 3081.8
9051 2820.8 3038.3
9052 2468.4 3144.8
9053 3053.4 3572.6
9054 3072.1 3656.6
44 347.9 5403.6
46 93.6 1715.6

 50BB260
S11P11 860830 102330 50260
 21 POINTS
015 4264.9 3312.4
016 2963.1 3876.4
017 2560.9 4942.3
018 4168.0 5198.0
1018 479.4 4132.6
1019 1010.2 4136.7
1021 359.9 3973.6
2009 2034.4 811.6
2011 2753.1 1182.1
2012 3688.4 1206.6
2013 4685.1 1125.9
2014 2705.4 2565.1
2015 3616.9 2299.9
2016 4858.6 2476.1
1114 1932.2 4608.4
1122 371.4 2722.2
1123 904.6 2747.7
1124 1432.8 1577.8
1125 1843.6 2869.4
1126 2036.1 2799.7
1048 1064.3 5545.3

 50BC261
S11P11 860830 102339 50261
 23 POINTS
019 2617.3 886.8
021 2686.1 1790.9
022 3611.0 1987.0
023 2664.9 2917.1
024 4348.6 2652.1
025 930.4 3750.1
027 2069.1 4222.1
028 3187.7 4678.7
030 1401.8 4758.4
1037 1469.1 1452.3
1042 938.1 1287.9
1043 1915.8 1413.3
1047 73.6 264.1
1076 130.4 2615.1
1078 819.4 2602.9
1079 1628.4 2499.1
1080 1551.2 2302.7
3044 617.4 5218.6
3045 15.7 4923.6
3047 4173.7 5337.4
3051 2398.1 5240.9
3001 3443.6 5482.6
3050 1411.9 5329.6

 51BD262
S11P11 860830 102347 51262
 17 POINTS
3002 3322.6 1270.9
3003 2401.1 1393.4
3024 2234.2 2480.2
3025 3739.6 2527.3
3027 799.3 2386.7
3029 437.6 1180.2
3017 1415.9 2714.1
3042 2838.7 4394.9
3016 1570.2 3791.1
3040 3078.9 5645.3
3048 2209.1 5594.1
3023 2086.6 4130.6
3004 1417.3 978.6
3035 501.5 5754.5
3053 1214.6 4891.4
3015 700.7 3993.8
101 300.6 5545.3

NºPT	COL	LINE

Digital simultaneous monoscopic measurements over IGN A strip

ign FRANCE
Institut Géographique National

Appendix II

1. Programme for Workshop
2. List of participants at the workshop.

ORGANISATION EUROPÉENNE D'ÉTUDES PHOTOGRAMMETRIQUES EXPÉRIMENTALES
(OEEPE)

WORKSHOP
TRIANGULATION OF SPOT DATA

September 27th and 28th, 1989

at

University College London

Programme

Wednesday 27th September

900	Registration	
930	Opening of Workshop	
Session 1	**Chairman P.Denis**	
1015	Background to test	I.J.Dowman I.Veillet
1045	Coffee	
1115	The role of the pilot centre and summary of results	I.J.Dowman
1230	Lunch	
Session 2	**Chairman D.Rosenholm**	
1345	Reports from participants	IGN Canadian Centre for Mapping Department of Geographic Information, Queensland
1715	Close	
2000	Workshop dinner	

Thursday 28th September

Session 3	**Chairman D.V.Kratky**	
930	Reports from participants	Hannover Politechnico Milano UCL and LaserScan Laboratories
1200	Other	Trifid Corporation UCL
1230	Lunch	
Session 4	**Chairman I.J.Dowman**	
1345	Report from SPOT Image	Ph. Munier
1430	Discussion	
1600	Discussion of future plans and final summing up	
1700	Close	

LIST OF PARTICIPANTS

	NAME	OCCUPATION
1	ISABELLE VEILLET	IGN
2	VLAD KRATKY	CCM
3	P. DENIS	IGN
4	PH. MUNIER	CNES
5	LUIS COGAN	KERN
6	KEITH MURRAY	ORDNANCE SURVEY
7	NIGEL HIGH	ORDNANCE SURVEY
8	RUSSEL PRIEBBENOW	QUEENSLAND
9	IAN DOWMAN	UCL
10	DAVID GUGAN	LSL
11	PETER MULLER	UCL
12	MARK O' NEIL	UCL
13	WAYNE WILSON	TRIFID CORP USA
14	GUSTAV PICHT	HANNOVER
15	AUKE DE HAAN	MILAN
16	FRANCELINA NETO	UCL
17	DAN ROSENHOLM	SWEDEN SPACE COR
18	TORBJORN WESTIN	SWEDEN SPACE COR
19	SAAD YASSEN	UNIV. OF GLASGOW
20	E. THEODOSSIOU	UCL
21	IAN HARLEY	UCL
22	ROGER KIRBY	UNIV. OF EDINBURGH
23	A. GEORGOPOULOS	NTU OF ATHENS

Appendix III

Input from SPOT Image

Ph. Munier of SPOT Image presentad a paper to the wokshop on the current status of mapping from SPOT data and this is included in this appendix.

Information was also presented to the Workshop on new developments in SPOT products. These included the new photogrammetric film product , level 1AP, with stretching in the cross track direction and better fiducial marks, and DORIS, a ranging system requiring transponders on the ground but giving bettter positional information , which would be flown on SPOT 2.

The participants in the workshop raised a number of points with SPOT Image which resulted in the following comments:

full geometric calibration data will be published;

orbit and attitude data could be provided on a floppy disc with annotations for ease of use;

better precision of scene centre time is required;

attitude calibration is done 'frequently' when the sensor is not imaging.

MAP PRODUCTION AND MAP UPDATING USING SPOT DATA

Philippe MUNIER

Jean Claude RIVEREAU

SPOT IMAGE - Toulouse - France

ABSTRACT

From concept and design to actual tested performances, SPOT imagery is perfectly adapted to cartographic applications. Regular topographic mapping or map updating is achieved at scales ranging from 1:100,000 to 1:25,000 and products such as Digital Elevation Models and spacemaps are emerging. Present trends to meet the users'needs and requirements lead to the development of new products with updated specifications, produced more rapidly and at a lower cost.Technical innovation and the need for equipment investments are slowing down the development of SPOT cartographic applications. Improvements in digital techniques will lead to a positive evolution and new products will certainly contribute to a significant increase in basic cartographic mapping suited for development projects in the world.

RESUME

De par sa conception et ses caractéristiques, SPOT est parfaitement adapté aux applications cartographiques ainsi que l'ont démontré les nombreux tests réalisés à ce jour. La cartographie régulière ainsi que la mise à jour des cartes peuvent être conduites à des échelles allant du 1/100.000 au 1/25.000 et des produits tels que les Modèles Numériques de Terrain et les spatiocartes commencent à apparaître. La tendance actuelle pour satisfaire les besoins et les exigences des utilisateurs va vers le développement de produits nouveaux avec de nouvelles spécifications, produits qui seront réalisés plus rapidement et à des coûts moindres. L'innovation technique et les contraintes d'investissement pour l'équipement freinent le développement des applications SPOT sur le marché de la cartographie. L'amélioration des techniques numériques va favoriser une évolution positive et les nouveaux produits contribueront à l'augmentation rapide d'une production cartographique adaptée aux projets de développement dans le monde.

1. - CARTOGRAPHIC APPLICATIONS OF SPOT IMAGERY

United Nations statistics regarding the state of topographic cartography in the world show that only 44% of the land masses are covered by maps belonging to the 1:50,000 and 1:100,000 scale groups, which are the most important for economic development. In addition, a large part of these maps is obsolete and does not meet the countries'needs for development purposes. Since Landsat 4-TM in 1982 and moreover SPOT 1 in 1986, one can state that spacemaps will represent the base of cartography at small and medium scales in the near future.

The uses of space imagery in cartography include **revision** of existing maps, compilation of **new maps** and remaking of maps at larger scales than those currently in use. Satellite imagery is suited for compiling **general topographic maps** as well as **thematic maps**: vegetation, agriculture, urban and rural land use, geology, pedology, water ressources, environment etc...

Before we review the different forms that spacemaps* may take, let us remind the SPOT characteristics and capacities in the field of cartography.

2. - SPOT CHARACTERISTICS AND CARTOGRAPHY

From concept and design to actual tested performances, SPOT is perfectly adapted to cartographic applications.

The key advantages of SPOT imagery for topographic mapping are the following:

A) **Data acquisition flexibility** and large ground coverage : the oblique viewing capability of the SPOT HRV imaging instruments to either side of the satellite ground track gives imaging access to all areas within a 950 km-wide corridor. This oblique or cross-track viewing capability considerably reduces the time required to access a given area or to obtain complete coverage of a country.

B) **Improved spatial resolution** which allows to identify most of the ground features for mapping at a scale of 1:50,000 and in some cases 1:25,000.

C) **Stereo capability.** Stereoscopic vision is obtained with SPOT by taking two oblique views of the same area from two different orbits. The B/H ratio can vary as the pointing mode possibilities range from + 27° to - 27° (B/H from 0 to 1.1). This introduces the possibility of relief perception in photointerpretation and photogrammetric relief plotting.

D) **Good geometric performances.**

The **geometric precision** and the **information content** are the main features for any cartographic use of SPOT imagery, and we are going now to deal with each of them.

GEOMETRIC PRECISION

SPOT accuracy performances were first checked by a team of the Institut Geographique National, France, (V. RODRIGUEZ A.C;, DE GAUJAC, P. GIGORD, P. MUNIER, 1986). The results demonstrated that the expected accuracy in terms of planimetry and altimetry were met. The assessment was performed on 60 stereopairs with 3 viewing configurations: . + 27° and - 27° with B/H = 1 . 0° and 27° with B/H = 0.5 . + 13° and - 13° with B/H = 0.5

177 check points and control points were determined with an accuracy of: 3 meters in X, Y and 1.5 meters in Z.

* In the text, the use of term spacemaps refers to any cartographic product based on space imagery while the term Imagemap refers to products presented with the image as a background.

The stereopairs were processed on a Matra-Traster analytical plotting equipement for:

- Plotting ground control points (GCPs) and modeling the SPOT view,
- calculation of deviation from true positions.

Practically 6 to 10 points from the topometric network were sufficient to establish the model for one stereopair, the remaining points being then used for stereoplotting. The raw results (G. BRACHET, P. DENIS, W. Nordberg Symposium, 1987) for all stereopairs indicate a RMS residual error for each point of:

8.0 m in X, 6.6 m in Y and 7.1 m in Z.
After filtering, the RMS residual errors were reduced to:
4.6 m in X, 4.4 m in Y and 5.3 m in Z,
3.5 m in Z with a B/H of 1 and 6.7 m with a B/H of 0.5.

The most significant results are presented in Table 1.

R.M.S.	X	Y	Z
RAW RESIDUES	8.0 m	6.6 m	7.1 m
FILTERED RESIDUES	4.6 m	4.4 m	5.3 m
CONFIGURATION + 27°/-27° RAW RESIDUES	8.1 m	5.5 m	4.3 m
CONFIGURATION + 27°/-27° FILTERING RESIDUES	3.8 m	4.2 m	3.5 m
CONFIGURATION 0°/±27° RAW RESIDUES	7.8 m	7.2 m	8.3 m
CONFIGURATION 0°/±27° FILTERED RESIDUES	4.6 m	4.4 m	6.7 m

TABLE 1

Professor G. KONECNY from the Institute for Photogrammetry and Engineering Surveys, University of Hannover, (G. KONECNY : The use of SPOT imagery on analytical photogrammetric instruments, SPOT 87) developped a mathematical model which avoids high correlations between the unknowns and is based on the use of photo coordinates. The unknowns of the orientations are approximated by the use of orbit data and in the course of adjustment, are partly formulated as additional parameters. The method has been implemented on Zeiss Planicomp and Orthocomp hardware and a bundle adjustment programme BINGO has been modified to handle SPOT geometry. The results of test are given in table 2.

NUMBER OF ADJUSTED POINTS	NUMBER OF CONTROL POINTS	ADD. PAR. LEFT/ RIGHT	INTERNAL ACCURACY				
			σ_0	σXYMAX	σXYMEAN	σZMAX	σZMAX
86	18	4/3	8.4	8.7	5.2	10.9	8.5
86	34	3/3	7.9	6.1	4.5	8.8	7.1
86	83	4/5	6.1	4.5	3.0	5.6	5.0
NUMBER OF INDEPEND. CHECK P.	NUMBER OF CONTROL POINTS	MEAN DIFFERENCES			MEAN SQUARE DIFFERENCE		
		X	Y	Z	X	Y	Z
68	18	7.9	10.4	4.8	10.9	13.7	6.5
52	34	8.3	10.5	4.5	11.3	13.8	6.2

TABLE 2

Similar results have been obtained by the University College London (Gugan, Dowman), Mc Donald Detwiler Ass. (Canada) and Ordnance Survey (Hartley) on analytical plotters or by automatic correlation techniques (INRIA-ISTAR, MDA, Geospectra), which give figures around 10 to 15 m in planimetry and better than 10 m in altimetry. I.J. Dowman, in his extensive review of SPOT prospects in cartography (I.J. Dowman, the prospects for topographic mapping using SPOT data, SPOT 87) concluded that the necessary accuracy for mapping at 1:50,00 scale with 20 m contour lines is achieved with SPOT and that organizations are prepared to produce imagemaps at scale 1:25,000 (orthophotos).

Following this description of the planimetric and altimetric performances of SPOT required for topographic cartography, we must recall that a large part of the needs is satisfied by maps realized with monoscopic viewing: the cartographic background is then made of accurately geometricaly processed images, but ignoring the effects of relief and incidence. That is why an accurate evaluation of the **standard SPOT level 2 product*** was made in 1988 by CNES and IGN (de Gaujac, Bégni, 1989). The operation concerned 11 level 2A scenes and 21 level 2B scenes (including 2 segments of 4 scenes). These images were distributed on several locations of the world (France, la Réunion Island, Marocco, Brazil, USA, Australia, Japan). Various check documents were used: 1:25,000 and 1:50,000 maps or stereopreparation network. The number of check points goes from 20 to 70 per scene. The results are given in table 3 below:

LEVEL	GLOBAL TRANSLATION	INTERNAL DISCREPANCIES
2A	412 m	28 m
2B	0 m	Pan: 10 m** XS: 14 m

TABLE 3

* SPOT level 2 products are rectified according to a given cartographic projection; level 2A without ground control points; 2B with ground control points (georeferenced)..

** NB: RMS obtained when control and check points are known at a better precision than 10 meters (1:25,000 maps or stereopreparation).

This evaluation demonstrates that the standard level 2 products perfectly fit with cartographic requirements at scales 1:50,000 and smaller. However, the precision of level 2 products depends on altitude differences and viewing angle (see fig. 1). Therefore every effort must be done to carry out vertical or near vertical viewing, in twin-HRVs mode, when a monoscopic imaging of large areas is required for basic mapping purposes in thematic studies and development projects.

FIGURE 1

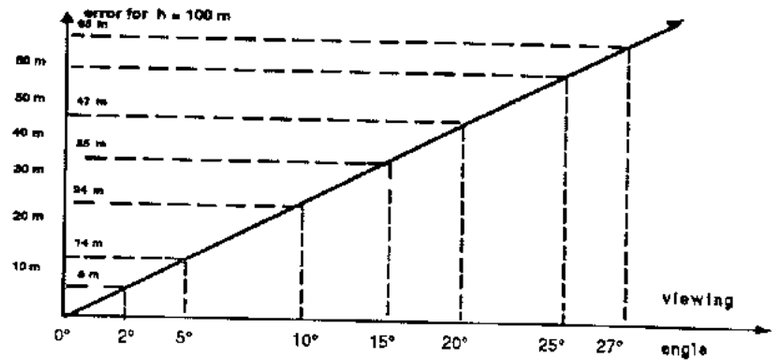

Maximum planimetric error for any point placed at height h = 100 m above or under the rectification level, as a function of the viewing angle for SPOT georeferenced products (Level 2).

We can thus rightfully conclude that the geometric performances of SPOT lies between 5 and 15 meters in planimetry as well as in altimetry allowing, as most authors agree, to compile maps at scale up to 1:50,000, and even 1:25,000, in the form of imagemaps as well as linemaps.

INFORMATION CONTENT

The specifications relating to the information content are much more difficult to be defined than the ones concerning the precision. Many tests have been made to evaluate the information content of SPOT images.

First of all, the digital nature of the images has to be underlined : the interpretation can be much improved by applying image processing (enhancement, filtering, etc..) (Gugan and Dowman, London 1987).

To this end, IGN France achieved in 1987 a series of topographic maps over the Ghardaïa area in Algeria, at 1:50,000, 1:100,000 and 1:200,000 scales, including linemaps, imagemaps and even mixed ones. An important field completion was necessary to reach the actual IGN specifications compatible with standard linemaps. Let us also mentioned the study made by Dowman et al. (1987) over the Aix-Marseille area, about stereocompiling Panchromatic images. The results are given by table 4:

	1:50,000, % errors		1:100,000, % errors	
	omission	commission	omision	commission
Roads (major)	13	0	0	
Canals (major)	0	0	0	
Rivers	0	0	0	
Railways	3	0	0	no
Buildings	33	9	25	
Minor roads, tracks	56	20	28	
Canals (minors)	100	0	100	
Streams	45	0	0	

TABLE 4

Results of a French-Canadian experiment about the SPOT image content performed by F. Salgé et al. and D. Begin et al. given in table 5 below are also significant:

	% well classified
Roads (major)	86
Roads (medium)	92
Tracks, pathes	91
Rivers	95
Streams, ditches	45

TABLE 5

As far as land use features are concerned, they are correctly interpreted for the 1:50,000 scale specifications, providing operators are carefully trained to SPOT images analysis. (F. Salgé et al., Sherbrooke 1988).

These various examples demonstrate that the SPOT imagery characteristics are compatible with cartographic specifications at 1:50,000 and 1:100,000 scales, and raise new and interesting possibilities in terms of rapidity of production, homogeneity of interpretation over large areas, reliability and flexibility of the digital information content.

3. - EVOLUTION OF TOOLS, METHODS AND PRODUCTS

In order to reduce production costs and to improve technical performances, most of the production process steps should yet be developed:

Geometric modelization and space triangulation:

When large areas are at stake, in monoscopic as well as stereoscopic viewing, a significant reduction of the ground control network can be reached, while procuring a better consistency of the work. I. Veillet (Sherbrooke, 1988) presented results on a two segment stereopair of 4 scenes each, which confirm the geometric performances of SPOT. Such methods, using spatial triangulation, will have to be used in the future when processing large areas.

Mosaïcs and orthomosaïcs:

A large part of the cartographic market at small scales is, from now on, based on mosaïcs or orthomosaïcs of space images. The product is an imagemap with conventional specifications concerning projection, sheet cutting, scale, framing and editing; the information is made of a mosaïcs of georeferenced images as a background, eventualy corrected by using a DEM and may include graphical overlays: toponyms, contour lines, administrative boundaries, etc.
These products present an undeniable economic interest: thanks to their small cost and short production time, they are excellent up dated cartographic documents. Many imagemaps projects over large areas of several hundreds of thousand of Sq-km have already been carried out. Cost of mapping, including SPOT data, turns around 2 US$ per Sq-km at a scale of 1:100,000 and 4 US $ per Sq-km at a scale of 1:50,000.

Stereocompiling:

The production activity in this field has been up to now relatively low. This is probably due to the particularities of the SPOT stereo programming, but mainly to the rate of development of the market of stereoplotters suited to SPOT imagery. Most manufacturers of analytical stereocompilers now propose a SPOT version (T5N of MATRA, DSR1 of KERN, Planicomp C100 of ZEISS, BC and AC of WILD, Intergraph-Intermap). Analytical stereocompilers are designed to process aerial photographs as well as SPOT images. Investment for an equipment of this type is arount US$ 150.000. For already acquired equipments, the cost of SPOT up grading software is around US$ 15.000. However the future in the field of the stereocompilation belongs to **fully digital** equipments. I2S, GEMS, KERN, Contexvision, MATRA and Intergraph are proposing or announcing such equipments for the near future.

SPOT IMAGE markets currently one product adapted to stereocompiling: the level 1A film with added digital file of auxiliary data, and a new product is to be released with the image being corrected for spacecraft attitude variation effects. Advices are taken from the main manufacturers and users, in order to improve the photogrammetric product specifications.

Lastly, let us mentioned **simplified equipments**, which have the advantage of operating in analog or digital mode and monoscopic or stereoscopic viewing. Quick extraction of a succinct information, change detection and revision of existing maps can be carried out on this type of machine.

Digital Elevation Model:

Digital Elevation Model can also be obtained with SPOT by automatic and digital correlation. Several softwares are already available and many more are in the experimental or implementation phase. The technique involves the matching of a pair of images in order to determine parallax difference from which a DEM is constructed. Orbital information, ground control points and geometric model are needed. Image correlation is based on feature points or edges structured along epipolar lines. ISTAR, IGN and SEP, France, Mac Donald Detwiler and DIGIM, Canada, University College London, UK, SATIMAGE's Terragon System, Sweden, Geospectra and R. Welch, USA, are currently producing DEM wih automatic correlation techniques.

Apart from topographic line maps and orthophotos, DEM are also used to generate 3D landscape perspectives in computers for site locations, environment studies, flight simulations and as an input in Geographical Information Systems.

Towards the tools of future ...

A new generation of integrated cartographic tools is brewing in the fields of high technology, such as CARTOSPOT of DIGIM (Canada) where the digital stereoscopic images are stored into memory and processed to yield a digital elevation model by **automatic correlation,** then geometricaly and radiometricaly corrected. The cartographer interprets the main details by viewing the images on a screen and can rapidly observe any detail of the stereoscopic model. Thanks to the flexibility of digital processing, observation conditions can be continuously modified: brightness, contrast, stretching, for a better confort and more precise interpretation. Assistance techniques, such as real time **aid for stereoscopic plotting**, or expert systems are also provided to carry out a great part of the **network extraction, segmentation and classification phases.**

... and new products:

As cartography aims at satisfying **users needs,** specifications will likely move to benefit fully from the characteristics of SPOT imagery, thus giving rise to new cartographic products. One of the main concern in defining such products will be time and cost savings.

It will also be necessary to improve the difficult **balance** between the image used as a **cartographic background** and the **overlaid cartographic elements**. We agree with the proposal of I.J. Dowman, London 1987 for an image map product at scale 1:50,000, with precision specifications corresponding to that scale and including graphic informations with specifications corresponding to the 1:250,000 scale (contour lines with equidistance down to 20 or 25 meters, in option: toponyms, administrative boundaries, main networks). Such a product, with lower cost and shorter production time, would certainly meet a large part of users requirements and contribute to development in many parts of the world.

4 - CONCLUSION

To conclude, we can think that we are in a paradoxal situation: on the one hand, the many experts who have tested and worked with SPOT data have praised the images quality, hardly minored by some restrictions. On the other hand, the operational applications of SPOT imagery in cartography has not yet reached the economical importance one may have expected.

Relating to this matter, two hypothesis can be put forward to explain causes of the slow break through:

1) Technical innovation which requires large investments in the production tool, not only in terms of equipment but also in studies, development and implementation, and this at a time when available budgets for cartography are steadily reduced.

2) This very technical innovation runs into the weight of users' and producers' practice: conflicts between current methods, old specifications and users'needs.

We are confident that from technical improvements will emerge more performant, less expensive and therefore more efficient products. These technical developments will question the conventional products and their actual uses and will lead to a positive evolution where new products will not stand against the cartographers'practice and certainly contribute to a significant increase in basic cartographic mapping suited for development projects.

REFERENCES

1. RODRIGUEZ Vincent, DE GAUJAC Anne Claire, GIGORD Patrick, MUNIER Philippe 1988. Evaluation of the stereoscopic accuracy of the SPOT satellite, Phot.Eng. & Remote Sensing, Feb. 1988.

2. G. BRACHET, P. DENIS, 1987. SPOT as a cartographic tool, early results and new developments, W. Norberg Symposium.

3. KONECNY G. , LOHMANN P., ENGEL H. , et PICHT,G., "The use of SPOT imagery on analytical photogrammetric instruments", SPOT 1 - Utilisation des images, CEPADUES-EDITIONS, pp. 1173-1186, 1988.

4. DOWMANN, I.J. "The prospects for topographic mapping using SPOT data", SPOT 1 - Utilisation des images, CEPADUES-EDITIONS, pp. 1163-1172, 1988.

5. A.C. de GAUJAC, G. BEGNI, 1989, Evaluation des produits de niveaux 2A et 2B du CRIS-Toulouse, CNES.

6. GUGAN, D.J. and DOWMANN, I.J. 1987. Accuracy and completeness of topographical mapping from SPOT data., ISPRS London 1987.

7. SALGE, F. et ROOS-JOSSERAND, M.J., "Apport des images satellite à la base de données cartographiques de l'I.G.N"., International Symposium on Topographic Applications of SPOT Data, Sherbrooke, 1988.

8. BEGIN, D. et LAPIERRE D., "Expériences franco-canadiennes, précision géométrique des données SPOT. Résultats canadiens". International Symposium on Topographic Applications of SPOT Data, Sherbrooke, 1988.

9. VEILLET I. "Expériences franco-canadiennes sur la spatiotriangulation et la précision planimétrique et altimétrique", International Symposium on Topographic Applications of SPOT Data, Sherbrooke, 1988.

10. J.C. RIVEREAU - M. POUSSE , "SPOT after three years in operation. An appraisal of results and a review of selected applications" SPOT IMAGE 1989.

LIST OF THE OEEPE PUBLICATIONS

State — August 1991

A. Official publications

1 *Trombetti, C.:* „Activité de la Commission A de l'OEEPE de 1960 à 1964" — *Cunietti, M.:* „Activité de la Commission B de l'OEEPE pendant la période septembre 1960—janvier 1964" — *Förstner, R.:* „Rapport sur les travaux et les résultats de la Commission C de l'OEEPE (1960—1964)" — *Neumaier, K.:* „Rapport de la Commission E pour Lisbonne" — *Weele, A.J. v. d.:* „Report of Commission F." — Frankfurt a. M. 1964, 50 pages with 7 tables and 9 annexes.

2 *Neumaier, K.:* „Essais d'interprétation de »Bedford« et de »Waterbury«. Rapport commun établi par les Centres de la Commission E de l'OEEPE ayant participé aux tests" — „The Interpretation Tests of »Bedford« and »Waterbury«. Common Report Established by all Participating Centres of Commission E of OEEPE" — „Essais de restitution »Bloc Suisse«. Rapport commun établi par les Centres de la Commission E de l'OEEPE ayant participé aux tests" — „Test »Schweizer Block«. Joint Report of all Centres of Commission E of OEEPE." — Frankfurt a. M. 1966, 60 pages with 44 annexes.

3 *Cunietti, M.:* „Emploi des blocs de bandes pour la cartographie à grande échelle — Résultats des recherches expérimentales organisées par la Commission B de l'O.E.E.P.E. au cours de la période 1959—1966" — „Use of Strips Connected to Blocks for Large Scale Mapping — Results of Experimental Research Organized by Commission B of the O.E.E.P.E. from 1959 through 1966." — Frankfurt a. M. 1968, 157 pages with 50 figures and 24 tables.

4 *Förstner, R.:* „Sur la précision de mesures photogrammétriques de coordonnées en terrain montagneux. Rapport sur les résultats de l'essai de Reichenbach de la Commission C de l'OEEPE" — „The Accuracy of Photogrammetric Co-ordinate Measurements in Mountainous Terrain. Report on the Results of the Reichenbach Test Commission C of the OEEPE." — Frankfurt a. M. 1968, Part I: 145 pages with 9 figures; Part II: 23 pages with 65 tables.

5 *Trombetti, C.:* „Les recherches expérimentales exécutées sur de longues bandes par la Commission A de l'OEEPE." — Frankfurt a. M. 1972, 41 pages with 1 figure, 2 tables, 96 annexes and 19 plates.

6 *Neumaier, K.:* „Essai d'interprétation. Rapports des Centres de la Commission E de l'OEEPE." — Frankfurt a. M. 1972, 38 pages with 12 tables and 5 annexes.

7 *Wiser, P.:* „Etude expérimentale de l'aérotriangulation semi-analytique. Rapport sur l'essai »Gramastetten«." — Frankfurt a. M. 1972, 36 pages with 6 figures and 8 tables.

8 „Proceedings of the OEEPE Symposium on Experimental Research on Accuracy of Aerial Triangulation (Results of Oberschwaben Tests)"
Ackermann, F.: „On Statistical Investigation into the Accuracy of Aerial Triangulation. The Test Project Oberschwaben" — „Recherches statistiques sur la précision de l'aérotriangulation. Le champ d'essai Oberschwaben" — *Belzner, H.:* „The Planning. Establishing and Flying of the Test Field Oberschwaben" — *Stark, E.:* Testblock Oberschwaben, Programme I. Results of Strip Adjustments" — *Ackermann, F.:* „Testblock Oberschwaben, Program I. Results of Block-Adjustment by Independent Models" — *Ebner, H.:* Comparison of Different Methods of Block Adjustment" — *Wiser, P.:* „Propositions pour le traitement des erreurs non-accidentelles" — *Camps, F.:* „Résultats obtenus dans le cadre du project Oberschwaben 2A" — *Cunietti, M.; Vanossi, A.:* „Etude statistique expérimentale des erreurs d'enchaînement des photogrammes" — *Kupfer, G.:* „Image Geometry as Obtained from Rheidt Test Area Photography" — *Förstner, R.:* „The Signal-Field of Baustetten. A Short Report" — *Visser, J.; Leberl, F.; Kure, J.:* „OEEPE Oberschwaben Reseau Investigations" — *Bauer, H.:* „Compensation of Systematic Errors by Analytical Block Adjustment with Common Image Deformation Parameters." — Frankfurt a. M. 1973, 350 pages with 119 figures, 68 tables and 1 annex.

9 *Beck, W.:* „The Production of Topographic Maps at 1 : 10,000 by Photogrammetric Methods. — With statistical evaluations, reproductions, style sheet and sample fragments by Landesvermessungsamt Baden-Württemberg, Stuttgart." — Frankfurt a. M. 1976, 89 pages with 10 figures, 20 tables and 20 annexes.

10 „Résultats complémentaires de l'essai d'«Oberriet» de la Commission C de l'OEEPE — Further Results of the Photogrammetric Tests of «Oberriet» of the Commission C of the OEEPE"
Härry, H.: „Mesure de points de terrain non signalisés dans le champ d'essai d'«Oberriet» — Measurements of Non-Signalized Points in the Test Field «Oberriet» (Abstract)" — *Stickler, A.; Waldhäusl, P.:* „Restitution graphique des points et des lignes non signalisés et leur comparaison avec des résultats de mesures sur le terrain dans le champ d'essai d'«Oberriet» — Graphical Plotting of Non-Signalized Points and Lines, and Comparison with Terrestrial Surveys in the Test Field «Oberriet»" — *Förstner, R.:* „Résultats complémentaires des transformations de coordonnées de l'essai d'«Oberriet» de la Commission C de l'OEEPE — Further Results from Co-ordinate Transformations of the Test «Oberriet» of Commission C of the OEEPE" — *Schürer, K.:* „Comparaison des distances d'«Oberriet» — Comparison of Distances of «Oberriet» (Abstract)." — Frankfurt a. M. 1975, 158 pages with 22 figures and 26 tables.

11 „25 années de l'OEEPE"
Verlaine, R.: „25 années d'activité de l'OEEPE" — „25 Years of OEEPE (Summary)" — *Baarda, W.:* „Mathematical Models." — Frankfurt a. M. 1979, 104 pages with 22 figures.

12 *Spiess, E.:* „Revision of 1 : 25,000 Topographic Maps by Photogrammetric Methods." — Frankfurt a. M. 1985, 228 pages with 102 figures and 30 tables.

13 *Timmerman, J.; Roos, P. A.; Schürer, K.; Förstner, R.:* On the Accuracy of Photogrammetric Measurements of Buildings — Report on the Results of the Test "Dordrecht", Carried out by Commission C of the OEEPE — Frankfurt a. M. 1982, 144 pages with 14 figures and 36 tables.

14 *Thompson, C. N.:* Test of Digitising Methods. — Frankfurt a. M. 1984, 120 pages with 38 figures and 18 tables.

15 *Jaakkola, M.; Brindöpke, W.; Kölbl, O.; Noukka, P.:* Optimal Emulsions for Large-Scale Mapping — Test of "Steinwedel" — Commission C of the OEEPE 1981—84. — Frankfurt a. M. 1985, 102 pages with 53 figures.

16 *Waldhäusl, P.:* Results of the Vienna Test of OEEPE Commission C — *Kölbl, O.:* Photogrammetric Versus Terrestrial Town Survey. — Frankfurt a. M. 1986, 57 pages with 16 figures, 10 tables and 7 annexes.

17 *Commission E of the OEEPE:* Influences of Reproduction Techniques on the Identification of Topographic Details on Orthophotomaps. — Frankfurt a. M. 1986, 138 pages with 51 figures, 25 tables and 6 appendices.

18 *Förstner, W.:* Final Report on the Joint Test on Gross Error Detection of OEEPE and ISP WG III/1. — Frankfurt a. M. 1986, 97 pages with 27 tables and 20 figures.

19 *Dowman, I. J.; Ducher, G.:* Spacelab Metric Camera Experiment — Test of Image Accuracy. — Frankfurt a. M. 1987, 112 pages with 13 figures, 25 tables and 7 appendices.

20 *Eichhorn, G.:* Summary of Replies to Questionnaire on Land Information Systems — Commission V — Land Information Systems. — Frankfurt a. M. 1988, 129 pages with 49 tables and 1 annex.

21 *Kölbl, O.:* Proceedings of the Workshop on Cadastral Renovation — Ecole polytechnique fédérale, Lausanne, 9—11 September, 1987. — Frankfurt a. M. 1988, 337 pages with figures, tables and appendices.

22 *Rollin, J.; Dowman, I. J.:* Map Compilation and Revision in Developing Areas — Test of Large Format Camera Imagery. — Frankfurt a. M. 1988, 35 pages with 3 figures, 9 tables and 3 appendices.

23 *Drummond, J.* (ed.): Automatic Digitizing — A Report Submitted by a Working Group of Commission D (Photogrammetry and Cartography). — Frankfurt a. M. 1990, 224 pages with 85 figures, 6 tables and 6 appendices.

24 *Ahokas, E.; Jaakkola, J.; Sotkas, P.:* Interpretability of SPOT data for General Mapping. — Frankfurt a. M. 1990, 120 pages with 11 figures, 7 tables and 10 appendices.

25 *Ducher, G.:* Test on Orthophoto and Stereo-Orthophoto Accuracy. — Frankfurt a. M. 1991, 227 pages with 16 figures and 44 tables.

B. Special publications

— Special Publications O.E.E.P.E. — Number I

Solaini, L.; Trombetti, C.: Relation sur les travaux préliminaires de la Commission A (Triangulation aérienne aux petites et aux moyennes échelles) de l'Organisation Européenne d'Etudes Photogrammétriques Expérimentales (O.E.E.P.E.). I[ère] Partie: Programme et organisation du travail. — *Solaini, L.; Belfiore, P.:* Travaux préliminaires de la Commission B de l'Organisation Européenne d'Etudes Photogrammétriques Expérimentales (O.E.E.P.E.) (Triangulations aériennes aux grandes échelles). — *Solaini, L.; Trombetti, C.; Belfiore, P.:* Rapport sur les travaux expérimentaux de triangulation aérienne exécutés par l'Organisation Européenne d'Etudes Photogrammétriques Expérimentales (Commission A et B). — *Lehmann, G.:* Compte rendu des travaux de la Commission C de l'O.E.E.P.E. effectués jusqu'à présent. — *Gotthardt, E.:* O.E.E.P.E. Commission C. Compte-rendu de la restitution à la Technischen Hochschule, Stuttgart, des vols d'essai du groupe I du terrain d'Oberriet. — *Brucklacher, W.:* Compte-rendu du centre «Zeiss-Aerotopograph» sur les restitutions pour la Commission C de l'O.E.E.P.E. (Restitution de la bande de vol, groupe I, vol. No. 5). — *Förstner, R.:* O.E.E.P.E. Commission C. Rapport sur la restitution effectuée dans l'Institut für Angewandte Geodäsie, Francfort sur le Main. Terrain d'essai d'Oberriet les vols No. 1 et 3 (groupe I). — I.T.C., Delft: Commission C, O.E.E.P.E. Déroulement chronologique des observations. — Photogrammetria XII (1955—1956) 3, Amsterdam 1956, pp. 79—199 with 12 figures and 11 tables.

— Publications spéciales de l'O.E.E.P.E. — Numéro II

Solaini, L.; Trombetti, C.: Relations sur les travaux préliminaires de la Commission A (Triangulation aérienne aux petites et aux moyennes échelles) de l'Organisation Européenne d'Etudes Photogrammétriques Expérimentales (O.E.E.P.E.). 2[e] partie. Prises de vues et points de contrôle. — *Gotthardt, E.:* Rapport sur les premiers résultats de l'essai d'«Oberriet» de la Commission C de l'O.E.E.P.E. — Photogrammetria XV (1958—1959) 3, Amsterdam 1959, pp. 77—148 with 15 figures and 12 tables.

— *Trombetti, C.:* Travaux de prises de vues et préparation sur le terrain effectuées dans le 1958 sur le nouveau polygone italien pour la Commission A de l'OEEPE. — Florence 1959, 16 pages with 109 tables.

— *Trombetti, C.; Fondelli, M.:* Aérotriangulation analogique solaire. — Firence 1961, 111 pages, with 14 figures and 43 tables.

— Publications spéciales de l'O.E.E.P.E. — Numéro III

Solaini, L.; Trombetti, C.: Rapport sur les résultats des travaux d'enchaînement et de compensation exécutés pour la Commission A de l'O. E. E. P. E. jusqu'au mois de Janvier 1960. Tome 1: Tableaux et texte. Tome 2: Atlas. — Photogrammetria XVII (1960—1961) 4, Amsterdam 1961, pp. 119—326 with 69 figures and 18 tables.

— „OEEPE — Sonderveröffentlichung Nr. 1"

Gigas, E.: „Beitrag zur Geschichte der Europäischen Organisation für photogrammetrische experimentelle Untersuchungen" — *N. N.:* „Vereinbarung über die Gründung einer Europäischen Organisation für photogrammetrische experimentelle Untersuchungen" — „Zusatzprotokoll" — *Gigas, E.:* „Der Sechserausschuß" — *Brucklacher, W.:* „Kurzbericht über die Arbeiten in der Kommission A der OEEPE" — *Cunietti, M.:* „Kurzbericht des Präsidenten der Kommission B über die gegenwärtigen Versuche und Untersuchungen" — *Förstner, R.:* „Kurzbericht über die Arbeiten in der Kommission B der OEEPE" — „Kurzbericht über die Arbeiten in der Kommission C der OEEPE" — *Belzner, H.:* „Kurzbericht über die Arbeiten in der Kommission E der OEEPE" — *Schwidefsky, K.:* „Kurzbericht über die Arbeiten in der Kommission F der OEEPE" — *Meier, H.-K.:* „Kurzbericht über die Tätigkeit der Untergruppe „Numerische Verfahren" in der Kommission F der OEEPE" — *Belzner, H.:* „Versuchsfelder für internationale Versuchs- und Forschungsarbeiten." — Nachr. Kt.- u. Vermesss.-wes., R. V, Nr. 2, Frankfurt a. M. 1962, 41 pages with 3 tables and 7 annexes.

— *Rinner, K.:* Analytisch-photogrammetrische Triangulation eines Teststreifens der OEEPE. — Österr. Z. Vermess.-wes., OEEPE-Sonderveröff. Nr. 1, Wien 1962, 31 pages.

— *Neumaier, K.; Kasper, H.:* Untersuchungen zur Aerotriangulation von Überweitwinkelaufnahmen. — Österr. Z. Vermess.-wes., OEEPE-Sonderveröff. Nr. 2, Wien 1965, 4 pages with 4 annexes.

— „OEEPE — Sonderveröffentlichung Nr. 2"

Gotthardt, E.: „Erfahrungen mit analytischer Einpassung von Bildstreifen." — Nachr. Kt.- u. Vermess.-wes., R. V, Nr. 12, Frankfurt a. M. 1965, 14 pages with 2 figures and 7 tables.

— „OEEPE — Sonderveröffentlichung Nr. 3"

Neumaier, K.: „Versuch »Bedford« und »Waterbury«. Gemeinsamer Bericht aller Zentren der Kommission E der OEEPE" — „Versuch »Schweizer Block«. Gemeinsamer Bericht aller Zentren der Kommission E der OEEPE." — Nachr. Kt.- u. Vermess.-wes., R. V, Nr. 13, Frankfurt a. M. 1966, 30 pages with 44 annexes.

— *Stickler, A.; Waldhäusl, P.:* Interpretation der vorläufigen Ergebnisse der Versuche der Kommission C der OEEPE aus der Sicht des Zentrums Wien. — Österr. Z. Vermess.-wes., OEEPE-Sonderveröff. (Publ. Spéc.) Nr. 3, Wien 1967, 4 pages with 2 figures and 9 tables.

— „OEEPE — Sonderveröffentlichung Nr. 4"

Schürer, K.: „Die Höhenmeßgenauigkeit einfacher photogrammetrischer Kartiergeräte. Bemerkungen zum Versuch »Schweizer Block« der Kommission E der OEEPE." — Nachr. Kt.- u. Vermess.-wes., Sonderhefte, Frankfurt a. M., 1968, 25 pages with 7 figures and 3 tables.

— „OEEPE — Sonderveröffentlichung Nr. 5"

Förstner, R.: „Über die Genauigkeit der photogrammetrischen Koordinatenmessung in bergigem Gelände. Bericht über die Ergebnisse des Versuchs Reichenbach der Kommission C der OEEPE." — Nachr. Kt.- u. Vermess.-wes., Sonderhefte, Frankfurt a. M. 1969, Part I: 74 pages with 9 figures; Part II: 65 tables.

— „OEEPE — Sonderveröffentlichung Nr. 6"

Knorr, H.: „Die Europäische Organisation für experimentelle photogrammetrische Untersuchungen — OEEPE — in den Jahren 1962 bis 1970." — Nachr. Kt.- u. Vermess.-wes., Sonderhefte, Frankfurt a. M. 1971, 44 pages with 1 figure and 3 tables.

— „OEEPE — Sonderveröffentlichung Nr. D–7"

Förstner, R.: „Das Versuchsfeld Reichenbach der OEEPE." — Nachr. Kt.- u. Vermess.-wes., Sonderhefte, Frankfurt a. M. 1972, 191 pages with 49 figures and 38 tables.

— „OEEPE — Sonderveröffentlichung Nr. D–8"

Neumaier, K.: „Interpretationsversuch. Berichte der Zentren der Kommission E der OEEPE." — Nachr. Kt.- u. Vermess.-wes., Sonderhefte, Frankfurt a. M. 1972, 33 pages with 12 tables and 5 annexes.

— „OEEPE — Sonderveröffentlichung Nr. D–9"

Beck, W.: „Herstellung topographischer Karten 1 : 10 000 auf photogrammetrischem Weg. Mit statistischen Auswertungen, Reproduktionen, Musterblatt und Kartenmustern des Landesvermessungsamts Baden-Württemberg, Stuttgart." — Nachr. Kt.- u. Vermess.-wes., Sonderhefte, Frankfurt a. M. 1976, 65 pages with 10 figures, 20 tables and 20 annexes.

— „OEEPE — Sonderveröffentlichung Nr. D–10"

Weitere Ergebnisse des Meßversuchs „Oberriet" der Kommission C der OEEPE. *Härry, H.:* „Messungen an nicht signalisierten Geländepunkten im Versuchsfeld «Oberriet»" — *Stickler, A.; Waldhäusl, P.:* „Graphische Auswertung nicht signalisierter Punkte und Linien und deren Vergleich mit Feldmessungsergebnissen im Versuchsfeld «Oberriet»" — *Förstner, R.:* „Weitere Ergebnisse aus Koordinatentransformationen des Versuchs «Oberriet» der Kommission C der OEEPE" — *Schürer, K.:* „Streckenvergleich «Oberriet»." — Nachr. Kt.- u. Vermess.-wes., Sonderhefte, Frankfurt a. M. 1975, 116 pages with 22 figures and 26 tables.

— „OEEPE — Sonderveröffentlichung Nr. D–11"

Schulz, B.-S.: „Vorschlag einer Methode zur analytischen Behandlung von Reseauaufnahmen." — Nachr. Kt.- u. Vermess.-wes., Sonderhefte, Frankfurt a. M. 1976, 34 pages with 16 tables.

— „OEEPE — Sonderveröffentlichung Nr. D–12"

Verlaine, R.: „25 Jahre OEEPE." — Nachr. Kt.- u. Vermess.-wes., Sonderhefte, Frankfurt a. M. 1980, 53 pages.

— „OEEPE — Sonderveröffentlichung Nr. D–13"

Haug, G.: „Bestimmung und Korrektur systematischer Bild- und Modelldeformationen in der Aerotriangulation am Beispiel des Testfeldes „Oberschwaben." — Nachr. Kt.- u. Vermess.-wes., Sonderhefte, Frankfurt a. M. 1980, 136 pages with 25 figures and 51 tables.

— „OEEPE — Sonderveröffentlichung Nr. D—14"

Spiess, E.: „Fortführung der Topographischen Karte 1 : 25 000 mittels Photogrammetrie" (not published, see English version in OEEPE official publication No. 12)

— „OEEPE — Sonderveröffentlichung Nr. D—15"

Timmerman, J.; Roos, P. A.; Schürer, K.; Förstner, R.: „Über die Genauigkeit der photogrammetrischen Gebäudevermessung. Bericht über die Ergebnisse des Versuchs Dordrecht der Kommission C der OEEPE." — Nachr. Kt.- u. Vermess.-wes., Sonderhefte, Frankfurt a. M. 1983, 131 pages with 14 figures and 36 tables.

— „OEEPE — Sonderveröffentlichung Nr. D—16"

Kommission E der OEEPE: „Einflüsse der Reproduktionstechnik auf die Erkennbarkeit von Details in Orthophotokarten." — Nachr. Kt.- u. Vermess.-wes., Sonderhefte, Frankfurt a. M. 1986, 130 pages with 51 figures, 25 tables and 6 annexes.

— „OEEPE — Sonderveröffentlichung Nr. D—17"

Schürer, K.: Über die Genauigkeit der Koordinaten signalisierter Punkte bei großen Bildmaßstäben. Ergebnisse des Versuchs „Wien" der Kommission C der OEEPE. — Nachr. Kt.- u. Vermess.-wes., Sonderhefte, Frankfurt a. M. 1987, 84 pages with 3 figures, 10 tables and 42 annexes.

C. Congress reports and publications in scientific reviews

- *Stickler, A.:* Interpretation of the Results of the O.E.E.P.E. Commission C. — Photogrammetria XVI (1959—1960) 1, pp. 8—12, 3 figures, 1 annexe (en langue allemande: pp. 12—16).
- *Solaini, L.; Trombetti, C.:* Results of Bridging and Adjustment Works of the Commission A of the O.E.E.P.E. from 1956 to 1959. — Photogrammetria XVI (1959—1960) 4 (Spec. Congr.-No. C), pp. 340—345, 2 tables.
- *N. N.:* Report on the Work Carried out by Commission B of the O.E.E.P.E. During the Period of September 1956—August 1960. — Photogrammetria XVI (1959—1960) 4 (Spec. Congr.-No. C), pp. 346—351, 2 tables.
- *Förstner, R.:* Bericht über die Tätigkeit und Ergebnisse der Kommission C der O.E.E.P.E. (1956—1960). — Photogrammetria XVI (1959—1960) 4 (Spec. Congr.-No. C), pp. 352—357, 1 table.
- *Bachmann, W. K.:* Essais sur la précision de la mesure des parallaxes verticales dans les appareils de restitution du I^{er} ordre. — Photogrammetria XVI (1959—1960) 4 (Spec. Congr.-No. C), pp. 358—360).
- *Wiser, P.:* Sur la reproductibilité des erreurs du cheminement aérien. — Bull. Soc. Belge Photogramm., No. 60, Juin 1960, pp. 3—11, 2 figures, 2 tables.
- *Cunietti, M.:* L'erreur de mesure des parallaxes transversales dans les appareils de restitution. — Bull. Trimestr. Soc. Belge Photogramm., No. 66, Décembre 1961, pp. 3—50, 12 figures, 22 tables.

- „OEEPE — Arbeitsberichte 1960/64 der Kommissionen A, B, C, E, F"

  Trombetti, C.: „Activité de la Commission A de l'OEEPE de 1960 à 1964" — *Cunietti, M.:* „Activité de la Commission B de l'OEEPE pendant la période septembre 1960—janvier 1964" — *Förstner, R.:* „Rapport sur les travaux et les résultats de la Commission C de l'OEEPE (1960—1964)" — *Neumaier, K.:* „Rapport de la Commission E pour Lisbonne" — *Weele, A. J. van der:* „Report of Commission F." — Nachr. Kt.- u. Vermess.-wes., R. V. Nr. 11, Frankfurt a. M. 1964, 50 pages with 7 tables and 9 annexes.
- *Cunietti, M.; Inghilleri, G.; Puliti, M.; Togliatti, G.:* Participation aux recherches sur les blocs de bandes pour la cartographie à grande échelle organisées par la Commission B de l'OEEPE. Milano, Centre CASF du Politecnico. — Boll. Geod. e Sc. affini (XXVI) 1, Firenze 1967, 104 pages.
- *Gotthardt E.:* Die Tätigkeit der Kommission B der OEEPE. — Bildmess. u. Luftbildwes. 36 (1968) 1, pp. 35—37.
- *Cunietti, M.:* Résultats des recherches expérimentales organisées par la Commission B de l'OEEPE au cours de la période 1959—1966. Résumé du Rapport final. — Présenté à l'XI^{e} Congrès International de Photogrammétrie, Lausanne 1968, Comm. III (en langues française et anglaise), 9 pages.
- *Förstner, R.:* Résumé du Rapport sur les résultats de l'essai de Reichenbach de la Commission C de l'OEEPE. — Présenté à l'XI^{e} Congrès International de Photogrammétrie, Lausanne 1968, Comm. IV (en langues française, anglaise et allemande), 28 pages, 2 figures, 2 tables.
- *Timmerman, J.:* Proef „OEEPE-Dordrecht". — ngt 74, 4. Jg., Nr. 6, Juni 1974, S. 143—154 (Kurzfassung: Versuch „OEEPE-Dordrecht". Genauigkeit photogrammetrischer Gebäudevermessung. Vorgelegt auf dem Symposium der Kommission IV der I.G.P., Paris, 24.—26. September 1974).
- *Timmerman, J.:* Report on the Commission C. "OEEPE-Dordrecht" Experiment. — Presented Paper for Comm. IV, XIIIth Congress of ISP, Helsinki 1976.
- *Beck, W.:* Rapport de la Commission D de l'OEEPE sur l'établissement de cartes topographiques au 1/10 000 selon le procédé photogrammétrique. — Presented Paper for Comm. IV, XIIIth Congress of ISP, Helsinki 1976.
- *Verlaine, R.:* La naissance et le développement de l'OEEPE — Festschrift — Dr. h. c. *Hans Härry*, 80 Jahre — Schweizerische Gesellschaft für Photogrammetrie und Wild Heerbrugg AG, Bern 1976.
- *Förstner, R.:* Internationale Versuche (Essais contrôlés) — Festschrift — Dr. h. c. *Hans Härry*, 80 Jahre. — Schweizerische Gesellschaft für Photogrammetrie und Wild Heerbrugg AG, Bern 1976.
- *Baj, E.; Cunietti, M.; Vanossi, A.:* Détermination Expérimentale des Erreurs Systématiques des Faisceaux Perspectifs. — Société Belge de Photogrammétrie, Bulletin trimestriel, Brüssel 1977, pp 21—49.
- *Timmerman, J.:* Fotogrammetrische stadskaartering de OEEPE-proef Dordrecht. — Geodesia 19, Amsterdam 1977, pp. 291—298.
- *Waldhäusl, P.:* The Vienna Experiment of the OEEPE/C. Proceedings — Standards and Specifications for Integrated Surveying and Mapping Systems. — Schriftenreihe HSBw, Heft 2, München 1978.
- *Bachmann, W. K.:* Recherches sur la stabilité des appareils de restitution photogrammétriques analogiques. — Vermessung, Photogrammetrie, Kulturtechnik, Zürich 1978, pp. 265—268.
- *Parsic, Z.:* Untersuchungen über den Einfluß signalisierter und künstlicher Verknüpfungspunkte auf die Genauigkeit der Blocktriangulation. — Vermessung, Photogrammetrie, Kulturtechnik, Zürich 1978, pp. 269—278.
- *Waldhäusl, P.:* Der Versuch Wien der OEEPE/C. — Geowissenschaftliche Mitteilungen der Studienrichtung Vermessungswesen der TU Wien, Heft 13, Wien 1978, pp. 101—124.
- *Waldhäusl, P.:* Ergebnisse des Versuches Wien der OEEPE/C. — Presented Paper for Comm. IV, XIVth Congress of ISP, Hamburg 1980.
- *Timmerman, J.; Förstner, R.:* Kurzbericht über die Ergebnisse des Versuchs Dordrecht der Kommission C der OEEPE. — Presented Paper for Comm. IV, XIVth Congress of ISP, Hamburg 1980.

- *Bernhard, J.; Schmidt-Falkenberg, H.:* OEEPE — Die Arbeiten der Kommission E „Interpretation". — Presented Paper for Comm. IV, XIVth Congress of ISP, Hamburg 1980.
- *Bachmann, W. K.:* Elimination des valeurs erronées dans un ensemble de mesures controlées. — Papers written in honor of the 70th birthday of Professor *Luigi Solaini* — Richerche di Geodesia Topografia e Fotogrammetria, Milano 1979, pp. 27—39.
- *Visser, J.:* The European Organisation for Experimental Photogrammetric Research (OEEPE) — The Thompson Symposium 1982. — The Photogrammetric Record, London 1982, pp. 654—668.
- *Spiess, E.:* Revision of Topographic Maps: Photogrammetric and Cartographic Methods of the Fribourg Test. — The Photogrammetric Record, London 1983, pp. 29—42.
- *Jerie, H.G. and Holland, E.W.:* Cost model project for photogrammetric processes: a progress report. — ITC Journal, Enschede 1983, pp. 154—159.
- *Ackermann, F. E.* (Editor): Seminar — Mathematical Models of Geodetic/Photogrammetric Point Determination with Regard to Outliers and Systematic Errors — Working Group III/1 of ISP — Commission A of OEEPE. — Deutsche Geodätische Kommission bei der Bayerischen Akademie der Wissenschaften, Reihe A, Heft Nr. 98, München 1983.
- *Brindöpke, W., Jaakkola, M., Noukka, P., Kölbl, O.:* Optimal Emulsions for Large Scale Mapping — OEEPE—Commission C. — Presented Paper for Comm. I, XVth Congress of ISPRS, Rio de Janeiro 1984.
- *Ackermann, F.:* Report on the Activities of Working Group III/1 During 1980—84. — Comm. III, XVth Congress of ISPRS, Rio de Janeiro 1984.
- *Förstner, W.:* Results of Test 2 on Gross Error Detection of ISP WG III/1 and OEEPE. — Comm. III, XVth Congress of ISPRS, Rio de Janeiro 1984.
- *Gros, G.:* Modèles Numériques Altimétriques — Lignes Characteristiques — OEEPE Commission B. — Comm. III, XVth Congress of ISPRS, Rio de Janeiro 1984.
- *Ducher, G.:* Preparation d'un Essai sur les Ortho- et Stereo-Orthophotos. — Comm. IV, XVth Congress of ISPRS, Rio de Janeiro 1984.
- *van Zuylen, L.:* The influence of reproduction methods on the identification of details in orthophoto maps. — ITC Journal, Enschede 1984, pp. 219—226.
- *Visser, J.:* OEEPE-News — The European Organization for Experimental Photogrammetric Research. — ITC Journal, Enschede 1984, pp. 330—332.
- *Brindöpke, W., Jaakkola, M., Noukka, P., Kölbl, O.:* Optimale Emulsionen für großmaßstäbige Auswertungen. — Bildmess. u. Luftbildw. 53 (1985) 1, pp. 23—35.
- *Thompson, C. N.:* Some New Horizons for OEEPE. Presented Paper to the Symposium of Commission IV, ISPRS in Edinburgh, 8.—12. September 1986, pp. 299—306.
- *Dowman, I.:* The Restitution of Metric Photography Taken From Space — Comm. II, XVIth Congress of ISPRS, Kyoto 1988.
- *Kilpelä, E.:* Statistical Data on Aerial Triangulation — Comm. III, XVIth Congress of ISPRS, Kyoto 1988.

The official publications and the special publications issued in Frankfurt am Main are for sale at the

Institut für Angewandte Geodäsie
— Außenstelle Berlin —

Stauffenbergstraße 13, D-1000 Berlin 30

Organisation Européenne d'Etudes Photogrammétriques Expérimentales

Publications officielles

Content